Optimization of a Dry, Mixed Nuclear Fuel Storage Array for Nuclear Criticality Safety

A Thesis

Presented in Partial Fulfillment of the Requirements for the

Degree of Master of Science

with a

Major in Nuclear Engineering

in the

College of Graduate Studies

University of Idaho

by

Benjamin T. Baranko

Major Professor: Akira Tokuhiro, Ph.D.

Committee Members: Robert Hiromoto, Ph.D.; Leland Montierth, Ph.D.;

Matthew Riley, Ph.D.

Department Administrator: Lee Ostrom, Ph.D.

May 2015

Authorization to Submit Thesis

This thesis of Benjamin T. Baranko, submitted for the degree of Master of Science with a Major in Nuclear Engineering and titled "Optimization of a Dry, Mixed Nuclear Fuel Storage Array for Nuclear Criticality Safety," has been reviewed in final form. Permission, as indicated by the signatures and dates below, is now granted to submit final copies to the College of Graduate Studies for approval.

Major Professor: _____ Date: _____

Akira Tokuhiro, Ph.D.

Committee Members: _____ Date: _____

Robert Hiromoto, Ph.D.

_____ Date: _____

Leland Montierth, Ph.D.

_____ Date: _____

Matthew Riley, Ph.D.

Department Administrator: _____ Date: _____

Lee Ostrom, Ph.D.

Abstract

A dry storage array of used nuclear fuel at the Idaho National Laboratory contains a mixture of more than twenty different research and test reactor fuel types in up to 636 fuel storage canisters. New analysis demonstrates that the current arrangement of the different fuel-type canisters does not minimize the system neutron multiplication factor (k_{eff}), and that the entire facility storage capacity cannot be utilized without exceeding the subcritical limit (k_{safe}) for ensuring nuclear criticality safety. This work determines a more optimal arrangement of the stored fuels with a goal to minimize the system k_{eff}, but with a minimum of potential fuel canister relocation movements. The solution to this multiple-objective optimization problem will allow for both an improvement in the facility utilization while also offering an enhancement in the safety margin. The solution method applies stochastic approximation and a Tabu search metaheuristic to an empirical model developed from supporting MCNP calculations. The results establish an optimal relocation of between four to sixty canisters, which will allow the current thirty-one empty canisters to be used for storage while reducing the array k_{eff} by up to 0.018 +/- 0.003 relative to the current arrangement.

Acknowledgements

The Monte-Carlo neutron transport (MCNP) analysis contained in this document builds upon existing nuclear criticality safety analysis that has been performed by others on the IFSF storage array. All calculations that are reported in this document are new MCNP input cases of unique arrangements that have been modified and performed by the author. However, the specific modeling of the IFSF structure and fuels is existing MCNP geometric input and material compositions that are already utilized for the IFSF nuclear criticality safety basis calculations. These original IFSF structure and fuel models were primarily developed by K. B. Woods, M. N. Neeley, and V. L. Putman, who all have performed previous supporting analysis of the IFSF array. This previous work serves as a foundation upon which this current work expands.

I wish to thank Professor Tokuhiro for the continual guidance and assistance provided over the course of this effort.

I wish to also thank the committee of Robert Hiromoto, Lee Montierth, and Matthew Riley for their investment of time and effort in fulfilling this role.

Dedication

This work is dedicated to my wife Linda, as my post-graduate education would not have been possible without her steadfast support, and to my parents Donna and Emil, who always emphasized educational pursuits and strived to provide the best possible educational opportunities.

Table of Contents

List of Figures

List of Tables

Nomenclature

AOA	area of applicability
ANECF	average neutron-energy causing-fission
ATR	Advanced Test Reactor
DOE	Department of Energy
eV	electron volt
EALF	energy of the average lethargy causing fission
ENDF	Evaluated Nuclear Data File
FRR	foreign research reactor
FSV	Fort Saint Vrain (reactor fuel)
HEU	highly-enriched uranium
HTGR	High Temperature Gas-cooled Reactor
IFSF	Irradiated Fuel Storage Facility
INL	Idaho National Laboratory
k_{eff}	k-effective (neutron multiplication factor)
k_{safe}	subcritical limit
LEU	low-enriched uranium
MCNP	Monte-Carlo N-Particle (radiation transport code)
MPR	multi-purpose reactor
MTR	Materials Test Reactor
MVDS	Modular Vault Dry Storage
NCS	nuclear criticality safety
ORSNF	Oak Ridge Spent Nuclear Fuel

PB	Peach Bottom
PBF	Power Burst Facility
RERTR	Reduced-Enrichment Research and Test Reactor
SBT	South Basin TRIGA
SNF	spent nuclear fuel
TRIGA	Training, Research, Isotopes-General Atomics (research reactor fuel)
TRIGA-IN	TRIGA-Incoloy [clad]
UBM	Uranium Bearing Material
UNF	used nuclear fuel
wt%	weight percent

Chapter 1.0 - Introduction

The Irradiated Fuel Storage Facility (IFSF) at the Idaho National Laboratory (INL) is used to store used nuclear fuels in a centralized, dry storage arrangement. This facility has been in operation since the 1970s and currently stores a mixture of more than twenty different research and test reactor fuels. The fuel is stored in an array of up to 636 fuel storage canisters. The IFSF is a unique facility among centralized dry storage facilities regarding the neutronically coupled storage configuration and the variety of stored fuel types. Nuclear Criticality Safety (NCS) is a primary limiting factor that dictates the allowed storage arrangement and the permissible fuel storage density. Nuclear criticality safety is maintained primarily by moderation control and through the control on neutron interaction and leakage provided by the credited geometry. The facility currently has a number of fuel storage positions that are empty and that could be used for additional storage capacity; however, in the NCS analysis the current storage arrangement approaches the allowable limit on the neutron multiplication factor for demonstrating subcriticality, or k_{safe}. The current fuel storage arrangement is known to not result in the minimum possible neutron multiplication factor, k_{eff}, for the given set of fuel storage canisters that are currently present in the fuel storage array. However the magnitude of a possible improvement has never been assessed or quantified. Ultimately, this situation means that the entire facility storage capacity cannot be utilized without surpassing the system minimum subcritical state (k_{safe}) for ensuring nuclear criticality safety, and the potential for improvement is unknown.

This work determines a more optimal arrangement for the stored fuels with a goal to minimize the system k_{eff}, but also with a minimum of potential fuel canister relocation movements. The primary goal is to establish a solution for this multiple-objective optimization problem by finding the Pareto Front for maximum k_{eff} reduction versus the number of canister relocations. The process first required additional analysis of the array by Monte-Carlo neutron transport codes (specifically, MCNP) to gain a greater understanding of the interaction characteristics of the disparate fuel types. Some stored fuels are composed of primarily metallic and oxide components that provide very little inherent moderation, while other fuel types contain graphite or zirconium-hydride which can contribute a significant amount of moderation. These factors cause a complex relationship within a fuel arrangement with respect to thermal utilization and axial leakage probability.

The MCNP analysis was applied to develop a simplified spreadsheet-based empirical model which simulates the array k_{eff} result. The empirical model was benchmarked against MCNP calculations for various arrangements and then employed in the optimization analysis. Heuristic treatments guided by the supporting analysis were applied with a stochastic approximation

optimization component. The optimization objective is to determine the minimum array k_{eff} for each of various numbers of possible canister relocation movements. The optimization algorithm interrogated the empirical model to determine the optimal rearrangement for a maximum of sixty canister relocation movements (or thirty canister swaps).

The likely candidate solutions for a given number of canister moves were analyzed in MCNP to confirm the best result. In this manner the Pareto Front was determined for the largest possible reduction in k_{eff} for between 4 and 60 canister relocation movements. The optimization result shows that a limited number of canister relocation movements could allow the existing empty array positions to be filled with common research reactor fuels while also yielding a reduction in the overall array k_{eff} relative to the current arrangement. This will impart an improvement in the facility capacity utilization while also offering an enhancement in the nuclear criticality safety margin.

Objectives

Specific objectives of this work include:

- To further the understanding of the criticality physics of complex arrangements of differing types of nuclear fuels in an under-moderated state. This is accomplished by investigating the spatial relationships of the NCS parameters that correlate the neutron interaction and leakage aspects of the subcritical system. This supports the determination of parametric values that can be utilized to create an empirical model.

- Develop an empirical model for a dry storage array of fissile material that effectively determines relative changes in system k_{eff} for movement of the locations of canisters with discreet fuel loadings.

- Develop a viable optimization treatment for the empirical model for the two-dimensional spatial arrangement, to enhance the nuclear criticality safety margin and maximize facility utilization.

Benefits

Specific benefits that will be realized by accomplishing the above objectives include:

- Improved knowledge of physics of complex interacting system
    - "Computer calculations are convenient and very fast; however, it is sometimes difficult to relate the basic output provided by the codes to the basic physics involved. Use of these codes can obscure the parameters that a particular fissile system may be sensitive to…further, practitioners must avoid using computer codes as devices that take inputs and simply provide outputs (i.e., a "black box")." - Douglas G. Bowen and Robert D. Busch, LA-14244-M
- Enhanced safety posture by increasing the safety margin associated with the array k_{eff}. This allows an increased tolerance for upset conditions and future changes.
- Quantification of margin that exists within the storage arrangement. Specific knowledge of the degree of subcritical margin present provides the vital data that is needed for decision making regarding improved operational utilization of facility. More informed decisions determined from cost-benefit analysis based on the analysis results would be possible.
- This quantification of safety margin is also valuable to facility life extension and aging management issues.
- This work will ultimately allow more complete utilization of a finite but unique existing resource for used nuclear fuel (UNF) storage.

Chapter 2.0 - Problem Description and Background

2.1 Centralized, Dry, Used Nuclear Fuel Storage

Intermediate-term storage of used nuclear fuel is an important issue facing the nuclear industry and the federal government. Extended storage of used nuclear fuel is required while an ultimate disposition method for the UNF is determined. This may require storage of the UNF for an additional 30 to 100 years. The benefits of dry fuel storage are widely established, and this method is the preferred storage type once the cooling of decay heat provided by underwater storage is no longer required for safety. Dry cask storage systems have become the most common method for interim dry UNF storage, particularly at nuclear power plants.

Centralized dry-storage of UNF provides a number of benefits compared to dry cask storage. A central storage location simplifies monitoring and reduces the staffing required during the storage period. Interim UNF storage requires surveillances regarding temperature and pressure, external radiation, containment of contamination, security, and potentially for hydrogen generation or maintenance of an inert gas environment. These tasks can be more efficiently provided by a smaller dedicated staff at a central facility as compared to multiple dry cask storage pads at reactor facilities, particularly regarding plants that have undergone permanent shutdown. Removing fuel from dry cask storage pads at the reactor facilities also provides the benefits of freeing sites that have completed deactivation for other uses, and reducing the risk to fuel from natural disaster or security related events, even if this may often be more of a perceived reduction in risk rather than a real benefit.

UNF can be stored in a more dense arrangement, or smaller overall footprint, if it is placed in a central shielded facility. These types of facilities provide all the benefits of centralized dry cask storage with additional benefits of even further ease of monitoring fuel condition, central cooling if needed, and containment, shielding, and filtration efficiency benefits. Central shielded facilities also allow ideal environments for handling and repackaging of the UNF into the configuration required for the permanent repository or other disposition path such as chemical or electro refining methods of reprocessing. This type of storage arrangement involves a shielded fuel handling cell with remote equipment that allows for re-configuration of stored fuels to allow for repackaging of fuels in storage devices of a design or material type that may be required for reprocessing or ultimate disposal. Fuels can also be batched for reprocessing by other fuel parameters such as burnup or enrichment.

Centralized dry fuel storage facilities exist in a number of places around the world in the form of Modular Vault Dry Storage (MVDS) facilities. These UNF storage facilities typically place

canistered UNF into concrete vaults designed to provide a degree of confinement and shielding. The vaults typically provide near-isolation of neutrons between adjacent vaults to a sufficient degree that significant neutron interaction does not occur from a nuclear criticality safety standpoint. That is, the separate vaults can be considered to provide effective isolation. Examples of MVDS type storage include the fuel storage facilities at Wylfa, United Kingdom and at the Pakks Nuclear Power Plant in Hungary.

Some other dry UNF storage facilities differ from the MVDS concept by also placing the fuel in metal canisters, but then the canisters are placed in wells in what is essentially a concrete slab. Provisions may be provided for cooling airflow. Here again, the significant thickness of concrete between the storage positions provides neutronic isolation such that interaction between stored canisters is not a NCS concern. Examples of this type of UNF storage include the Canister Storage Building at the United States Department of Energy (DOE) Hanford site, WA, and the Nuclear Regulatory Commission (NRC) licensed Fort St. Vrain power plant fuel storage facility near Greeley, CO.

2.2 Irradiated Fuel Storage Facility (IFSF)

A unique version of a central shielded dry UNF storage facility exists at the Idaho National Laboratory. This facility, called the Irradiated Fuel Storage Facility, differs from the MVDS facilities in that the fuel is stored in canisters that are placed in an open frame steel rack. Containment and shielding is provided by thick exterior concrete walls and HEPA filtration on the ventilation that provides cooling airflow and maintenance of the negative differential pressure to ensure containment of contamination.

The fuel storage array of the IFSF consists of a triangular-pitch arrangement of steel fuel storage canisters that hang from the top surface of an open, steel-framed storage rack by a flange at the top of the canister. The fuel storage canisters are constructed of 18 inch Schedule 10 pipe that is either carbon steel or stainless steel. The canisters are approximately 11 feet tall with a 10 foot 9 inch (327.7 cm) usable interior height. The storage array alternates between 17 or 18 canisters arranged in the north-south direction, with 38 rows of canisters. Rows 36 through 38 only contain between three to fifteen canisters due to the presence of the canister shuttle bin that moves the fuel storage canisters between the fuel handling cave and the storage area. Figure 1 shows an isometric cut-away view of the IFSF storage area. The fuel handling cave is used to unload the transport casks and load the fuel storage canisters in a configuration acceptable for storage. There are a total of 636 fuel canister storage

positions in the fuel storage rack. The bottoms of the canisters are suspended approximately 2.5 inches above the concrete floor. A sheet steel cover encloses the top surface of the storage rack around all the canister openings. Figure 2 shows a view of a canister and a section of the fuel storage rack.

The IFSF walls are modeled as a minimum of 71 cm of concrete, while the floor and ceiling modeled as 61 cm thick. The walls are modeled as immediately adjacent to the exterior canisters, while the bottoms of the canisters are modeled as only 1 mm above the floor. The ceiling is modeled as being 632.66 cm above the top surface of the storage array.

The canister movement operations are performed remotely by a bridge crane. Operations are viewed through an oil-filled shield window and by cameras.

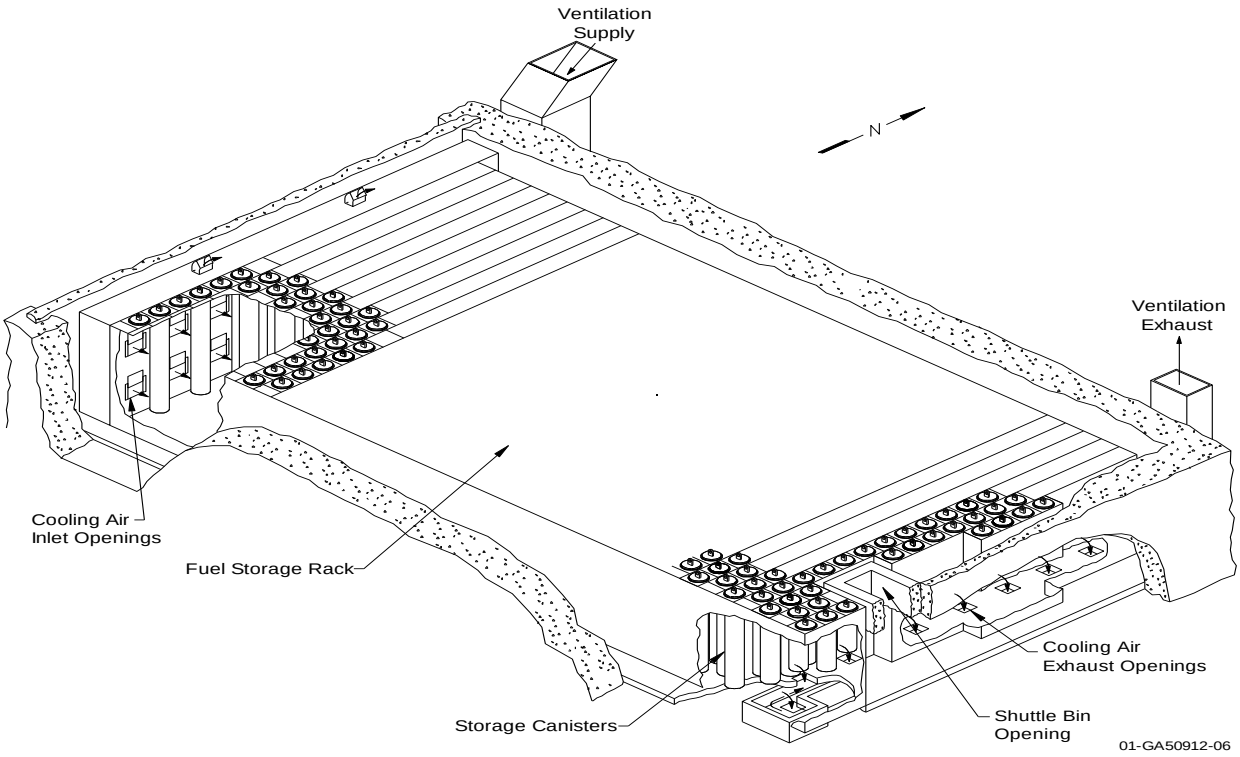

Figure 1 - Cut-away view of the IFSF fuel storage area.

A variety of carbon or stainless steel fuel storage buckets, baskets, or inserts are used to handle the fuel and serve as an inner storage container within the fuel storage canisters. No fuel storage arrangement results in a stack of fuel storage buckets/baskets more than three tiers high in a canister. These devices serve to maintain the credited fuel storage configuration and geometry during fuel storage and handling.

Some fuels are also stored in a fuel storage can. Fuel storage cans are generally utilized for fuels that may be damaged, or in cases where the fuel was cut or disassembled for post-irradiation examination for materials science research. Fuel where the cladding is removed, that may have degraded during extended underwater storage, or some processing residues are also stored in fuel cans.

The storage facility was originally intended for fuels that resulted in a sufficiently low neutron multiplication factor that the fuel canisters could be placed in the storage array in any arrangement, and the specific locations did not need to be restricted or controlled. Likewise, the neutron multiplication calculations performed at the time of facility startup confirmed that the entire array could be filled with canisters of the fuels originally intended for storage in any arrangement, crediting the controlled loading of fuel quantity and the geometric configuration within the storage canisters, and the storage canister spacing.

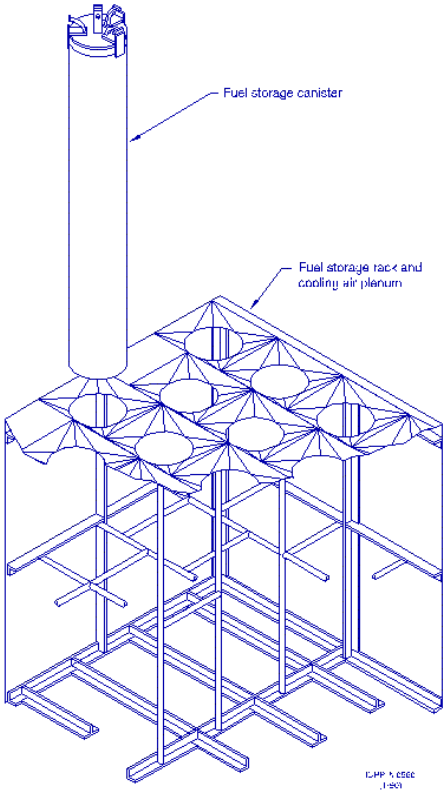

Figure 2 - Cut away view of the IFSF fuel storage rack and fuel storage canister.

The fuels the facility was originally intended to store are graphite based gas-cooled reactor fuels. Over time other fuels were desired to be stored in the IFSF that would result in an unsafe neutron multiplication factor if too many overall canisters of the more reactive fuels were placed in the

array, or if too many canisters or a more reactive fuel type/configuration were placed in a cluster. At this time a controlled arrangement of the array was analyzed that dictated the acceptable and required controlled storage arrangement. The total number of canisters of each fuel type to be stored was credited and controlled, and a specific arrangement was analyzed and controlled. This calculation is known as the "base case", which is updated each time a new fuel type or storage configuration is desired to be stored in the array, or if the total canister quantity of a current fuel configuration was desired to be increased. The base case models the empty positions of the array as containing an empty canister, and no fuel is allowed to be stored in the positions that are modeled as empty. The current base case model fuel storage arrangement is shown in Figure 3. In the figure north is at the top of the page with landscape orientation, and east is the right side. The cardinal directions will be used to refer to different directions within the array with this orientation throughout this document.

There are currently 13 empty storage positions at the perimeter of the array or at the northeast and southeast corners. These positions are not utilized due to limitations on crane travel or difficult viewing relative to the shielded window. There are eight empty positions in row 28, seven empty positions in row 30, 13 empty positions in row 32, and three empty positions in row 33 that could be utilized. These empty positions total 31 empty canisters. The current array neutron multiplication has approximately a 0.7% margin (0.007 delta-k_{eff}) below the subcritical limit of 0.95. This margin is insufficient to allow filling of the remaining empty 31 positions with any of the fuel types/configurations that are most likely to be desired to be stored at the IFSF. These fuels include MTR type fuels (designated as Aluminum-plate fuels in the fuel categorizations used in this document) or standard TRIGA fuel (low enriched [20 wt% U-235]), which is also designated the "group 2 TRIGA" category in this document. HEU TRIGA may also be referred to as "group 1 TRIGA". Calculations presented in chapter 6.1.6 show that filling these empty positions with AL-plate fuel or LEU TRIGA fuel results in exceeding the array acceptance criteria for subcriticality of 0.95 by approximately 2% and 3% respectively. This demonstrates that the full capacity of the fuel storage array cannot be utilized at the present time based on the arrangement and quantities of fuels that are currently stored in the array. Calculations presented in chapter 6.1.5 show the result of filling the open array positions with LEU TRIGA and AL-plate fuel. The ability to use these 31 additional positions represents the potential to store a significant amount of additional UNF. Each canister can hold more TRIGA elements than are present in an entire core, and the AL-plate canisters can store more than 20 kg of U-235.

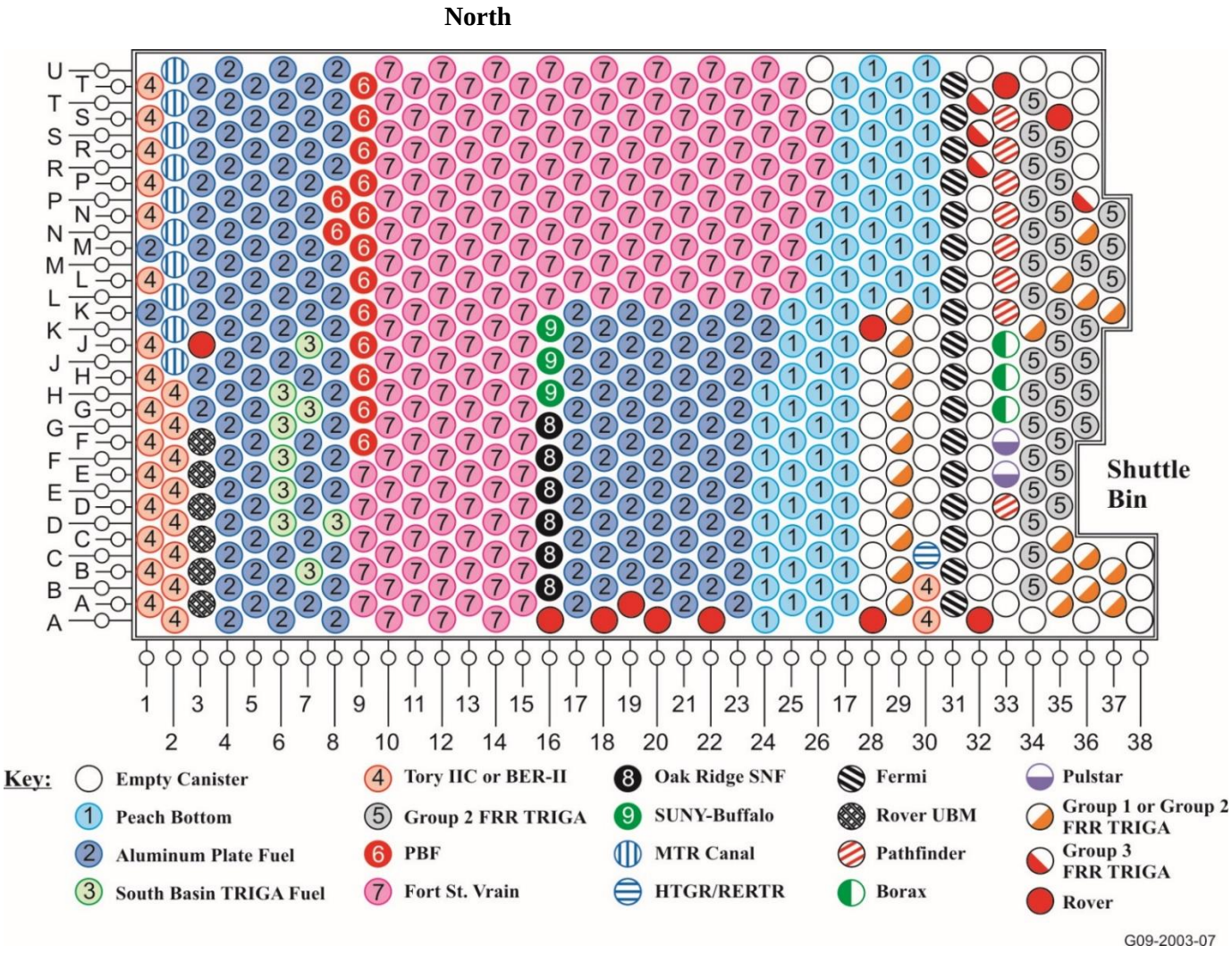

Figure 3 - Current IFSF fuel storage arrangement.
North is the side at row “U”, west is the side at row “1”. Directions relating to this orientation of the array are used throughout this document.

At the present time the fuel canisters are not stored in the array in an arrangement that minimizes the neutron multiplication factor for the overall array. The analysis of this document confirms this. What is unknown is the possible beneficial reduction in the array neutron multiplication factor that could result from potentially less reactive arrangements of the currently stored fuels, and whether a reasonable rearrangement or shuffling of some canister locations could result in a reduction that allows utilization of the remaining empty canister positions. Answering this question is one of the primary objectives of this new work. The IFSF presents a unique but finite resource for cost-effective interim storage of research and test reactor fuels that are owned or managed by the Department of Energy, and maximizing the potential utilization of the facility would serve as a valuable benefit in the management of UNF. Existing central dry storage facility resources are limited, and dry storage is the preferred interim storage method for UNF.

From a criticality physics standpoint, the IFSF system is a strongly coupled arrangement of interacting units. This is demonstrated by the fact that for all canister storage configurations considered, the concrete corner reflected, single canister neutron multiplication (typically 0.15 to 0.66, with the majority on the lower end) is drastically lower than the full array results for a given canister type (0.4 to 1.26). Similarly, at least a 10 by10 arrangement of canisters is required to begin to approach the k_{eff} of the full array for the better moderated fuel types.

2.3 Problem Constraints

Various aspects of the existing array modeling and practical limitations of the facility operation serve to limit which characteristics of the facility can be assumed to change.

The canister size, spacing, number of array positions is a constant that cannot change. This overall effort is to address the specifics of the current IFSF design from a practical standpoint that could be readily implemented operationally, and will not consider hypothetical improvements regarding these aspects, i.e. a re-design. Similarly, the analytic focus is on determining the potential benefit and optimization of a limited number of canister relocation movements, since a complete array re-arrangement is also not practical.

The existing empty wall and corner positions at the east side of the array will be assumed to be unavailable to receive a relocated canister. This is a constraint that complicates the optimization of the array with a goal to minimize the system neutron multiplication factor. The corner and edge positions present the greatest potential for neutron leakage and reduced interaction with other fissile material for fuels that are stored in these positions. Eliminating these positions as candidate locations for the more

reactive fuels removes some "easy" solutions to the array k_{eff} reduction goal, and complicates the process.

Precision is fundamentally limited by the inherent statistical uncertainty that exists with Monte-Carlo calculations of the neutron multiplication factor. In addition, many potential canister moves of fuel canisters with a similar reactivity will not result in a statistically significant impact to the array k_{eff} due to the global nature of the system behavior. The reality is that many of these canisters moves will result in a very small change to the overall system k_{eff} that is not discernable within the statistical uncertainty. The array system is effectively infinite in the horizontal directions, and the overall array k_{eff} can be fundamentally driven by a localized region of the array. The system k_{eff} is dictated by the most reactive general region of the array, unless a collection of fuel is present that could be perfectly arranged with consistent neutron multiplication through a broad region of the array center. Localized neutron multiplication will always be lower at the margins of the array, where neutron leakage is greater and interaction with other fissile material is reduced. In this way, the goal of minimizing the array neutron multiplication is similar to flux flattening efforts for a reactor core. Similar to placement of higher enrichment or fissile mass density fuels at the exterior of a core, the optimization of the IFSF array to minimize k_{eff} can involve placement of the more reactive fuels at the perimeter of the array. However reactivity of the fuels in the IFSF is primarily driven by the relative fissile mass and moderation present in the fuel. Therefore the placement of fuels relative to the moderation state of neighboring fuels also is impactful regarding the overall neutron multiplication. In this way the IFSF array can be thought of as a very large reactor core that is undermoderated, and undermoderated at a varying and inconsistent degree depending on location.

This effort is not concerned with the efficiency of solution within reasonable practical computer time constraints. The precision needed for the ultimate approximate solution is constrained by the statistical uncertainty of the MCNP models used as the baseline calculation method and by the inherent insensitivity to single canister moves that can be exhibited by a strongly coupled large fissile material arrangement that exhibits very "global" behavior. That is, the k_{eff} of the array is not strongly tied to any one single canister, but by a collective regional arrangement of canisters.

The goal is not to determine the optimal rearrangement to minimize the array k_{eff} for a "clean-slate" or complete rearrangement of the entire array. While this is a challenging problem, it is not operationally practical to perform such an activity. Relocation of more than 60 canisters is not a reasonable effort to operationally undertake. However if a significant reduction in array reactivity can be shown for a feasible number of canister relocation movements, this information can be important for potential improvement in the practical utilization of the facility.

Chapter 3.0 - Literature Review

A review of published works has not yielded research or analysis on systems similar to the considered large array of strongly interacting but widely differing fuel types, particularly with degrees of moderation that differ greatly. This is not surprising since the IFSF is a unique facility which contains a variety of fuel types that would be difficult to surpass elsewhere. The INL and the Savannah River Site are the two primary nuclear facilities in the United States that reprocessed DOE owned fuels, but the INL has had a greater focus on development of different reactor types. The INL has also received fuels from a wider variety of research reactors, many of which have been stored since reprocessing operations were terminated in the 1990s. The IFSF therefore contains some fuels which were never reprocessed, often due to a composition that posed reprocessing challenges. Some fuels date to the first few decades of reactor development when interesting and different reactor and fuel designs were being developed that differ from the current types that became more common.

The primary relevant result from the literature search was a conference proceedings paper related to improving efficiency of fissile material storage for the design of a new facility (Reference i). The paper considered the impact of a number of factors such as neutron poisons and fire suppression water in addition to arrangement of the physical units. The paper provides relevant discussion relating the impact of neutron capture and leakage to the criticality physics of storage arrangements, and provides an interesting consideration for storage cell unit fissile mass versus a larger overall storage volume. However the focus on fissile mass and the limited consideration of different moderation states reduces the overall applicability of the methods that were developed to the problem of IFSF storage optimization.

Much work does exist from the past nuclear criticality safety evaluations (CSEs) and the supporting analysis that have been performed for the IFSF. Older CSEs considered varying arrangements of the stored fuels after the point when fuels were received that would exceed the subcritical limit if they were assumed to fill the array. At this time the controlled, credited mapped array arrangement became required. However these past analyses that varied the arrangements did not consider the full variety and quantities of fuels that are currently stored. Recent IFSF analysis has not attempted to determine if the array can be filled, and has not been tasked with determining better arrangements of the fuels based on the current stored fuels or additional expected fuels.

Some past work however has provided helpful insight into determining alternate methods by which to consider the interaction problem posed by the IFSF. Specifically, the Limiting Surface

Density developed by J. T. Thomas (Reference ii), and simplified methods for considering interaction developed by H. K. Clark (Reference iii) have inspired this attempt to determine an empirical model to determine the k_{eff} of the array based on the fuel types and arrangement.

For example, the "criticality" factor of Reference iii relates interaction as a function of spacing, whereby the relationship between unit fissile mass and allowed spacing on k_{eff} can be determined. This has been shown to be the case for the condition where all the units are not moderated, or all the units are moderated. These hand calculations do require use of different characteristic constants that vary depending on the specifics of the problem. These constants have been determined ahead of time based on the results of experiments or calculational analyses.

These methods however raised the question on whether factors or similar characteristic constants could be determined to relate the mixing of moderated and unmoderated stored units where the unit spacing is not variable but instead is held constant. In this case a relationship between the known unit fissile mass and moderation could be established to determine k_{eff}. Supporting analysis will be needed to determine the values for the constants that will be used to account for the interaction effect between the fuel storage canisters with different fissile mass and moderation states. Determination of these constants could allow the development of an empirical model that could treat coupling of a multi-group problem in a practical way. The initial analysis performed in chapter 6.1 is an attempt to determine the impact of mixing of fuel canister types with different fissile mass and moderation states, and to determine the weighting factors that could be applied to treat the interaction effect correctly.

Chapter 4.0 - Detailed Background

4.1 Nuclear Criticality Safety

Nuclear criticality safety is one of the primary safety disciplines affecting the operation of a nuclear fuel storage facility. Nuclear criticality must not occur except when desired and controlled in a nuclear reactor, which is designed to regulate the reactivity increase and operating power level, provide sufficient heat removal to ensure integrity of the fuel materials, and provide shielding of the substantial quantities of neutron, gamma, and neutron capture-gamma radiation. The fuel storage array of the IFSF must be demonstrated to be operated in a manner such that the potential for an accidental criticality event is sufficiently low as required by Department of Energy orders and national standards. Subcriticality must be maintained for all normal and credible upset operating conditions.

The determining factor dictating whether the arrangement is adequately subcritical is whether the system effective neutron multiplication factor, k_{eff}, remains below an established subcritical limit, k_{safe}. The neutron multiplication factor is effectively a ratio of the neutron production from fission to neutron loss from capture and leakage over the three dimensional geometry of the physical fissile system. The k_{eff} value can also be described as the ratio of the number of neutrons present in the system over a set unit of time to a subsequent identical unit of time. In this way, a supercritical system with a k_{eff} >1.0 is increasing in power (and neutron population) over time, a system with a k_{eff} of <1.0 is subcritical and is decreasing in power and neutron population, and a system with a k_{eff} of exactly 1.0 is at a constant power level (with delayed neutrons considered). The k_{safe} for the IFSF is considered to be 0.95, which provides a degree of minimum required safety margin. An additional validation bias and statistical uncertainty are separately applied to the calculation k_{eff} result with two-sigma uncertainty for the purposes of demonstrating subcriticality for the safety basis.

Nuclear criticality safety of a fissile material system is often discussed in the context of nine primary parameters that impact the k_{eff} of the system. These parameters can be controlled or restricted by operational requirements, through design of physical equipment, or may be inherent to a process.

4.2 NCS Parameter Discussion

4.2.1 Fissile Mass

Fissile mass is one of the NCS parameters that varies significantly among the stored fuel types and allowed canister storage configurations. This parameter contributes significantly to the overall array neutron multiplication. Sufficient fissile mass is required for criticality to be possible. For an optimized single unit criticality is possible with a little under 1 kg U-235 with idealized moderation, geometry, and reflection. For unmoderated oxide or metal tens of kilograms of U-235 are required. Most of the IFSF storage configurations contain between 4 and 12 kg U-235 for canisters with hydrogen moderation and significant graphite moderation and may contain 30 kg U-235 or more for unmoderated metallic fuels. Some canisters of metallic fuels may store up to 80 kg U-235, which is only possible from the reduced U-235 density in the alloys and the controlled geometry of the fuel pins. The ability to store these significant masses of fissile material shows the inherent contribution to controlling k_{eff} that occurs from the storage geometry, generally undermoderated state, and the leakage that occurs due to the spacing between canisters. This spacing effectively decreases the fissile density within the array. The fissile mass per canister can also be thought of as the fissile density loading per canister since all canisters have the same interior volume due to identical diameters and the fact that most fuels fill the majority of the canister diameter and height. The amount of fissile mass that can be stored in a canister or in a general region of the array is closely tied to the degree of moderation that is present in a canister or in a localized region of the array, which dictates the utilization of the fissile mass.

4.2.2 Moderation

Moderation is also an NCS parameter that is a primary controlled aspect of the storage array that significantly impacts the array neutron multiplication. The factor of moderation impacts the fission process due to the fact that lower energy neutrons are much more likely to be captured by fissile isotopes and cause fission than high energy neutrons. Neutrons released from fission have an average energy of ~2 MeV which cause a fission from interaction with a fissionable isotope a much smaller percentage of the time compared to low energy neutrons interacting with fissile isotopes, i.e. high energy neutron are much less likely to be captured by a fissile isotope. In this document the bin labels of “Fast” is applied to neutrons with an energy greater than 100 keV, “thermal” neutrons have an energy less than 0.625 eV, and epithermal neutrons have an energy between fast and thermal. True “thermal” neutrons have an average energy at equilibrium with the temperature of the materials of the system, over a Maxwellian distribution. Thermal cross-sections are generally specified at 0.025 eV.

Moderating materials are those materials that cause a reduction in neutron energy through neutron interaction or scattering. Elastic and inelastic collisions result in a decrease in the energy of the impinging neutron. A greater percentage of the neutron energy can be imparted to the target atom in a single collision with lighter isotopes than can be with heavier isotopes. Typically low atomic number ("Z") elements are considered better moderators than high Z materials. The single best moderator is a free hydrogen atom since it is the lightest isotope, closest to the mass of a neutron. However some materials or heavier elements such as deuterium and carbon can result in systems with lower minimum critical masses than hydrogen, due to the fact that there is less parasitic neutron capture with these elements and isotopes compared to hydrogen. Hydrogen has a small but non-trivial neutron capture cross-section.

The primary moderators in the IFSF storage array include the carbon present in the graphite and carbide based fuels, the hydrogen present in zirconium hydride based fuels, any water that is modeled with some fuels, and some epoxy that is modeled with some fuels.

While sufficient moderation for criticality is present with many of the graphite based fuels, they are safe instead by spacing or interaction control provided by the canister configuration. Most of the other fuels are intended for use in light water reactors, and when stored in a dry configuration are safe due to the undermoderated state of the system. The mixing of different inherently moderated fuels such as graphite (gas cooled reactor fuels) and TRIGA fuels (Zr-hydride fuels) with other fuel types that are stored in a more dense state compared to what would occur in a light water reactor results in the potential to challenge an acceptable subcritical safety limit for the fully loaded array. The moderation or energy state of the array is therefore a key controlled factor.

4.2.3 Interaction/Spacing

Similar to moderation, interaction or spacing is a primary NCS controlled parameter that ensures subcriticality of the IFSF array.

Spacing and array pitch is constant throughout the array, which is modeled as a triangular-pitch arrangement with a 22.5 inch pitch. The edge-to-edge spacing is therefore held constant between all canisters. From this standpoint interaction is constant within the array between canisters, from a geometric standpoint. Canisters are of an essentially identical diameter and height, and the stored fuels generally fill a similar fraction of the canister diameter. Likewise, most fuels are modeled at the full canister height or are considered to be stacked to nearly the full canister height. For example, the solid angle for interaction between any given canister and the neighboring canisters is constant. Calculations that follow will relate the height of the fuel storage array to an equivalent number of canister rows,

which gives some insight into the degree of leakage that can occur over the top surface based on the results of the partial array calculations. The number of canisters that must be present for an effectively infinite system to result in the radial direction varies depending on the moderation state of the canisters. An effectively infinite system is one in which a fission neutron produced near the center of the fissile system has a nearly zero probability of reaching the exterior border of the system without being absorbed by either fissile or not fissile atoms. That is, the non-leakage probability over much of the fissile system is 100%.

4.2.4 Geometry/Shape

Geometry and shape can be thought of from both the standpoint of within the fuel storage canisters, and the geometry of the overall array. Geometry and shape is controlled in the IFSF array through the use of the various storage devices to contain the fuel. For a single-unit the geometry dictates the neutron leakage of the system, such as with a favorable diameter cylinder that is too narrow in diameter to allow sufficient interaction distance with the moderator for fission energy neutrons to be sufficiently thermalized. In the case of coupled systems of interacting units such as the IFSF array, the geometry or size of the unit impacts the degree of interaction for a given unit spacing. Ultimately the canisters themselves restrict the geometry of the fuel unit to the canister internal diameter, which is constant for all fuels. The canister diameter relative to the edge-to-edge spacing between canisters (controlled by the designed array pitch) limits the degree of interaction and the effective overall fissile density loading at a large scale.

This parameter does not vary significantly since most of the stored fuel types occupy the majority of the canister diameter for the modeled configuration.

The overall array is effectively infinite in the radial directions, but not axially, which is important when considering the impact of reflection. From the standpoint of the overall array geometry this parameter is closely related to interaction and leakage from the array.

4.2.5 Enrichment/Isotopics

The criticality physics of a system is influenced by the enrichment of the fissile material. The enrichment dictates whether a homogeneous or heterogeneous configuration of the fissile material and other materials such as moderators can potentially be more reactive, due to the impact of fast fission with U-238 relative to the potential for resonance absorption (resonance self-shielding). The presence of a significant quantity of U-238 can also increase the thermal absorption of neutrons for a well-moderated system, that is, a loss of the neutron instead of a neutron-producing fission capture.

The majority of the fuels modeled are highly enriched uranium (HEU). For HEU a homogeneous treatment is more conservative towards producing a higher k_{eff} than a heterogeneous treatment by increasing thermal utilization. However, most fuels are modeled discreetly, where the undermoderated aspect of the array could increase the impact of resonance absorption and fast fission. However these factors have much less of an impact with HEU fuels. Some fuel models also contain U-233, and a few models contain small amounts of Pu-239, generally neglecting the non-fissile (even number atomic weight value) Pu isotopes. Note that burnup of the fuels is not considered in the models, other than from a conservative standpoint. The fuel models consider either beginning of life fissile loading or consider beginning of life U-235 values with end of life U-233 values for the thorium converter fuels.

4.2.6 Density/Concentration

Density and concentration are not factors that significantly impact the physical IFSF system or the neutronics modeling of the arrangement. Density and concentration are often related, as density is considered regarding the bulk density of the fissile material, such as for oxides or metal, while concentration concerns mixtures of the fissile material with non-fissionable elements. The concentration of a uranium solution dictates the degree of moderation of system, and for example overmoderated systems cause additional thermal absorption by hydrogen or other isotopes with appreciable thermal absorption. The fuel meat matrices (e.g. UO_2, U-AL, U-ZrH) are typically modeled at a full theoretical density to envelope the expected density of the material. Fuels that are modeled in a degraded state are modeled at an optimal concentration (height for the container) for the other materials that may be present with the fissile material. For mixtures of fissile material and moderator, concentration is related to moderation, which dictates whether an undermoderated or overmoderated state is present. For the IFSF, nearly all fuel arrangements are undermoderated, based on the limited quantities of moderator present and the significant amounts of fissile material considered in the storage containers.

4.2.7 Volume

The volume of the individual canisters and the overall array volume are constant. The parameter of volume is related to geometry, as there is maximum volume that is favorable for maintaining subcriticality, in that insufficient moderation or excessive neutron leakage take place. The constant volume aspects of the canisters means that the degree of geometric neutron interaction between canisters is fixed for a system of interacting units with fixed spacing. The constant volume aspect of the canisters and the fact that most of the fuels fill or are stacked to the majority of the

canister height and diameter allows the canister fissile and moderator masses to also be treated as fissile density or moderator density at the macroscopic scale.

4.2.8 Absorbers

Elements that have a significant neutron capture cross-section are important in the control of a fissile material system. The presence of absorbers is fairly constant across all the fuel storage canister arrangements present in the storage array as modeled. As expected of a nuclear reactor fuel, the structural materials such as cladding used in the fuel are intended to minimize neutron losses from the presence of absorbers. Most fuels are constructed of neutron transparent or materials with a minimal neutron absorption cross-section such as zirconium, aluminum, graphite, and oxide and carbide compounds. Some fuels have stainless steel cladding, which is considered a neutron absorber due to the iron and nickel present, but the cladding is present in a thin layer that minimizes the effect.

A much more substantial contribution to neutron absorption is from the steel of the IFSF canisters that are modeled in the neutron transport calculations for all positions, and the steel of many of the buckets/baskets and fuel cans is modeled as well. Therefore the degree of neutron absorption present throughout the array is fairly constant. The steel present from buckets/baskets and fuel storage cans is most often modeled with the more reactive configurations in an effort to reduce the reactivity for the higher neutron multiplication fuels. For example, fuels modeled in fuel storage cans are generally modeled in a homogeneous condition (e.g. the fuel is not discreet pins) with some moderation to envelope a degraded state, but modelling the additional steel of the fuel storage cans offsets this impact somewhat.

4.2.9 Reflection

Reflection will be shown to be an important aspect that impacts the neutron multiplication of the IFSF array, or more specifically, the limited axial reflection as it relates to neutron leakage. While the IFSF array has been previously shown to be effectively infinite in size in the two horizontal directions (East-West/North-South, or directions perpendicular to the canister major axis), new analysis in this document will show the impact of leakage in the axial direction on maintaining a subcritical system. The walls, floor, and ceiling of the array are an infinite or near-infinite thickness of concrete, which is an effective reflector for neutrons. The primary elements of concrete are sufficiently high atomic mass that they can cause a significant degree of high angle (back) scattering while preserving much of the overall neutron energy. The reflection effectiveness of concrete is also increased due to its density and the resultant overall atom density, and the fact that the elements that comprise concrete do not exhibit significant thermal neutron absorption. For these reasons, the

effectively-infinite thickness of concrete is approximately twice that of full-density water. The shielding wall thickness of the IFSF exceeds an effectively infinite thickness (approximately 60 cm) for concrete for fission energy neutrons.

While the reflection is constant around each given face of the array, this analysis will show that the impact of neutron leakage and importance of the reflector varies depending on the moderation state of the fuels in a given localized region.

4.3 MCNP Calculations

The MCNP calculations in this analysis are performed with MCNP5 Version 1.51, with the ENDF/B-V cross section data set. The ".50c" cross section data was used with all isotopes with the exception of iron which used ".55c", and which corrects a known error with the "0.50c" iron cross-section data. The calculations are performed on the Idaho Cleanup Project (ICP) workstation cluster of Hewlett Packard 585 G6 machines with Advanced Micro Devices Opteron processors running Red Hat Enterprise Linux. The MCNP code is configuration controlled on this system and is verified and validated. This is the same computing system, code, and cross section data set that have been used for a number of years to provide the NCS calculations for the IFSF safety basis documents.

Consistent with the current process regarding IFSF NCS calculations, a validation area of applicability (AOA) bias of 0.05 is applied to calculations that involve the full array with a mixed arrangement of fuels. This AOA bias addresses the validation challenges that this mixed arrangement of varied fuels presents, and which also results in a system where an epithermal neutron spectra dominates. There are far fewer benchmark experiments pertaining to epithermal systems as compared to thermal and fast systems, and there are no benchmark experiments that remotely consider such a diverse collection of fuel compositions, types, and fissile isotopes present. Calculations with single fuel types, or three or fewer fuels, will be reported at nominal values without bias to simplify comparisons.

The kcode calculations that involve mixed arrangements of fuel are run with 5,500 neutrons per generation, for 550 generations with 70 initial generations skipped to allow for source convergence. The resultant 2,640,000 source neutrons typically yield a sigma of 0.0005 or less for the calculation statistical uncertainty of the k_{eff} value final answer.

4.4 IFSF Stored Fuels

Table 1 presents a listing of the 26 fuel model configurations considered in the current IFSF storage arrangement. Some fuel models are a variation with the same fuel type and storage configuration but with small quantities of water moderation added. The table includes the number of canisters considered in the current storage arrangement for each type, the general fuel matrix composition, and whether the model considers a discreet fuel geometry or a homogenized fuel unit. The fuels are listed in decreasing order based on the number of canisters present. Generally the fuels stored in fuel storage cans are considered as a homogenized unit. The fuels present a wide range of differing research and test reactor fuel types of metallic, oxide, hydride, and carbide compositions. Graphite gas-cooled conversion reactor fuels and uranium-aluminum plate type MTR fuels compose the two general fuel types that are present in the array in the largest quantities. LEU TRIGA is stored and modeled in different six-position storage buckets that allow either five or six elements per position.

Table 1 - IFSF Fuel Models – Current Array Storage

Modeled Fuel	Number of Canisters	Fuel Matrix	Modeled State
Fort St. Vrain	188	Th/U Carbide pins in graphite	Discreet elements
AL Plate	157	U-AL metal	Discreet elements
Peach Bottom	63	Th/U Carbide in graphite	Homogenized element
LEU TRIGA (group 2, 6x5)	32	$U\text{-}ZrH_{1.65}$	Discreet elements
Tory-IIC	23	UO_2, Y_2O_2, ZeO_2 in BeO	Homogenized in fuel storage can
HEU TRIGA (group 1)	23	$U\text{-}ZrH_{1.65}$	Discreet elements
Fermi Driver	16	U-Mo metal	Discreet pins in fuel storage cans
PBF	14	UO_2, CaO, ZrO_2	Discreet Rods
Rover Parka	11	UO_2 in Graphite	Discreet rods in tubes
MTR Canal	10	UO_2 and polyethylene	Homogenized in fuel storage can
South Basin TRIGA (TRIGA-AL)	9	$U\text{-}ZrH_{1.0}$	Homogenized slurry in fuel storage can
Peach Bottom-mod	8	Th/U Carbide in graphite	Homogenized element
Pathfinder	8	UO_2 cermet	Discreet assemblies
Oak Ridge Canistered	6	U, Pu metal and graphite	Homogenized in fuel storage can
TRIGA-IN (Group 3, MPR)	4	$U\text{-}ZrH_{1.65}$	Discreet elements
Pulstar-dry	3	UO_2	Discreet assemblies
Pulstar-mod	2	UO_2	Discreet pins in fuel storage cans
Rover UBM 4	3	Al_2O_3, U_3O_8, and graphite	Homogenized in fuel storage can
Borax V	3	UO_2 Cermet	Discreet plate fuel elements
BER-II (Berliner TRIGA)	2	$U\text{-}ZrH_{1.0}$	Homogenized elements
Rover UBM1	1	Al_2O_3, U_3O_8, and graphite	Homogenized in fuel storage can
Rover UBM 2	1	Al_2O_3, U_3O_8, and graphite	Homogenized in fuel storage can
Rover UBM 3	1	Al_2O_3, U_3O_8, and graphite	Homogenized in fuel storage can
Fermi Driver-moderated	1	U-Mo metal	Discreet pins in fuel storage cans
LEU TRIGA (group 2, 6x6)	1	$U\text{-}ZrH_{1.65}$	Discreet elements
HTGR (General Atomics)	1	$U\text{-}ZrH_{1.65}$	Homogenized in fuel storage can
Total	591		

Table 2 presents the same listing of fuel models but includes data on the fissile isotopes present, the enrichment of the uranium, the total fissile mass present per canister, and the type and quantity of moderator present in the canister. HEU fuel is the predominant enrichment for the array, though FSV and Peach Bottom fuels that are present in large numbers both have an appreciable amount of U-233. The values show the much greater quantities of carbon moderator that are able to be stored compared to hydrogen moderator. This is because the maximum energy that can be lost by a neutron collision with hydrogen is 3.5 times greater than with a collision with a larger carbon atom. Also, a for a given mass of hydrogen or carbon the hydrogen atom density will greatly exceed the atom density of carbon in graphite, again due to the much smaller and lighter atom. This relationship is exemplified by a comparison of the physical arrangements of graphite moderated reactors compared to light water reactors. The physical core of a graphite reactor must be much larger than a light water reactor to ensure geometric buckling is sufficiently low, and a much larger mass of graphite must be present comparted to water (integral to the core) to ensure sufficient thermalization. This inherent variation can be seen in the difference in the diffusion length, migration area, and neutron age between light water and graphite.

Table 2 - IFSF Fuel Model Fissile Mass and Moderation Values

Modeled Fuel	Fissile Isotopes	Enrichment	Total Canister Fissile Mass (kg)	Moderator Presence (kg)
Fort St. Vrain	U-235, U-233	93	U-235: 5.410 U-233: 1.120	Carbon – 282.0
AL Plate	U-235	93	32.700	None
Peach Bottom	U-235, U-233	93	U-235: 2.790 U-233: 0.444 Pu-239: 0.012	Carbon – 509.2
LEU TRIGA (group 2, 6x5)	U-235	20	3.510	Hydrogen – 3.359
Tory-IIC	U-235	93	5.370	BeO – 77.0 kg Be
HEU TRIGA (group 1)	U-235	70	11.508	Hydrogen – 3.066
Fermi Driver	U-235	26	86.688	0.715 kg H
PBF	U-235	18.5	7.881	None
Rover Parka	U-235	93	25.200	Carbon – 190.0, Hydrogen – 1.48
MTR Canal	U-235	31 to 93.4	1.960	Water and polyethylene: H – 4.107, C – 27.97
South Basin TRIGA (TRIGA-AL)	U-235	20	4.788	Water and Zr-H; H – 3.18
Peach Bottom-mod	U-235, U-233	93	U-235: 2.790 U-233: 0.444 Pu-239: 0.012	Carbon – 509.2 and 5 liters of water (H-0.55)
Pathfinder	U-235	93.5	7.688	None
Oak Ridge Canistered	U-235, U-233, Pu-239	97	U-235: 10.920 U-233: 0.360 Pu-239: 4.680	Carbon – 234.0
TRIGA-IN (Group 3, MPR)	U-235	93	13.776	Hydrogen – 2.419
Pulstar-dry	U-235	6	15.908	None
Pulstar-mod	U-235	6	12.086	Water, H-2.956
Rover UBM 4	U-235	93	51.072	H – 0.381, C – 1.02
Borax V	U-235`	93	14.600	None
BER-II (Berliner TRIGA)	U-235	44	2.635	Hydrogen – 1.6
Rover UBM1	U-235	93	28.380	Carbon, water, and hydrocarbon; H – 3.61, C – 39.2

Modeled Fuel	Fissile Isotopes	Enrichment	Total Canister Fissile Mass (kg)	Moderator Presence (kg)
Rover UBM 2	U-235	93	9.936	Carbon, water, and hydrocarbon; H – 3.61, C – 39.3
Rover UBM 3	U-235	93	85.116	H – 0.381, C – 1.02
Fermi Driver-moderated	U-235	26	77.056	Water. H – 2.38
LEU TRIGA (group 2, 6x6)	U-235	20	4.212	Hydrogen - 4.031
HTGR (GA)	U-235	100	3.915	Water and hydrogen in ZrH; H – 2.661

Based on the fissile mass values and moderation values presented in Table 2, the modeled fuels can be considered according to the following groupings presented in Table 3. In the context of this table the "high' moderation fuels are relative to the standpoint of a dry storage array and relative to the metallic and oxide fuels that provide no moderation. When the reactivity impact is assessed some of the fuels merit additional discussion. The Fermi and Rover UBM 3 and 4 arrangements are fuel models with particularly high fissile mass values. Similarly, the Peach Bottom-mod, MTR Canal, and HTGR fuel models result in reactivity values that approach those of the high fissile mass-high moderation fuels due to the fact that these fuels models consider homogenized, degraded fuel uniformly mixed with moderator. Note that "high" fissile mass threshold for the high fissile mass/high moderation fuels is a much lower cut-off (~10.0 kg U-235) than the "high" fissile mass fuels that are not moderated (~32 kg U-235).

Table 3 - IFSF Fuel Model Categorizations

Category	Low fissile mass – low moderation	High Fissile mass – low moderation	Low fissile mass – high moderation	High fissile mass – high moderation
Applicable Fuel Models	Tory-IIC PBF Pathfinder Pulstar-dry Borax V BER-II	AL Plate **Fermi Driver** **Rover UBM 4** **Rover UBM 3** **Fermi Driver-moderated**	Fort St. Vrain Peach Bottom LEU TRIGA (group 2, 6x5) **MTR Canal** South Basin TRIGA **Peach Bottom-mod** LEU TRIGA (group 2, 6x6) **HTGR**	**HEU TRIGA (group 1)** **Rover Parka** **Oak Ridge Canistered TRIGA-IN (Group 3, MPR)** **Pulstar-mod** **Rover UBM1** **Rover UBM 2**
Number of canisters in current storage arrangement	53 canisters	178 canisters	312 canisters (343 when 31 in-service empty are filled with LEU TRIGA)	48 canisters

Fuels that are **bolded** result in a k_{eff} greater than or equal to 1.0 when that fuel type alone fills the entire array. There are 88 of these canisters present in the currently analyzed fuel storage array. See chapter 6.1.1.

The categorization of the fuel model fissile mass and moderation values will be shown to correlate well with the calculations performed in chapter 6.1.1 that fill the entire array with a single fuel model configuration at a time. The values of moderator present in the model are the cause of the resultant neutron spectra of the fuel model system as seen by the EALF and percentage of fissions caused by thermal neutrons. Much of the fundamental supporting analysis of this document will focus on six fuel types that represent the predominant types of quantities of fuels present in the IFSF fuel storage array. AL-plate is present in large quantities and is a high fissile mass-low moderation fuel. Fermi is a very high fissile mass and low moderation fuel that impacts the reactivity of the east end of the array where k_{eff} is highest. FSV and LEU TRIGA are fuels present in large quantities with significant moderation but lower fissile mass. HEU TRIGA is the high fissile mass and high moderation fuel that is present in the largest quantities. Peach Bottom fuel is also present in significant quantities as well and is sometimes considered as well.

Figure 4 – presents a comparison of U-235 equivalent mass per canister to hydrogen equivalent mass per canister for the IFSF fuel canister models. Labelled values are the k_{eff} for the array when filled entirely with the same fuel model, as determined in chapter 6.1.1. The U-235 and hydrogen equivalence relationships are determined in chapter 6.1.2.1. The figure shows that either higher amounts of fissile mass or higher quantities of moderator result in a greater k_{eff} for the array, and which typically exceeds a subcritical acceptance criterion. Significant quantities of both fissile mass and moderator result in very high k_{effs} if these canister arrangements were to fill the array. Limited numbers of these fuel canister arrangements can be tolerated in the array, and only in restricted arrangements, before an excessively high k_{eff} results. The figure shows that much greater quantities of fissile mass can be stored if the fuel is lacking in moderation. The moderated single-fuel empirical model is developed to determine the balance of fissile mass and moderation that results in a given k_{eff}, and the entire array empirical model is developed to accurately determine the impact of mixing fuel canisters of different fissile mass and moderator contents. The imperfect direct relationship of fissile mass or moderation to the single canister array fill k_{eff} value results from the impact of geometry and homogeneity effects from modelling larger homogeneous fissile units in some cases, the presence of greater quantities of steel in some models, and the fact that a few models do not have the moderation present uniformly around the fuel. That is, a few fuel models such as Fermi model the water as present in the bottom of a fuel storage can of pins, as opposed to uniformly dispersed amongst the fuel as is the case with the homogeneous models. The impact of these variations will be addressed in the empirical model development.

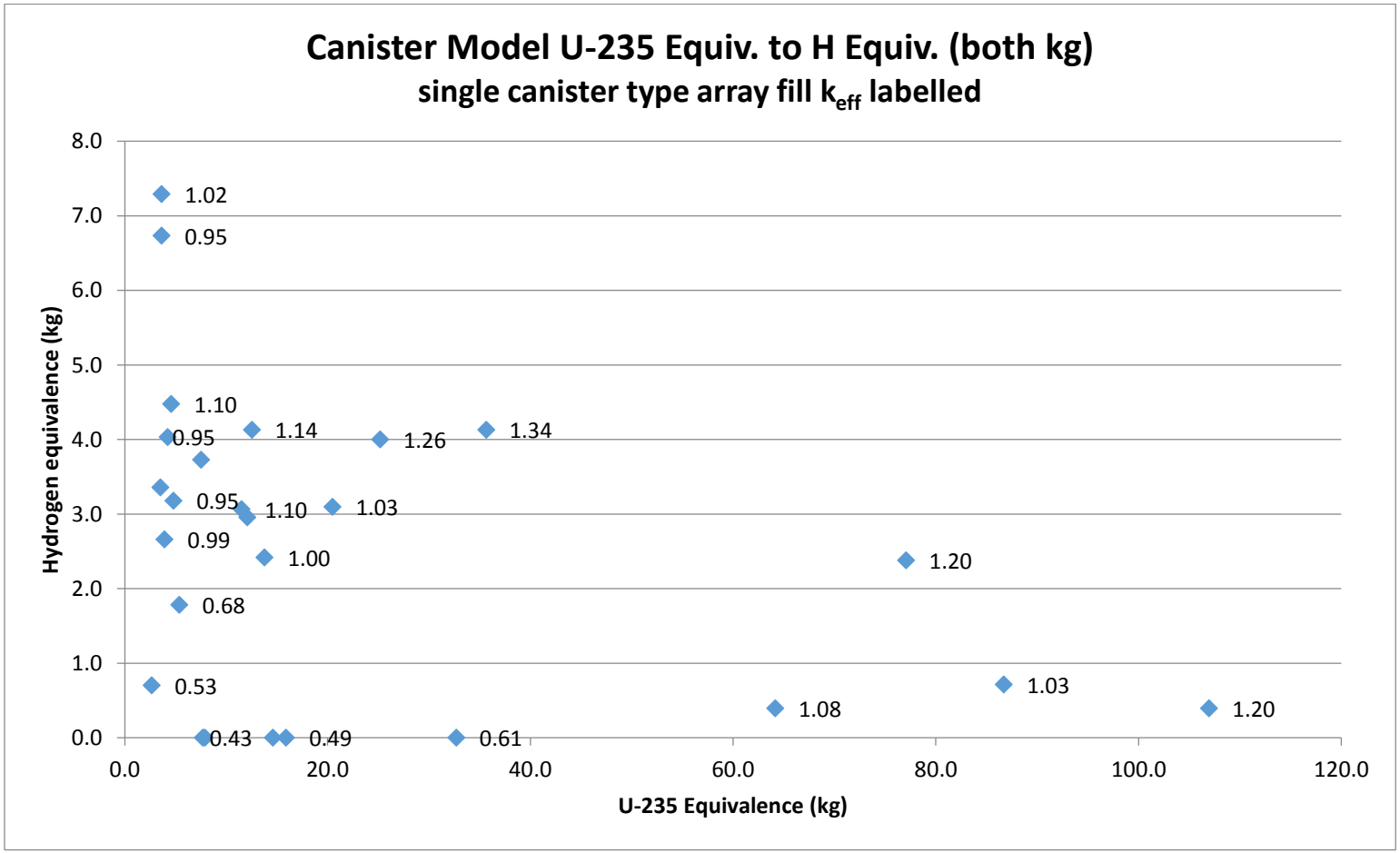

Figure 4 – Comparison of U-235 equivalent mass per canister to hydrogen equivalent mass per canister for the IFSF fuel canister models.

Labelled values are the k_{eff} for the array when filled entirely with the same fuel model, as determined in chapter 6.1.1.

4.5 Multiple-Objective Optimization

The fundamental problem of optimizing the IFSF arrangement to reduce k_{eff} is a complex problem due to the number of variables that are present. The fact that there are 26 different fuel storage canister configurations, varying in count between one and 188, with a total of 636 possible storage positions, means that the number of possible arrangements is extremely large. For example, if 26 unique canister swap movements were performed using all the (26) unique fuel models in the array, approximately 10^{72} different arrangements are possible with the 636 potential canister positions. The possible arrangements among these variables comprise the feasible design space, or the space that contains all possible solutions (optimal or not). This multiple-objective optimization problem can be considered a nondeterministic polynomial time, or NP-complete problem. The problem also has characteristics of a combinatorial optimization problem. There are constraints on the problem in the form of maintaining the existing number of canisters, as well as the fixed arrangement spacing, shape, and quantity of storage positions.

In light of the nature of the problem, the solution method will use approximation, randomization, and heuristics guided by the understanding of the criticality physics will be employed in the solution algorithm. In practical terms it is not possible to find one true absolute optimal result for the problem. This is partly due to the reality of the manner in which the results are confirmed. The MCNP calculations which are used to ultimately confirm the k_{eff} of the array have a statistical uncertainty associated with their results. Even if an experiment could be run to confirm the arrangement, measurement or experiment uncertainty would mean that confirmation of a single absolute solution would not be possible. For a system with such true global behavior and complex interplay of many units, the impact of some minor perturbations is indistinguishable. For example, the impact a minor shift in location of two canisters with a similar reactivity, or fissile mass or moderation state may not be significant to the overall global reactivity of the array. Because of this fact, and that fact that for some NP-complete problems only an approximate solution can be found in reasonable time-frames, a search for approximate solutions will be employed. Similarly, a gradient based approach to determine a precisely optimal solution is not possible based on the nature of the problem, and because a heuristic approach can be employed to capitalize on the innate interaction effects between the different mass and moderation states. This method does require the initial up-front analysis to determine the heuristic parameters to be applied, but this initial analysis is of a manageable degree for this problem.

Stochastic aspects or randomization of the search will be utilized to reduce the possibility that a preferred movement or sequence is missed, particularly due to heuristic restrictions or preferences that may be overly weighted. This could lead to a result that involves a localized optimum instead of the global optimal solution. However, the nature of the empirical model that will be developed also helps ensure that local minima are not found at the expense of the global array k_{eff} minimum. The empirical model will display a k_{eff} result that is based on the impact of the neighboring canisters, that is, it will show the canister centered at the location of the maximum k_{eff} or fission density. This ensures that if a set of canister movements creates the condition where the location of the array maximum k_{eff} region has changed, that this is immediately recognizable. That is, if a sequence of movements changes the region that was formerly producing the array maximum regional k_{eff}, the movements could have created a new worst maximum somewhere else, or if the movements are truly an improvement then a new, lower regional k_{eff} value becomes the new maximum. Finding this lowest possible regional k_{eff} value for a given number of canister movements is the ultimate goal.

While there are a huge number of permutations by which the set of 26 canister types of varying quantities could be placed in the array, some characteristics of the system greatly reduce the number of feasible solutions. For example, if the eastern third of the array is known to drive the reactivity of the array and effectively produce the k_{eff} result, then canister movements performed only in the less reactive region of the array will not reduce the array k_{eff}. Manipulation within or between low reactivity regions of the array will not have an effect, and will not produce a detectable change in the MCNP calculation result. Likewise, it is already known that some fuel types, or a single reactive fuel type, cannot be grouped together beyond a certain extent without producing a large k_{eff}. Obviously moving these fuels closer together by a significant degree with not aid in minimizing the k_{eff}. Other innate aspects that apply include placing more reactive fuels near the edge of the array where the potential for interaction with other fuel is reduced. These conditions can be applied in the form of constraints or heuristic guides in the solution algorithm to reduce the number of potential permutations searched and to increase the speed of the process. The supporting calculations that will be initially performed will both aid in development of the empirical model and serve to determine and support the heuristic conditions (applied rules) that comply with the understood behavior of the system. The heuristic constraints and preferences will be implemented by prohibiting or biasing certain canister relocation movements for the array rearrangement permutations performed on the spreadsheet empirical model.

Ultimately, the optimization method applied consists of a hybrid of the Tabu metaheuristic (Reference iv) with a stochastic approximation component. A Tabu search metaheuristic is an

enhancement of a local search. Changes considered in the search that have been determined to not result in an overall improvement regarding the objective, or that are already known to not have a desired result, are restricted from further consideration, or are "taboo". A number of canister type movements or movement locations are known, or are confirmed, to not result in a reduction in k_{eff}, and are therefore considered the "taboo" movements that are not further considered. The method seeks to avoid a trap of a local minimum by exploring changes generally adjacent to the location of concern, and by allowing changes that are not a direct immediate improvement if no changes that could generate an improvement remain. Due to the nature of the spatial aspects of this problem, a more broad stochastic aspect will investigate the wider ranging possibilities. For example, it is generally preferred to break up grouped collections of more reactive canisters or relocate more reactive canisters away from the center of the array, but the specific canister to swap with, or more precisely the best canister fuel type to replace the removed canister is not as certain, and which requires more permutations to investigate. The randomized aspect accomplishes this and assists the algorithm in determining a best approximate solution. The optimization method attempts to strive for a solution that provides for significant improvement, but in a reasonable amount of time, compared to the truly complete optimal or absolute best solution. Hence the "approximation" aspect, since a brute force or exhaustive search would be prohibitively time consuming. The optimization searches will be performed until diminishing returns are reached such that further searches do not return improved results of a statistical significance.

The primary overall objective is to find the greatest reduction in k_{eff} with the least number of canister moves. Minimizing k_{eff} and minimizing the number of canister relocation movements are competing objectives. The problem is discreet since canister loadings are fixed and highly variable among the parameters that impact the answer, and integer based since only whole number canister movements are possible. The objective function can be stated as a goal to minimize the maximum positional k_{eff} value returned by the empirical model for search iteration (tested canister relocation arrangement) n+1 relative to the preceding iteration n. This search is also repeated for varying total numbers of potential canister relocation movements, since the other objective of the multiple objective problem is to minimize the total number of canister relocation movements. These objectives comprise the feasible criterion space in which the solution must exist. The constraints on the problem include the controlled arrangement and number of possible storage positions, the restrictions on positions that will remain empty, and the current fuel storage configurations in the canisters.

A solution is optimal when it satisfies Pareto efficiency or Pareto optimality. When two objectives are in competition, a Pareto optimal solution is one by which an improvement cannot be

made to the desired outcome of one objective without causing a detriment to the desired outcome of the other objective. The Pareto Front or Frontier is the set of Pareto efficient solutions that define that competing boundary (Reference v). In the case of this problem the Pareto Front will define the curve by which any further reduction in array k_{eff} will require additional canister moves, or conversely a relocation of less than a given number of canisters will require an increase in the array k_{eff}. For most multiple-objective optimization problems this front does not present a single answer to the problem, but a set of possible solutions, that is, there is not a single "utopia' point. The ultimate answer depends on the priorities regarding the needs for the system performance. The determination of the Pareto Front provides a decision maker with the information needed to make a cost-benefit decision based on hard data. In the case of the IFSF, a practical improvement of significance will be found if the open positions of the array can be determined to be filled without exceeding the subcritical limit. This will allow full utilization of the facility.

One item worth noting is that no attempt will be made to optimize the current array configuration with the currently empty positions. While a reduction in k_{eff} could surely be obtained, this new arrangement would almost certainly not be optimal for the placement of a new fuel type. The optimization effort would then need to be repeated with the newly added fuel. The overall effort is therefore made more efficient by starting with the condition where the array in the current arrangement has the open positions filled with the desired fuel. This starting point will exceed the allowable k_{safe}. A fuel type with a reactivity and moderation state that is enveloping of the fuel types that would be expected to be received will be chosen as the fuel to fill the open positions in the array.

Chapter 5.0 - Methodology

5.1 Array k_{eff} Empirical Model Development

The overall goal of the empirical model development is to create a model of the array that returns a fast but accurate estimate of the array reactivity and which also correctly determines the localized region of the storage array where the peak neutron multiplication (or flux or fission density) is occurring. Determination of this location allows identification of the best candidate canisters for relocation. The empirical model is developed to be calculated in a Microsoft Excel spreadsheet. The innate layout of a spreadsheet format is conducive to representing a two dimensional array. MCNP calculations are time consuming to perform, while the spreadsheet model can return a near instantaneous answer to a perturbation of the array. In this way a large number of different canister arrangements and relocation sequences can be evaluated in a much more time efficient manner.

The process of developing the empirical model requires further investigation of the neutronic behavior of the array system, which serves to enhance the understanding of the criticality physics of the system and the intrinsic aspects of interaction of fuels with different moderation states. The empirical model will be used to apply stochastic optimization that is guided by the understanding of the physics of the system to determine potential candidate optional rearrangements of the array. The candidate rearrangements that are identified will then be confirmed by MCNP calculations performed with the proposed rearrangements. Various potential rearrangement cases for a given number of canister relocations will be confirmed with the MCNP calculations, which will serve as a check on the empirical model, as well as to allow an estimate of the uncertainty. Based on this effort to determine the maximum possible reduction in array k_{eff} for each of various numbers of canister relocation moves, the Pareto Front can be determined. The ultimate spreadsheet-based empirical model is a stand-alone entity separate from the optimization treatment, and which is developed from the supporting calculations and benchmarked by additional MCNP comparison calculations. The empirical model is then subjected to the optimization algorithm, which is a set of rules (constraints and preferential canister movements) and random canister movements that is imposed onto the empirical model in order to search for the lowest possible k_{eff} to result for a given number of canister movements. The preferred movements are determined based on the underlying known criticality physics behavior of the system as supported and confirmed by additional MCNP calculations.

5.2 Solution Development Methodology

The specific methodology to determine a solution to the multiple-objective optimization problem of the maximum reduction of the IFSF storage array k_{eff} for the minimum number of canister relocation movements is as follows:

1) Perform MCNP calculations that model every storage position of the IFSF array as containing the same fuel storage canister fuel type and configuration. These calculations will be used to determine the fuels that drive the array neutron multiplication and to provide data on the neutron spectra for the various fuels. EALF and the percent fissions in the thermal, epithermal, and fast energy bins will be considered. These calculations are a fundamental basis for correlating the differences in fuel canister fissile mass and moderation. The calculation results will be compared to the subsequent calculations to determine the proper treatment of the interaction of the different fuels type in the empirical model.

2) Perform MCNP calculations that consider the current fuel storage arrangement, but with the interior empty canister positions all filled with the same common fuel storage canister fuel configurations. This is repeated with different important and common fuels types present in the empty interior positions. These calculations will be used to assess the sensitivity of the current storage arrangement to the addition of different fuel types. The storage array in the current arrangement with empty positions filled with an enveloping fuel type that can likely be expected to be received by the IFSF in the future will serve as the baseline for improvement of the array arrangement.

3) MCNP calculations will be performed that consider the IFSF storage array with either a single fuel type configuration or the current storage arrangement with either the floor removed or the ceiling moved closer to the top of the fuel storage rack. These cases will demonstrate the impact of axial leakage on limiting the array k_{eff}, and the variation of this effect depending on the degree of moderation present in the array.

4) The fuels and fuel canister storage configurations will be grouped into categories based on degree of fissile mass and moderation present in the canister.

5) An attempt will be made to develop an empirical model that simulates the k_{eff} of the full IFSF storage array filled with a single fuel storage configuration at a time.

6) MCNP calculations will be performed with varying mixtures of moderated and unmoderated fuels. These calculations will be used to develop the empirical model for mixed arrangements of fuels, primarily by determining weighting factors that will be applied to the fuels when present in mixed groups in the array, and when mixing fuels of disparate moderation levels.

7) MCNP calculations will be performed with partial array arrangements and with a concrete wall of the array moved to model smaller regions of the array with full exterior reflection. These cases will be used for two purposes. One reason is to determine the regions of the array in the current arrangement that produce the greatest neutron multiplication, that is, that drive the array reactivity. This knowledge will be useful in evaluating the effectiveness of the empirical model to identify the more reactive regions of the array. Knowledge of the localized region or canisters that drive reactivity is vital in the determination of which canisters are the best candidates to be relocated to reduce the overall array k_{eff}. Second, these calculations will be used to develop the treatment of the reflection of the concrete walls in the empirical model. It is currently known that the center of the east end of the array is the region with the greatest neutron multiplication with the current arrangement. However as more reactive fuels are moved to the perimeter of the array and the fission density of the center of the array is reduced (similar to flux flattening with a reactor core), the importance of the reflection from the walls increases relative to the k_{eff} that results for the overall array arrangement. That is, proper treatment in the empirical model of the exterior wall reflection is important for the optimization effort as more canisters are moved.

8) The empirical model developed from the above steps will be compared to the MCNP calculation results for various mixed arrangements of fuel, to serve to benchmark the empirical model. The empirical model is developed by determining a weighted average of a set number of canisters of neighboring canisters for each position of the array. This is initially developed for arrangements that were calculated in MCNP with moderated fuels. Once the data is fit for the moderated fuels, the model is expanded to include mixtures of unmoderated fuels with the moderated fuels to determine a correction factor based on the degree of

moderation around the unmoderated fuels. Finally the data is also fit to the concrete wall calculations to determine the appropriate treatment of the concrete wall reflection.

9) Stochastic Approximation Optimization will be applied to the empirical model. Constraints are imposed on the optimization treatment in light of the criticality physics knowledge of the behavior of the system. Intrinsic aspects of the empirical model structure assist in ensuring a best solution is found, since the model readily identifies the region of the array producing the largest and the smallest neutron multiplication. This reduces the chance that focus continues to be applied towards reducing the neutron multiplication of a given reactive region of the array when in fact a new peak multiplication factor region has been created or made worse. The empirical model will identify when this has occurred. However, a degree of randomness will ensure that different fuels types are considered in the swaps, as initial reductions in array k_{eff} may be driven not by where a more reactive fuel is moved to, but instead by what fuel is chosen to move into the place formerly occupied by that more reactive fuel. The search will be performed until no further reduction in k_{eff} for the number of canister relocation movements of interest. The candidate best arrangements for a given number of relocation movements will be calculated in MCNP to determine the best case arrangement and lowest k_{eff} for a given number of canister movements. These arrangements comprise the Pareto Front for lowest possible array k_{eff} for the least number of canister movements.

Chapter 6.0 - Results

6.1 Empirical Model Development Calculations

6.1.1 Single Fuel Data

The MCNP calculations presented in Table 4 consider the entire IFSF array with each fuel position filled with the same fuel configuration model. The table presents the nominal k_{eff} result (without statistical uncertainty), as well the spectral information returned by the code. The statistical uncertainty for these calculations is always less than 0.0016. These results provide an important starting point for the comparison of the different fuel type configurations.

Table 4 – Single fuel configuration array fill MCNP calculations

Fuel Configuration	Nominal k_{eff}	prompt removal life (seconds)	ANECF (MeV)	EALF (eV)	% fissions Thermal	% fissions Epithermal	% fissions Fast
HEU TRIGA (group 1)	1.09334	4.09E-04	3.39E-02	4.99E-01	73.59	24.18	2.24
LEU TRIGA (group 2, 6x5)	0.84424	5.74E-04	2.61E-02	1.39E-01	88.57	10.17	1.27
LEU TRIGA (group 2, 6x6)	0.92196	4.99E-04	2.51E-02	1.34E-01	89.04	9.75	1.21
LEU TRIGA (LWT basket)	0.75181	4.62E-04	2.82E-02	1.56E-01	87.27	11.34	1.39
TRIGA-IN (group 3)	1.00177	4.90E-04	4.38E-02	1.10E+00	63.81	32.99	3.20
AL plate	0.61172	8.97E-04	1.99E-01	1.60E+02	29.73	47.62	22.65
Berliner (BER-II)	0.53701	7.23E-04	3.60E-02	3.70E-01	77.09	20.76	2.15
BORAX	0.49401	9.36E-04	1.82E-01	7.33E+01	34.47	43.88	21.65
Fermi	1.03123	5.33E-04	5.72E-01	1.45E+03	16.19	47.99	35.82
Fermi - moderated	1.20777	3.63E-04	3.11E-01	2.72E+01	40.95	41.61	17.44
FSV	0.81347	5.77E-04	2.21E-02	1.32E+00	55.72	42.59	1.69
HTGR	0.99733	5.99E-04	3.51E-02	1.13E-01	87.13	11.26	1.61
MTR Canal	1.11439	3.06E-04	1.82E-02	8.60E-02	89.90	9.16	0.94
ORNL canistered	1.03214	6.49E-04	5.87E-02	1.91E+01	27.47	67.39	5.14
Pathfinder	0.43289	9.52E-04	1.30E-01	4.56E+01	33.10	52.43	14.47
Peach Bottom	0.95134	5.17E-04	9.22E-03	3.47E-01	73.85	25.41	0.74
PB w/ water	1.02843	4.73E-04	8.02E-03	1.73E-01	81.07	18.32	0.61
PBF	0.39752	9.57E-04	2.22E-01	1.33E+01	47.85	37.31	14.85
Pulstar moderated	1.10066	1.19E-04	2.39E-01	1.84E+00	64.62	25.83	9.55
Pulstar dry	0.44982	8.10E-04	7.67E-01	1.20E+03	24.94	35.02	40.04
Rover- light load	0.19386	1.31E-03	1.35E-01	5.14E+00	50.76	39.27	9.97
Rover - heavy load	1.26733	3.98E-04	7.33E-02	1.31E+01	34.05	59.82	6.12
Rover UBM 1	1.34331	3.26E-04	4.12E-02	1.34E+00	59.80	37.10	3.11
Rover UBM 2	1.14185	4.23E-04	1.71E-02	2.43E-01	78.88	19.83	1.29
Rover UBM 3	1.21657	4.76E-04	2.20E-01	9.77E+02	11.86	66.92	21.22
Rover UBM 4	1.08414	4.82E-04	1.38E-01	3.75E+02	11.52	74.61	13.88
TORY IIC	0.68672	6.93E-04	2.22E-02	2.51E+00	49.58	48.36	2.06
TRIGA AL	0.95849	4.51E-04	3.20E-02	1.08E-01	86.44	11.98	1.58
Current IFSF arrangement	0.94011	5.68E-04	9.32E-02	1.46E+00	63.35	31.88	5.77

Key conclusions that can be drawn from the single fuel results is the fact that a number of fuels can be fully loaded in the array without approaching the subcritical limit of 0.95, generally unmoderated fuel canisters except those with very high fissile mass, while other fuels far exceed this acceptance criterion (always the case for high fissile mass and high moderation fuels). This knowledge can be used in the optimization effort as strategic groupings of fuel can be assembled to effectively isolate the more reactive fuels from one another. For example, a large collection of only LEU TRIGA fuel (in the 30 elements per fuel bucket [6x5] configuration) will not result in a k_{eff} greater than 0.85. Calculations presented later will show that a few intervening rows of a well moderated fuel such as LEU TRIGA reduces the effective interaction between more reactive fuel types. Likewise, a region of a low moderation canister type can serve to produce a low reactivity region of the array where neutron leakage of adjacent high moderation fuel canisters is increased. This is important, since both FSV (a moderated but lower reactivity fuel configuration, k_{eff} ~0.81) and AL-plate (low moderation, k_{eff} ~0.61 when moderator absent) fuels are two of the fuel types present in the largest quantity numbers in the array.

6.1.2 Empirical Model for Single Canister Fuel Type Array Fill Cases

6.1.2.1 Unmoderated Fuels

The unmoderated fuels present a rather simple case where the dominating aspect is the fissile mass loading. This can be shown by the four factor equation for a one group system, since for a one-group (fast) system the four factor equation simplifies to (Reference vi):

$k_\infty = \Pi f =$(eta{number of neutrons produced per fission} * fuel utilization) (Equation 1)

$$= \Pi \Sigma_{af}/(\Sigma_{af} + \Sigma_{am})$$

Where the new terms are the macroscopic absorption cross section in the fuel and moderator

$$= \Pi/(1+\Sigma_{am}/\Sigma_{af}) =$$

$$= \Pi / (1 + N_m\sigma_{am}/N_f\sigma_{af})$$

Where the macroscopic cross section is expressed in terms of the atom density of the fissile isotope or moderator (N_f and N_m respectively) times the respective microscopic cross section (σ) of the fissile isotope or moderating element.

The terms in the final arrangement of the expression are relatively constant between fuel arrangements of unmoderated fuels, with the exception of N_f, therefore k_{eff} is essentially proportional to N_f (and therefore fissile mass per canister). The theory of the four factor equation therefore shows the applicability of an empirical model for the unmoderated fuels where k_{eff} is directly proportional to canister fissile mass quantity or density. This one-group treatment however only remains true if moderation is very minimal. The treatment is therefore only applicable to metal, oxide, or carbide fuels without the presence of materials containing light elements. The presence of more than 0.5 kg of hydrogen (or ~ 5 liters of water) in the canister would invalidate use of this unmoderated model.

Figure 5 shows that for truly unmoderated fuels that k_{eff} of the array is directly proportional to the canister fissile mass (which is the same as the array fissile density due to the controlled spacing and geometry). The fuels in the figure are Pathfinder, PBF, Borax, Pulstar-dry, AL-plate, and Fermi in order of increasing fissile mass. The data fit is k_{eff} = 0.0078 *(canister U-235 mass in kg) + 0.355. This fit is valid between fissile masses of 7 to 100 kg and fuels that are unmoderated.

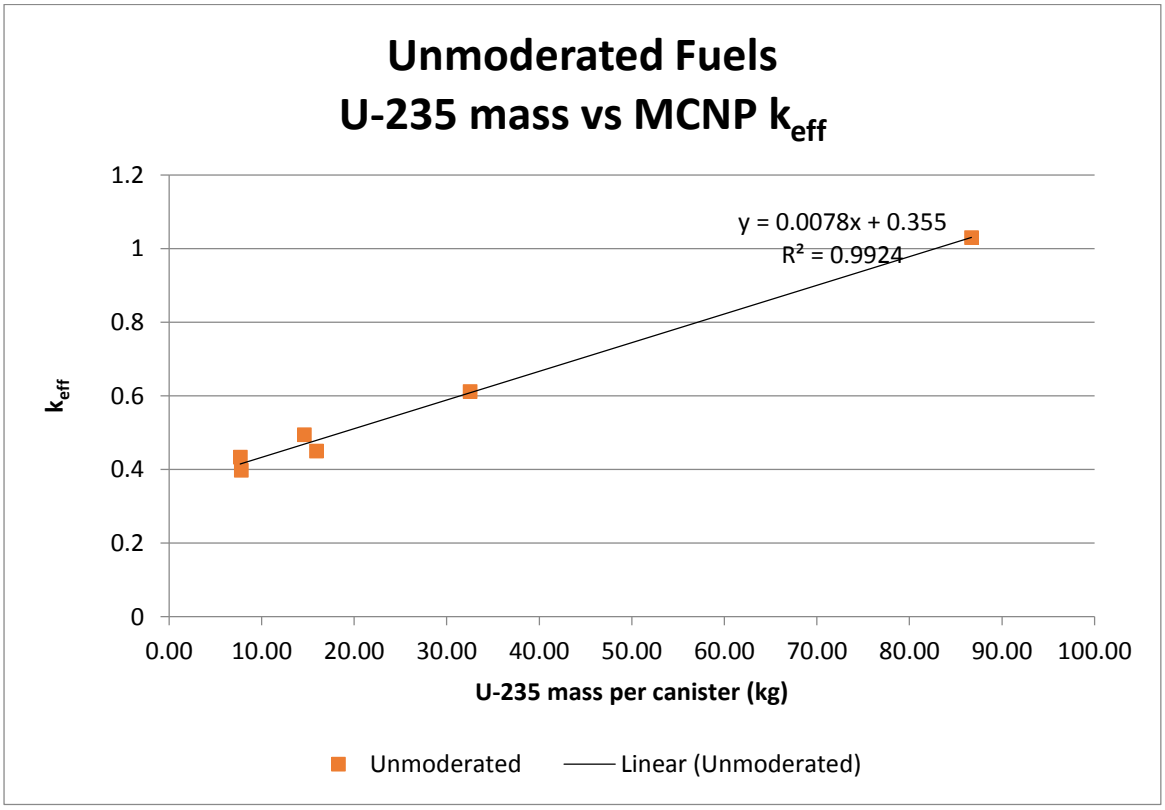

Figure 5 – Unmoderated fuel array k_{eff} dependence on canister fissile mass.

6.1.2.2 Moderated Fuels

Moderation is one of the most important controlled parameters regarding the neutron multiplication of the IFSF array, and is one of the primary variables concerning the different fuel storage types and configurations. This importance is because absorption and fission cross-sections increase by many orders of magnitude for lower neutron energies. For example, the microscopic fission cross-section of U-235 increases from the range of single digits in units of barns for fast neutrons to 10,000+ barns for 0.025 eV neutrons (Reference vii). It will also be shown that moderation significantly influences leakage in the axial direction. This is because less moderation means a longer/larger diffusion length, neutron age, and migration area. This can be related to the fast non-leakage factor $P_f = 1/(1+B^2 \tau)$ where B represents buckling and τ represents neutron age which is equal to the diffusion constant divided by the macroscopic cross-section for removal from the fast spectrum (Reference vi). Increased moderation of the systems means that there is less leakage from the top and bottom surfaces of the array. This can also be thought of as the geometric buckling decreases as moderation of the system increases, since the vertical distance of the array is effectively larger for the better moderated condition. Therefore, for a fixed axial height, the leakage probability decreases as neutron moderation increases.

A comparison of the single canister configuration array fill results for the moderated fuels shows that fissile mass alone and moderator mass alone do not correlate well with the k_{eff} result. This is not unexpected, as a multi-group model is required for the moderated case. Figure 6 and Figure 7 show this poor correlation of fissile mass and moderation alone to k_{eff} for the moderated fuel configurations.

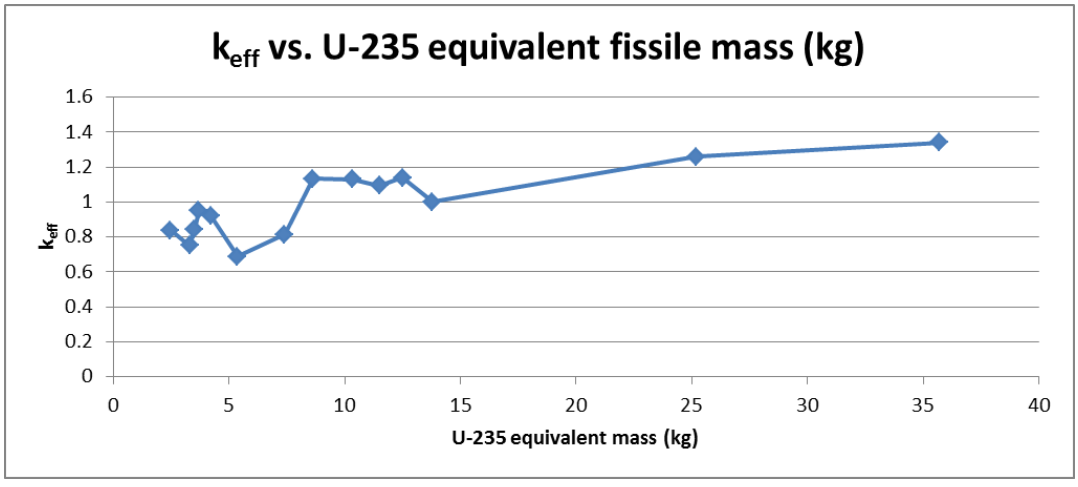

Figure 6 – Plot of moderated fuel array k_{eff} versus canister U-235 equivalent fissile mass.

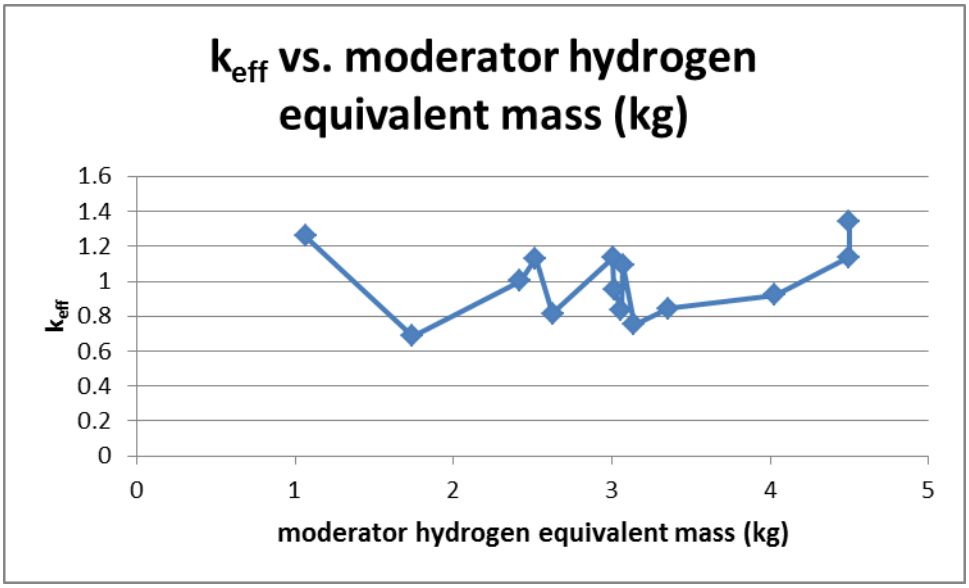

Figure 7 – Plot of moderated fuel k_{eff} versus canister hydrogen equivalent moderator mass.

In order to compare the fuel types with differing moderators, a moderator equivalence is established. The primary moderating elements present in the IFSF array are hydrogen, carbon, and beryllium. An equivalence is established based on average energy loss per collision for elastic scattering, based on the average logarithmic energy decrement denoted by ξ. Elastic scattering dominates for neutrons with fission energies. ξ can be expressed as:

$$\xi = \ln (E_i/E_f) \qquad \text{(Equation 2, Reference viii)}$$

where E_i is the average initial neutron energy and E_f is the average final neutron energy. ξ is often used in the expression:

$$N = [\ln (E_{fast}/E_{thermal})/ \xi$$

to calculate the "N" number of collisions to thermalize a neutron from fission energy to thermal energy (or any starting energy to a finishing energy of interest). The value of ξ can be expressed by the relationship:

$$\xi = 1+ (\alpha/(1-\alpha)) \ln(\alpha)$$

where

$$\alpha = [(A-1)/(A+1)]^2$$

and A is the atomic weight of the target isotope.

This expression for ξ is often simplified to:

$$\xi = 2/(A+2/3) \text{ for } A \geq 10.$$

The values of ξ for hydrogen, beryllium, and carbon are one, 4.8, and 6.3 respectively. This equates to 19 and 114 collisions for a neutron to moderate from fission energy of 2 MeV to thermal energy 0.025 eV for hydrogen and carbon respectively when present in water and graphite at normal density. The number of collisions a neutron will undergo is dependent on the atom density of the moderating elements. Since the moderators are not present in the IFSF canisters at normal full density, these factors will be reduced to a mass based value by dividing by the atomic weight. This is applicable because an equal mass of hydrogen and carbon present in the same volume (such as in a canister) means that the atom density of carbon is $1/12^{th}$ the atom density of hydrogen. Therefore a collision with a hydrogen atom is twelve times more likely than a collision with a carbon atom if the elemental masses are equal. Therefore the ultimate expression for hydrogen moderator equivalence is moderator mass divided by the element ξ, then divided by the element value for A. Both of these values are essentially one for hydrogen, establishing hydrogen mass as the baseline for the equivalence.

Since more collisions are required with carbon atoms than with hydrogen atoms for a comparable decrease in neutron energy this shows that larger physical cores are required with graphite moderated fuels for a similar moderation state and non-leakage probability as compared to water moderated reactors. For very well moderated systems carbon and beryllium do have one advantage as a practical material for moderation in that there is less parasitic neutron capture with C and Be as compared to hydrogen, since the microscopic absorption cross section is lower.

Some of the moderated fuels also have various fissile isotopes present, mainly U-233 and Pu-239 in addition to U-235. The fissile mass equivalence for different fissile isotopes is well established in the NCS community. The equivalence factor used is 1.9 to relate U-233 and Pu-239 mass to U-235 equivalent mass.

These canister fissile mass and moderator masses are normalized based on the values present and then a weighted relationship is determined that relates them to the resultant k_{eff}. The normalizing factors are dividing the fissile mass by 24.5, and dividing the hydrogen equivalent mass by 5.0, except when graphite is the predominant moderator which used a value of 7.5. These values are approximately the maximum values for any of the canister modelled arrangements for each category,

and were determined by a data fit. The resultant values are summed to arrive at the nominal score. If the fuels were present in a significantly homogenized arrangement, a geometry correction was applied by multiplying the summed score by 1.2 to arrive at the final score; this was applied to TORY IIC, SBT, ORSNF, BER, and HTGR. The summed score was divided by 1.1 for Rover Parka where the geometric configuration in the moderating fiberboard tubes is less ideal and more heterogeneous than for other fuels. These correction factors for geometry were also determined by a data fit. Figure 8 presents the results of the application of the moderated, single-fuel canister empirical model to the moderated fuel configurations, with a comparison to MCNP results for singe-fuel canister arrays.

This model stands for well moderated fuels, but neither this moderated model nor the unmoderated model remains valid with mixing of moderated fuels with unmoderated fuels in the same array. Similarly, fuels that are present at the boundaries of the moderated empirical model and the unmoderated model do not fit either model well, such as moderated Fermi and Rover UBM. The final empirical model for mixed arrangements must be able to treat this combined, mixed state of all fuels. For these reasons, the ultimate array empirical model will be based on the single canister full array fill k_{eff} for each given fuel position, but with a weighted average of the surrounding canisters. The moderation values are used to determine a modification of the unmoderated fuel k_{eff} effective depending on the degree of moderation present in the neighboring canisters around the unmoderated fuel canister. These additional weighting factors and modifiers will be developed in the subsequent sections based on calculations that mix fuel types in the array with differing moderation states. Section 6.2 will detail the development of the final array empirical model.

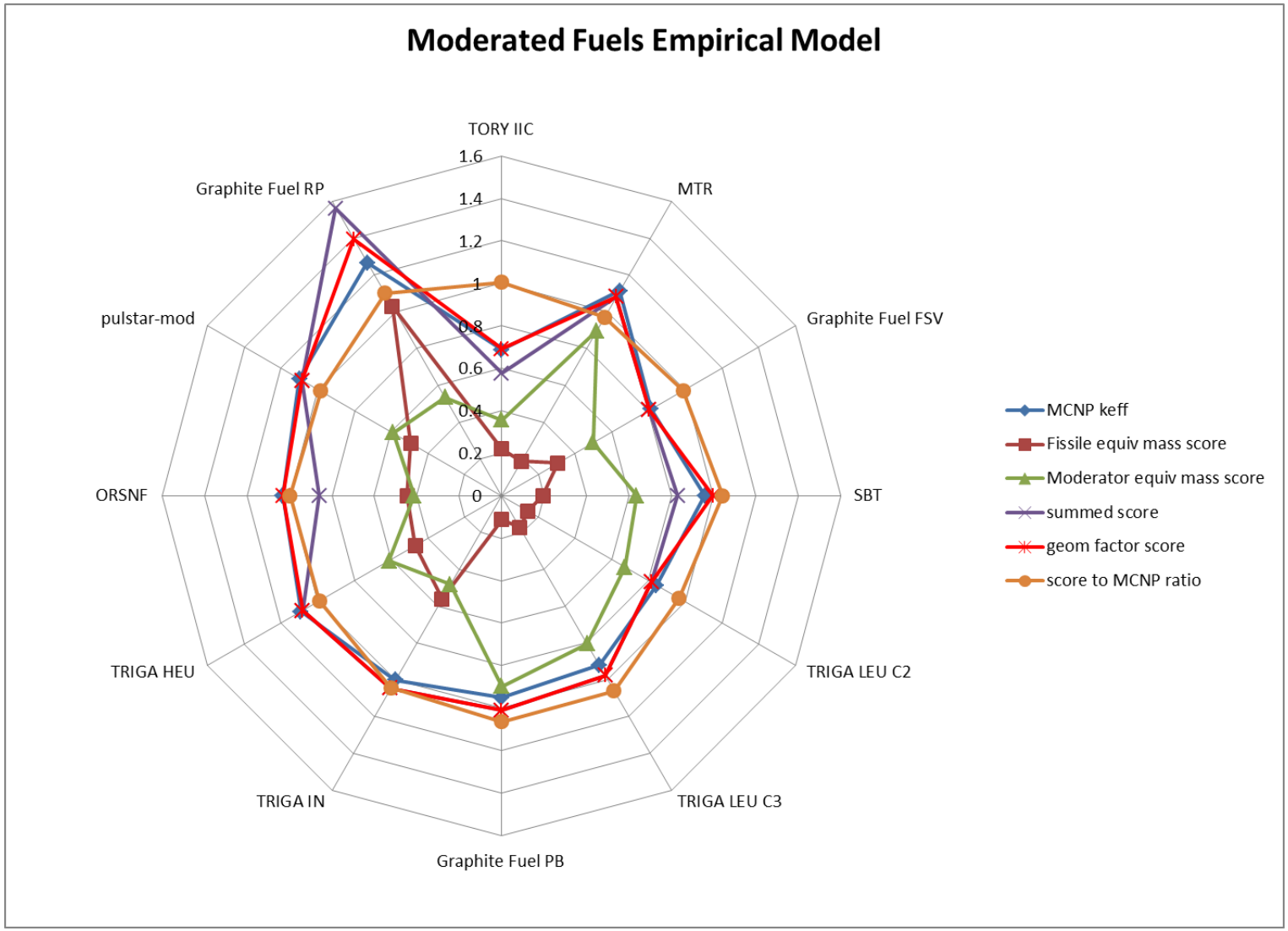

Figure 8 – Moderated single-fuel empirical model results.

6.1.3 Axial Reflection Cases

The MCNP calculations in this section are performed to verify that neutron leakage in the axial direction from the array is a characteristic that limits the array k_{eff}. The storage array is effectively infinite in dimension in the horizontal directions, as will be shown by the partial array cases. The calculations of this section also demonstrate that axial neutron leakage is much greater with unmoderated fuel configurations than for moderated fuel configurations. The calculations consider the storage array entirely loaded with one fuel type at a time, but with the concrete ceiling moved to be immediately above the top surface of the storage rack, therefore increasing reflection at the top surface of the array. A companion calculation then uses the same comparison cases of the array filled with one fuel at a time, but with the floor removed. In this case there is no bottom reflector for the array, which shows the effect of increased neutron leakage from both the top and bottom surfaces of the array. The results for the six primary scoped fuel types are shown in Table 5.

Table 5 - Axial Reflection Effect Cases

Fuel	Condition	k_{eff}	% of Nominal	Effect Rank
	Close ceiling	1.11758	102.2	5
HEU TRIGA	Nominal	1.09334		
	No floor	1.00419	91.8	6
	Close ceiling	0.69574	113.7	1
AL Plate	Nominal	0.61172		
	No floor	0.41887	68.5	1
	Close ceiling	1.08716	105.4	2
Fermi	Nominal	1.03123		
	No floor	0.81853	79.4	2
	Close ceiling	0.84187	103.5	3
FSV	Nominal	0.81347		
	No floor	0.73832	90.8	4
	Close ceiling	0.87026	103.1	4
LEU TRIGA C2	Nominal	0.84424		
	No floor	0.73984	87.6	3
	Close ceiling	0.96587	101.5	6
PB	Nominal	0.95134		
	No floor	0.87038	91.5	5

Fuel	Condition	k_{eff}	% of Nominal	Effect Rank
	Close ceiling	0.91364	102.6	
Current array Storage arrangement	Nominal	0.89011		
	No floor	0.83094	93.4	

The maximum fuel region height is 10.8 feet. This height is equivalent to ~ 6 to 7 rows of array length or width. The partial array fill cases show that this distance is not effectively infinite, particularly for regions of the array with poor moderation. However this height is effectively much closer to infinite for lower neutron energy regions of the array. Therefore, there is less neutron leakage from the top and bottom surfaces of array for the better moderated fuels/regions of the array. The influence of the top and bottom reflector is most significant for poorly moderated fuels. This has also been confirmed by calculations with shorter fuel regions as shown in Table 6. Ultimately, the fuel region is far from infinite thickness for fission energy neutrons in the vertical direction.

The axial leakage impact is important to the resultant array or array region neutron multiplication and is directly dependent on the moderation state of a region of the array, since the axial height is constant. This result explains why particularly well moderated, high fissile mass fuels (and therefore more reactive) result in a lower k_{eff} region when placed in or adjacent to a region of undermoderated fuels which results in maximal neutron leakage and a minimal overall k_{eff} value. This is only possible when the unmoderated fuels outnumber the well moderated fuels in the region. The calculations also show that the current array configuration gives a result similar to the better moderated fuels such as TRIGA and Peach Bottom, showing that the current configuration of stored fuels is an overall moderated arrangement for the region driving reactivity. This similarity is expected given the large collection of TRIGA and Peach Bottom fuel in the east side of the array.

Another way to look at the axial leakage aspect is the fact that neutron leakage is tied to the number of neutron collision mean free paths present over the given dimension. After a certain number of mean free paths of thickness, the thickness of the region approaches infinite for the majority of the fission energy neutrons born in the fissile region. With an increasing density of moderator present the mean free path is shorter. Therefore the effective thickness of the fissile region is greater in the regions of the array with increasing moderator density. The problem can also be considered with respect to the solid angle for a canister axial position, versus the density and thickness of fissile material and moderator impinged upon to reach the top or bottom surface of the array. For this reason, alternating canisters or high fissile-mass/low moderation fuels and canisters with significant moderation is not desirable in reducing array reactivity, as a much greater quantity or percentage of neutrons can be

thermalized by the moderated canister and then impinge upon a neighboring high fissile mass canister. This can also be explained by the relationship of geometric buckling [smaller value meaning less leakage] to a larger material buckling value (utilization).

Table 6 - Cases with fuel canisters containing two buckets/baskets of fuel instead of three.

Case	Description	k_{eff}
all-g1	Case with entire array filled with HEU TRIGA	1.09334
g1isrt	Like above, but fuel baskets in canister stacked two high instead of three.	1.00568
all T 20 frr 65	Case with entire array filled with LEU TRIGA (30 element buckets).	0.84424
frr65srt	Like above, but fuel baskets in canister stacked two high instead of three.	0.74939
all-g2	Case with entire array filled with LEU TRIGA, in NAC-LWT baskets (29 element baskets).	0.75181
g2inacsrt	Like above, but fuel baskets in canister stacked two high instead of three.	0.68949

6.1.4 Array Size and Concrete Reflection Cases

These MCNP calculations will be used to develop the capability of the empirical model to treat the neutron reflection contribution provided by the exterior concrete walls correctly, and to demonstrate the ability of the empirical model to correctly identify the more reactive region. The cases also confirm that the east side of the current storage arrangement is driving the current overall array k_{eff} value, by determining the k_{eff} of specific sub-sections of the array. The calculations simply take a comparison array arrangement and decrease the size in the east-west direction by moving the opposing concrete wall reflector, which increases the relative importance of the reflection of the arrangement in the horizontal (radial to the canisters) direction. Table 7 and Table 8 present the results of MCNP calculations with partial regions of the array with concrete reflection on all sides.

Table 7 - Concrete Reflection of Partial Array arrangements.

Array size	k_{eff}	% of nominal k_{eff}	% full array
Current complete mixed array of 38 rows – Nominal Value	0.89011		
east 8 rows	0.84966	95.5	22
east 15 rows	0.8894	99.9	42
east 22 rows	0.88958	99.9	61
west 8 rows	0.82963	93.2	22
west 15 rows	0.83137	93.4	42
west 22 rows	0.82881	93.1	61
middle 20 rows	0.67956	76.3	56

Table 8 - Concrete Reflection of Partial Array arrangements – East Side – Fewer rows

Concrete cases	Description	k_{eff}
fbc-g2-r32	Comparison case for below, full array.	0.93153
fbc-g2-r32	Concrete wall added just west of row 32 – current array.	0.84167
fbc-g2-r34	Concrete wall added just west of row 34 – current array.	0.77576
bf-g2-m6-6	Comparison case for below, full array.	0.87935
m6-6-r22	Concrete wall added just west of row 22 – modification to case bf-g2-m6-6.	0.86442
m6-6-r24	Concrete wall added just west of row 24 – modification to case bf-g2-m6-6.	0.85741
m6-6-r26	Concrete wall added just west of row 26 – modification to case bf-g2-m6-6.	0.839
m6-6-r28	Concrete wall added just west of row 28 – modification to case bf-g2-m6-6.	0.80527
m6-6-r30	Concrete wall added just west of row 30 – modification to case bf-g2-m6-6.	0.7845

The concrete wall partial array results provide insight into the comparative k_{eff} value resulting from different sections of the array and the degree to which a number of rows must be present to produce a result that approaches the overall array result. This allows for a determination of the number of rows that should be included in the calculation of the array k_{eff} by the empirical model. These results are also used to determine the multiplication factor to apply to the walls in the empirical model.

6.1.5 Multiple Fuel Arrangement Data

6.1.5.1 Two Fuel Mixes

The MCNP calculations presented in Table 9 consider the IFSF array with two different canister models stored at varying proportions. The results presented in the table give the k_{eff} value for the array filled with a single fuel types, and then with a second fuel type introduced in every sixth row, fifth row, fourth row, etc. through a 50/50 mix where the rows alternate, and continuing until the array is filled with the second fuel. Figure 9 and Figure 10 show a view of the MCNP model for the 50% fill fraction arrangement and the 80%/20% fill fraction arrangement respectively. Figure 11 plots the results.

Table 9 - MCNP calculations with the storage array filled with two different fuel models.

% of array (first fuel listed)	FSV and AL (case name)	k_{eff}	HEU TRIGA and FSV	k_{eff}	HEU TRIGA and AL	k_{eff}	LEU TRIGA and AL	k_{eff}	LEU TRIGA and FSV	k_{eff}
100	allfsv	0.81347	all-g1	1.09334	all-g1	1.09334	all-g2	0.75181	all-g2	0.75181
86	fsv6dal	0.80106	g1d6fsv	1.0768	g1d6al	1.07812	g2d6al	0.76469	g2d6fsv	0.75934
83	fsv5dal	0.80129	g1d5fsv	1.07034	g1d5al	1.07473	g2d5al	0.76852	g2d5fsv	0.7618
80	fsv4dal	0.79535	g1d4fsv	1.06155	g1d4al	1.06562	g2d4al	0.77384	g2d4fsv	0.76521
75	fsv3dal	0.79138	g1d3fsv	1.04816	g1d3al	1.0529	g2d3al	0.78258	g2d3fsv	0.76886
50	fsv2dal	0.77532	fsv2dg1	1.01743	al2dg1	1.0187	al2dg2	0.78707	fsv2dg2	0.77874
25	al3dfsv	0.73596	fsv3dg1	0.97167	ald3g1	0.95915	ald3g2	0.76706	fsv3dg2	0.78496
20	al4dfsv	0.71098	fsv4dg1	0.94691	ald4g1	0.91959	ald4g2	0.74355	fsv4dg2	0.78871
17	al5dfsv	0.69348	fsv5dg1	0.93225	ald5g1	0.88674	ald5g2	0.72749	fsv5dg2	0.79332
14	al6dfsv	0.68316	fsv6dg1	0.92082	ald6g1	0.87059	ald6g2	0.71429	fsv6dg2	0.79429
0	all-al	0.61172	all-fsv	0.81347	all-al	0.61172	all-al	0.61172	all-fsv	0.81347

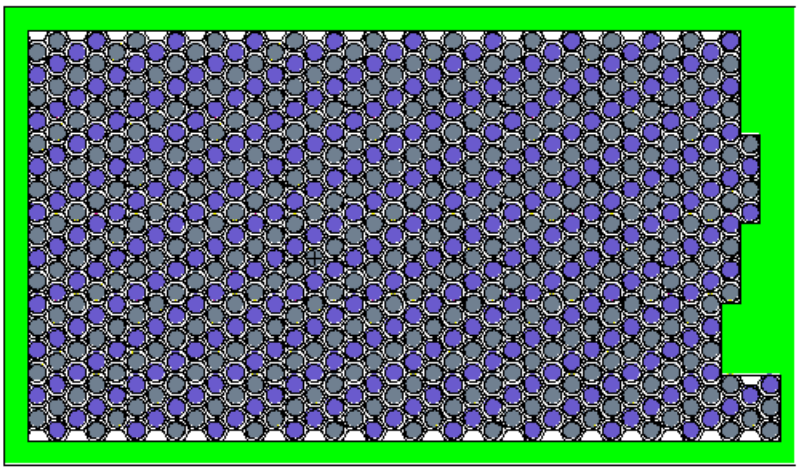

Figure 9 – Plot of MCNP model geometry for two-fuel array fill calculation with 50% fill fraction.

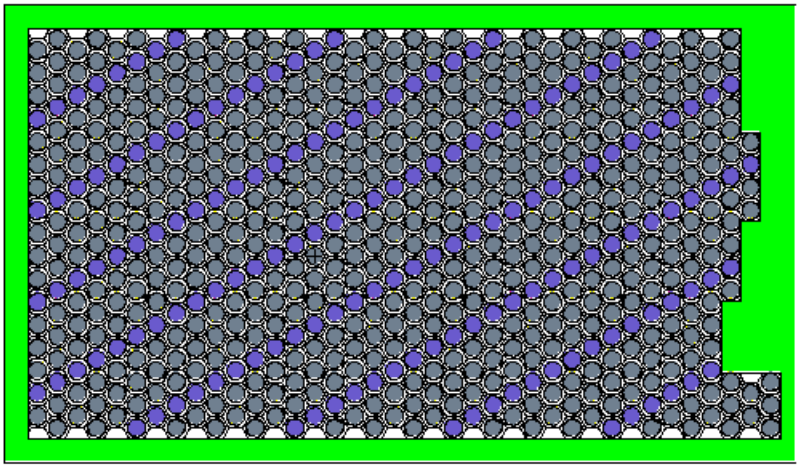

Figure 10 - Plot of MCNP model geometry for two-fuel array fill calculation with 80%/20% fill fraction.

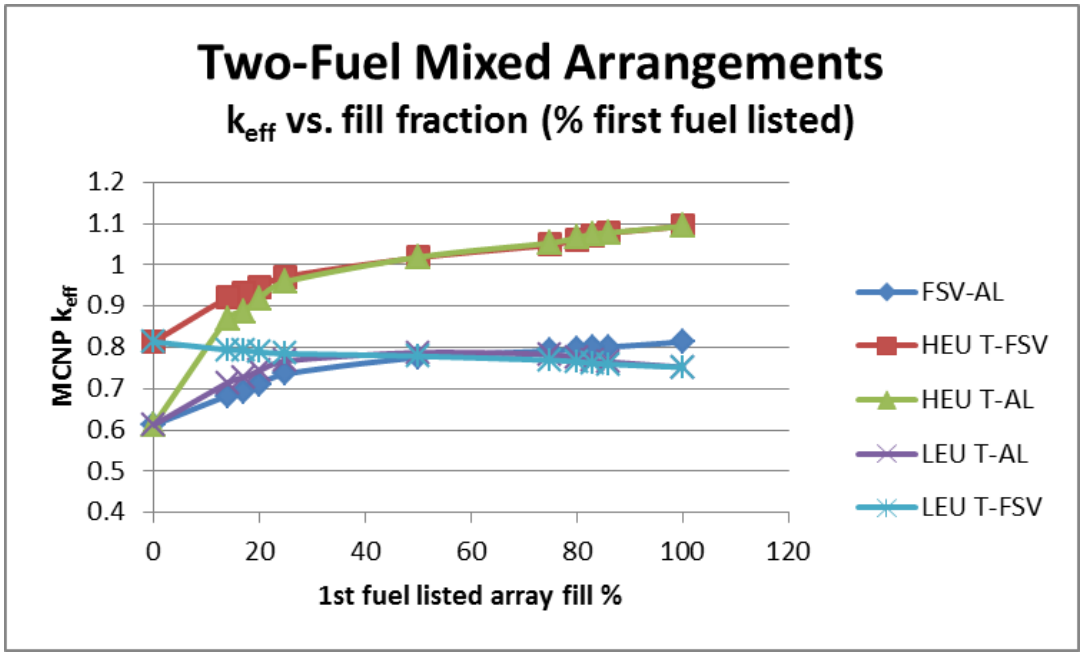

Figure 11 – Plot of results of MCNP calculations with varying proportions of two different fuels.

Calculations with 50/50 mixtures where the rows of two different fuels alternate were also performed with Fermi fuel and other key moderated fuels. These calculations are presented in Table 10.

Table 10 – Two fuel 50/50 mixtures (alternating rows) with Fermi fuel.

Case Name	Fuels Considered	Nominal k_{eff}	All second fuel k_{eff}
All-fermi-917.o	Fermi only	1.03123	N/A
fermi2dal.o:	Fermi and AL-plate	0.89640	0.61172
fermi2dg1.o:	Fermi and HEU TRIGA	1.09308	1.09334
fermi2dg2.o:	Fermi and LEU TRIGA (6x5)	1.09085	0.75181
fsv2dfermi.o:	Fermi and FSV	0.97388	0.81347

The results show that the impact of the high fissile mass but undermoderated fuel canisters is greatly increased when they are present in a well moderated region of the array or present among neighboring well moderated fuel canisters. The Fermi fuel canisters (with a full array k_{eff} of 1.03)

exhibit the condition where there is no decrease in k_{eff} when mixed with group 1 HEU TRIGA fuel. This is the only fuel to cause this. Even more pronounced is the fact that mixing Fermi 50/50 with LEU TRIGA produced nearly as high an overall result than mixing Fermi with HEU TRIGA, even though LEU TRIGA alone yields a much lower k_{eff} than HEU TRIGA alone. This is because the LEU TRIGA is one of the best moderated fuels with a large degree of hydrogen present. When mixed with a very high fissile mass fuel such as Fermi that has no inherent moderation, this thorough mixing of the high fissile mass fuel with the high moderation fuel results in a large increase in the utilization of the high fissile mass fuel. The resultant k_{eff} produced by the high fissile mass fuel is effectively increased or enhanced in relative reactivity contribution worth.

Aluminum plate fuel when mixed with other high moderation fuels also can cause an increase of a magnitude more similar to other fuels that are much more reactive than AL-plate in the single canister type array model. Recall that the AL-plate single canister k_{eff} is approximately 0.61, while FSV is 0.81. However AL-plate canisters mixed with HEU TRIGA result in a more reactive system for the same number of canisters, for example, compared to mixing with FSV. This trend continued until a 50/50 mixture of the fuels, below which FSV becomes the fuel that causes higher reactivity when mixed with HEU TRIGA. This shows the degree of moderation required for the effect to occur.

6.1.5.2 Two fuel cases with 50/50 mixtures and grouping of fuel type rows

The next set of two fuel mixing calculations consider a 50/50 mixture of two different fuels types, but where the rows of the different fuels are progressively clumped together. These cases are presented in Table 11 for AL-plate fuel mixed with HEU TRIGA fuel. Additional results are presented in Appendix A.

Table 11 – Mixtures of two fuels in rows with varying grouping of row fuel type.

Grouped rows	Arrangement	k_{eff}
AL-plate fuel and HEU TRIGA		
al2dg1	Alternating rows	1.01870
al2dg1-2.o:	Alternating 2 rows grouped	1.01698
al2dg1-3.o:	Alternating 3 rows grouped	1.02008
al2dg1-4.o:	Alternating 4 rows grouped	1.01989
al2dg1-5.o:	Alternating 5 rows grouped	1.02964
al2dg1-6.o:	Alternating 6 rows grouped	1.03008
al2dg1-7.o:	Alternating 7 rows grouped	1.04208

Grouped rows	Arrangement	k_{eff}
al2dg1-8.o:	Alternating 8 rows grouped	1.04118
al2dg1-9.o:	Alternating 9 rows grouped	1.05304
al2dg1-10.o:	Alternating 10 rows grouped	1.05827
al2dg1-11.o:	Alternating 11 rows grouped	1.06583
al2dg1-12.o:	Alternating 12 rows grouped	1.06990
al2dg1-13.o:	Alternating 13 rows grouped	1.07461
al2dg1-14.o:	Alternating 14 rows grouped	1.07579
al2dg1-15.o:	Alternating 15 rows grouped	1.07863
al2dg1-16.o:	Alternating 16 rows grouped	1.07855
al2dg1-17.o:	Alternating 17 rows grouped	1.07416
al2dg1-18.o:	Alternating 18 rows grouped	1.07023

These results are used for data fitting in the empirical model development to address mixtures of different fuels and different moderation states. The results also show the impact of the number of adjacent canister rows of more reactive fuels to result in k_{eff} values that approach the single fuel type k_{eff} for the more reactive fuel. An interesting result is that groups of two rows typically result in a slightly lower k_{eff} than alternating rows of a moderated and unmoderated fuel. However the results also show that grouping the more reactive fuels in rows more than two wide is undesirable for minimizing the array k_{eff}.

6.1.5.3 Two fuel cases with single rows of different fuels.

A final set of two fuel mixing cases is presented in Table 12 that considers the case where the array is filled with a single fuel type with every sixth row empty, except for one central row that is filled with a different fuel type. These cases provide additional data to verify the treatment in the final empirical model to properly address mixed arrangements of fuels, particularly for different moderation states.

Table 12 – Two fuel cases with single rows of different fuels.

Case Name	Nominal fuel	Added fuel	k_{eff}	% increase
g1d6v.o:	HEU TRIGA	none	1.04287	
g1d6vg2.o:	HEU TRIGA	add LEU TRIGA	1.0502	100.7
g1d6vfsv.o:	HEU TRIGA	add FSV	1.05158	100.8
g1d6vpb.o:	HEU TRIGA	add PB	1.05589	101.2
g1d6val.o	HEU TRIGA	add AL	1.05747	101.4
g1d6vg1.o:	HEU TRIGA	add HEU TRIGA	1.06847	102.5
g1d6vfermi.o:	HEU TRIGA	add Fermi	1.06855	102.5
	Nominal fuel	Added fuel		
g2d6v.o:	LEU TRIGA	None	0.71776	
g2d6vg2.o:	LEU TRIGA	add LEU TRIGA	0.73446	102.3
g2d6vfsv.o:	LEU TRIGA	add FSV	0.73741	102.7
g2d6val.o:	LEU TRIGA	add AL	0.73815	102.8
g2d6vpb.o:	LEU TRIGA	add PB	0.74115	103.3
g2d6vfermi.o:	LEU TRIGA	add Fermi	0.77761	108.3
g2d6vg1.o:	LEU TRIGA	add HEU TRIGA	0.80001	111.5
	Nominal fuel	Added fuel		
fermi6dv.o:	Fermi	None	0.97147	
fermi6dval.o:	Fermi	add AL	0.97984	100.9
fermi6dvfsv.o:	Fermi	add FSV	0.98911	101.8
fermi6dvpb.o:	Fermi	add PB	0.99367	102.3
fermi6dvg2.o:	Fermi	add LEU TRIGA	0.99449	102.4
fermi6dvfermi.o:	Fermi	add Fermi	0.9976	102.7
fermi6dvg1.o:	Fermi	add HEU TRIGA	1.01431	104.4

The results of these calculations further confirm the previous results regarding the mixing of moderation states and the magnitude of the impact. With the well moderated fuels the biggest increase in k_{eff} results from inclusion of the highest fissile mass fuels. The converse is true as well, the array of Fermi fuel is markedly impacted by adding a single row of a moderated fuel. The primary exception is HEU TRIGA which is always a driving reactivity fuel, though high fissile mass fuels such as AL-plate and Fermi still provide a greater relative increase than other fuel type categories. The ranked order of the reactivity impact of the results directly follows the degree of moderation or lack thereof for the differing fuel type. Note that the largest overall impact when different fuel types are considered is present from adding any new fuel to an array that is primarily lower mass with high moderation (the LEU TRIGA case), with a very large impact resulting from the introduction of high mass fuels such as Fermi to a region of LEU TRIGA fuel.

6.1.5.4 Single fuel empty row calculations

Calculations were performed that considered a single fuel type filling the array but with increasing numbers of empty rows. While these calculations were not ultimately utilized in the development of the empirical model since it is not a goal of the empirical model to treat empty positions, they show an interesting result and therefore are reported. The trend lines that are fitted to the data presented in Figure 12 extrapolate to a Y-axis intercept that approximates the result for one single reflected canister k_{eff} quite well. The MCNP results for single canisters in a concrete corner for these fuels include 0.63 for HEU TRIGA (intercept 0.70), 0.26 for AL-plate (intercept 0.29), 0.26 for FSV (intercept 0.29), 0.41 for Peach Bottom (intercept 0.36), and 0.44 for LEU TRIGA (intercept 0.47).

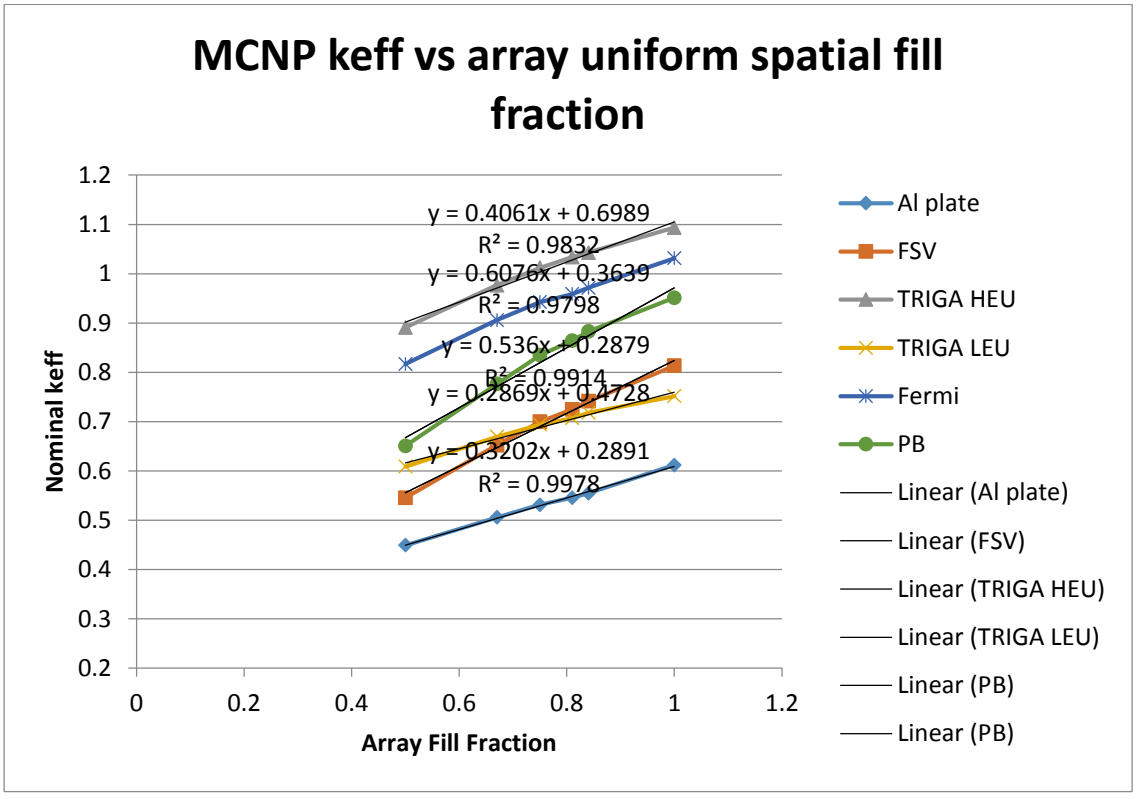

Figure 12 – Plot of MCNP nominal k_{eff} vs. array fill fraction for single fuel filling

6.1.5.5 Three Fuel Mixtures

The MCNP calculations in Table 13 model arrangements of three fuels in equal 1/3 proportions by alternating rows of each fuel considered. The rows are ordered diagonally. The fuels considered are AL-plate, HEU TRIGA, LEU TRIGA, FSV, and Fermi.

Table 13 – Uniform Mixtures of Three Fuels.

Case Name	Fuels Considered	k_{eff}
all-g1	All HEU TRIGA for comparison	1.09334
alg1fsv	AL-HEU TRIGA-FSV	0.98027
alg1g2	AL-HEU TRIGA-LEU TRIGA	0.93619
g2g1fsv	LEU TRIGA-HEU TRIGA-FSV	0.93059
alg2fsv	AL-LEU TRIGA-FSV	0.78759
fermig1fsv.o:	Fermi-HEU TRIGA-FSV	1.04653
fermig1g2.o:	Fermi-HEU TRIGA-LEU TRIGA	1.10039
fermig2fsv.o:	Fermi-LEU TRIGA-FSV	1.04278

The results of the three fuel mixtures confirm the results of the two fuel mixtures, in that the enhancement or multiplying effect of mixing high fissile mass/low moderation fuels with high moderation fuels can be very pronounced. For example, mixing AL-plate fuel, though it is less reactive than FSV or LEU TRIGA when considered in isolation, results in a more reactive configuration mixed with these fuels and HEU TRIGA in 1/3rd proportions than when LEU TRIGA or FSV are mixed with HEU TRIGA as 2/3 and 1/3 respectively (from the two fuel mixing cases). This shows the effective reactivity and neutron multiplication increase experienced by adding a significant amount of fissile mass in a well distributed manner to regions of the array where substantial moderation is present. The results also show that FSV fuel also experiences some degree of effective reactivity increase when present in an area with increased moderation as well. FSV fuel does not have as much moderation as Peach Bottom fuel in the models that compare the graphite fuels, and which is confirmed by the spectral results in Table 4. ORSNF and Rover Parka are also somewhat less moderated and could be expected to experience an effective increase in well moderated regions as well. However, this shows that among the moderated fuels that FSV is a preferable fuel to have in the vicinity of the higher mass fuels, due to the lower effective moderation. An important result is that in a well moderated region of the array, the addition of AL-plate fuel would result in a higher k_{eff} compared to the addition of LEU TRIGA, even though AL-plate is a much less reactive fuel when the single fuel array case is considered. Likewise, in a poorly moderated region of the array the addition of LEU TRIGA would result in a much greater k_{eff} comparted to the addition of high fissile mass

undermoderated fuels such as AL-plate. Ultimately the calculations show that uniform mixing of the high mass/low moderation fuels is not a preferable arrangement, and that lower regional k_{eff} results can be produced by grouping the higher mass/low moderation fuels such as AL-plate together. This is true as long as there are not an excessive number of high reactivity fuels placed together. This strategy will be utilized as long as the high fissile mass/high moderation fuels can be placed where they are not grouped together to a significant degree, i.e. multiple rows wide.

6.1.6 Array Fill Cases – Fill all central empty positions with one fuel type – current IFSF arrangement

The calculations in Table 14 consider the fuel storage array with the current arrangement of fuels with the exception that the empty positions in rows 28, 30, 32, and 33 are all filled, and are filled with the same fuel type configuration at one time. These empty positions are present in a well-moderated region of the array due to the presence of a large number of TRIGA fuels and PB fuel. The fuel configurations added are AL-plate, Fermi, FSV, HEU TRIGA, LEU TRIGA, and Peach Bottom. The increase in array k_{eff} trends similarly to the impact demonstrated in the previous calculations for the addition of a fuel to a well moderated region. As expected the largest increase is from the addition of HEU TRIGA and Fermi, followed closely by Peach Bottom. LEU TRIGA results in a slightly smaller increase than FSV since the region is already well moderated, therefore the addition FSV with more fissile mass results in a larger increase. Even though LEU TRIGA yields a greater singe canister array fill k_{eff} than FSV, the FSV is not as well moderated as LEU TRIGA, therefore putting FSV in a well moderated region causes a much improved utilization of the fissile mass. AL-plate results in the smallest increase, but proportionally larger than a fuel such as LEU TRIGA, since again the region is already well moderated such that the fissile mass of the much higher fissile mass AL-plate is also much better utilized. Note that all fuels result in the subcritical limit of 0.95 being exceeded, demonstrating that these 31 empty positions cannot be filled with these fuel types.

The condition of the current array with the interior 31 empty positions filled with LEU TRIGA is chosen as the starting condition for the optimization of the array for a few reasons. With HEU TRIGA there will not be a solution that would allow the addition of 31 canisters of such a reactive fuel type, and this additional quantity of HEU TRIGA no longer exists in the world. Some capacity remains in the actual array for HEU TRIGA and most of the HEU TRIGA has already been received as part of reduced enrichment research reactor initiatives. The PB and FSV fuels were not chosen because there are not significant quantities of other graphite fuels remaining to be stored by DOE.

There are significant quantities of AL-plate and LEU TRIGA remaining at research reactors that could eventually be stored at the IFSF. The LEU TRIGA is a more challenging fuel for which to optimize the arrangement because it elevates the array k_{eff} to a greater degree and because it provides an increase in the array moderation, which is the driving factor for array k_{eff}. The presence of additional AL-plate fuel would present a simpler optimization case because more canisters of low moderation fuel allow the creation of more blocks of low moderation regions or an increase in the surface area of low moderation regions which can be used to maximize neutron leakage near the more reactive fuels.

Figure 13 presents a depiction of the array with the above described empty positions filled with LEU TRIGA fuel, while Table 15 serves as a legend for Figure 13. This depiction is from a view of a component of the empirical model spreadsheet that shows the arrangement of the array being considered. This view incorporates a color coded depiction of the fuels that assists in visualizing the placement of the fuels according to relative reactivity. The coloring is according to the canister reactivity for the single fuel array fill calculations. Red represents fuels with a single fuel array k_{eff} > 1.0, orange for fuels with k_{eff} between 1.0 and 0.90, yellow for fuels with k_{eff} between 0.9 and 0.8, and green for fuels with k_{eff} less than 0.80. Purple corresponds to very high mass Fermi and Rover UBM fuels. Blue is for empty positions to be preserved empty. Grey represents the concrete walls. This color coding will be used in subsequent similar views of different array fuel canister arrangements to assist in depicting the changes and variations.

Table 14 – Empty array position fill cases.

Case Name	Description	k_{eff} w/ 0.05 bias
fbc-al.o:	Current storage array canister arrangement with empty positions of rows 28, 30, 32, and 33 filled with AL-plate fuel.	0.96784
fbc-fermi.o:	Like above, but fill empty positions with Fermi fuel.	1.01542
fbc-fsv.o:	Like above, but fill empty positions with FSV fuel.	0.98576
fbc-g1.o:	Like above, but fill empty positions with HEU TRIGA fuel.	1.05197
fbc-g2.o:	Like above, but fill empty positions with LEU TRIGA fuel (6x5 configuration).	**0.98153**
fbc-pb.o:	Like above, but fill empty positions with Peach Bottom fuel.	1.00976

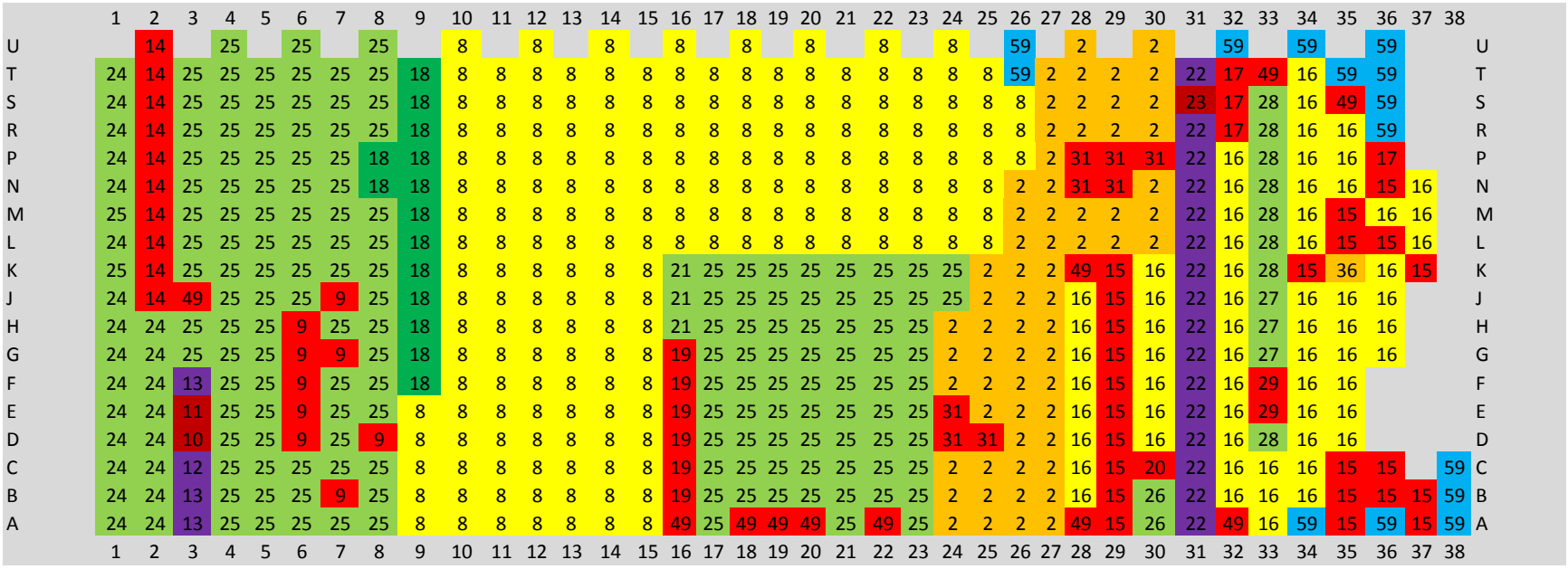

Figure 13 – Array fill case for the current storage arrangement with rows 28, 30, 32, and 33 empty positions filled with LEU TRIGA fuel.

The numbers correspond to the MCNP calculation universe number for the fuel canister model. This figure therefore depicts an identical arrangement as Figure 3 with the exception that the intended empty positions are filled with LEU TRIGA.

Table 15 – Legend for Figure 13

Fuel and MCNP calculation input universe number and color coding				
PB = 2	Rover UBM 4 = 13	ORSNF = 19	AL-Plate = 25	TRIGA LEU (6x6) = 36
FSV = 8	MTR Canal = 14	HTGR = 20	BER = 26	Rover = 49
SBT = 9	HEU TRIGA = 15	SUNY Pulstar = 21	Borax V = 27	
Rover UBM 1 = 10	LEU TRIGA (6x5) = 16	Fermi = 22	Pathfinder = 28	
Rover UBM 2 = 11	TRIGA-IN (MPR) = 17	Fermi-mod = 23	Pulstar – mod = 29	
Rover UBM 3 = 12	PBF = 18	Tory IIC = 24	PB-mod = 31	
Color coding – single fuel model array fill k_{eff} and color – identical color coding is used with subsequent spreadsheet array fill views				
Red >1.0	1.0> orange >0.90	0.90> yellow > 0.8	green <0.80	Purple – Fermi and high fissile mass Rover UBM
Blue – empty	Gray - walls			

6.1.7 Concentric Arrangement Calculations – Initial Application of Optimization Heuristics

This set of cases attempts to assess the impact of different discreet collections of three different fuel types to determine the potential reduction in array k_{eff} that is possible by arranging a certain fuel type near the perimeter of the array compared to a fuel type that is placed at the center of the array. These calculations therefore consider two concentric (rectangular) rings of two fuel types surrounding a center collection of a third fuel type. All cases have approximately 208 of each of the three fuel types, or each comprises approximately one-third of the fuel storage positions. See Figure 14 for a representation of the arrangement. The fuel types considered are AL-plate as the low moderation-high fissile mass fuel, FSV as the high moderation-low fissile mass fuel, and HEU TRIGA as the high moderation-high fissile mass fuel. This collection of fuels is representative but enveloping of the actual storage array since AL-plate fuel is present in the largest proportion for low moderation fuels, but bounds the fissile mass of the low moderation fuels for the vast majority of that type. FSV is the overall most numerous fuel type and is therefore applicable for this analysis. HEU TRIGA is a limiting fuel type for the high fissile mass high moderation fuels, and is enveloping for the most plentiful of that type which is Peach Bottom.

The fuels are arranged such that the outer ring is two or three rows deep (all but one side two deep), the inner ring is three or two rows deep (all but one side three deep), and the third fuel is in the remaining center positions. The results are shown in Table 16. As expected the results show that the presence of over 200 HEU TRIGA canisters far exceed a safe k_{eff} when all the HEU TRIGA is grouped together in the center of the array, and the configuration is also quite reactive when present in the inner ring. Placement of this fuel in the inner ring is not ideal since this most reactive fuel is grouped together in a thicker region that when in the outer ring and is surrounded by and interacting with another fuel that contributes significant quantities of moderated neutrons (FSV).

The case where HEU TRIGA is in the inner ring and FSV is in the center with AL-plate-placed at the perimeter has a higher k_{eff} than if the FSV and AL-plate were swapped because FSV is a more reactive and better moderated fuel than AL-plate. FSV is therefore a worse fuel than AL-plate to have in the center where peak fission density can potentially be highest from a geometric standpoint, and a very reactive fuel is surrounding this second most reactive fuel of the three. Likewise, the outside of the inner ring is the side of the fuel collection with the most surface area and is therefore the side most affected by having interaction with a low moderation fuel. In this way the interaction between different fuels can be thought of as being analogous to reflection. AL-plate is a much less

effective reflector to surround the more reactive fuel than FSV would be (in this case a multiplying reflector).

The ideal arrangement for these three fuels is to array them with the HEU TRIGA on the perimeter, with AL-plate intervening between the center FSV region and the HEU TRIGA. This decreases interaction between the more reactive fuels that are the only source of moderated neutrons. The intervening AL-plate fuel therefore serves to isolated the two fuels somewhat, and to also decrease the overall reactivity of the thin collection of HEU TRIGA by allowing greater leakage from this region of fuel that has a smaller effective size. Note however that there is not a large difference (~0.007 delta-k_{eff}) between this case and the case where HEU TRIGA is at the perimeter and AL-plate is in the center. All of these cases exceed the subcritical limit when the 0.05 bias is applied, however the 200+ canisters of HEU TRIGA that is considered far exceeds the number of canisters with this reactivity that is present in the actual IFSF arrangement.

Two other cases were performed that considered the best arrangements determined above (HEU TRIGA at the perimeter, outer ring), but with 104 HEU TRIGA canisters at the perimeter and 105 PB canisters comprising the remainder of the outer ring. These cases (conc1-pb and conc2-pb) resulted in a k_{eff} that would be acceptably subcritical, and which better represent the number of higher reactivity canisters stored in the actual array.

Table 16 – Concentric fuel arrangements of AL-plate, HEU TRIGA, and FSV fuel.

Case Name	Center Fuel	Inner Ring	Outer Ring	k_{eff} (without bias)
conc1a.o:	AL-plate	FSV	HEU TRIGA	0.95615
conc2.o:	FSV	AL-plate	HEU TRIGA	0.94876
conc3.o:	HEU TRIGA	FSV	AL-plate	1.07334
conc4.o:	HEU TRIGA	AL-plate	FSV	1.06756
conc5.o:	AL-plate	HEU TRIGA	FSV	1.01054
conc6.o:	FSV	HEU TRIGA	AL-plate	1.00435
conc1-pb.o:	AL-plate	FSV	Half HEU TRIGA Half PB	0.87617
conc2-pb.o:	FSV	AL-plate	Half HEU TRIGA Half PB	0.87113

The next case provides a comparison to show the potential benefit or detriment that could be obtained with either a preferred grouping of the three fuels (high mass-high moderation fuel on the perimeter) or the worst case arrangement (the high mass-high moderation fuel grouped in the center

with the second most reactive and well moderated fuel surrounding the center group). This case considers the same quantities and types of fuels as the above cases but arranges them uniformly alternating in both horizontal directions. This arrangement could be thought of as the most homogeneous arrangement of the fuels. In this case the high fissile mass fuel with low moderation is as maximally mixed with the moderated fuels as is possible with discreet canisters of one fuel type. This mixed state is a poor arrangement, as the calculation result shows, since this configuration is increasing utilization of the low moderation fuel. Since two thirds of the canisters present are well moderated the overall system is well moderated also. This arrangement is depicted in Figure 15 and the result is shown in Table 17.

Table 17 - Uniform Arrangement of AL-plate, FSV, and HEU TRIGA fuel

Case Name	Description	k_{eff} (without bias)
alfsvg1-unf.o:	Two dimensional uniform arrangement alternating AL-plate, FSV, and HEU TRIGA fuels	0.99065

A third comparison set is performed by grouping the same three fuel types in alternating diagonal rows, similar to the row grouping cases performed for the two-fuel arrangements. The results presented in Table 18 show that alternating every single row or every other row both result in a less reactive arrangement than the uniform arrangement case, but not as low as the best concentric arrangement. This shows that placement of a reactive fuel such as HEU TRIGA in more than three rows wide is undesirable, at least when another well moderated fuel is present. The two row fuel grouping case is slightly preferable to the alternating row case (0.0016 delta-k_{eff} lower), since this reduces the potential exposure of the high fissile mass fuel to moderated neutrons from the other two fuel types. However grouping the rows of the fuel types to a greater degree result in a more reactive arrangement because an excessive amount of the more reactive fuel is placed together.

Table 18 - Grouping of rows of three different fuels – AL-plate, FSV, and HEU TRIGA

Case Name	Description	k_{eff} (without bias)
alg1fsv	Alternating rows of AL-HEU TRIGA-FSV	0.98027
2-alg1fsv.o:	Alternating paired rows of AL-HEU TRIGA-FSV	0.97862
3-alg1fsv.o:	Alternating groups of three rows of AL-HEU TRIGA-FSV	0.98533
4-alg1fsv.o:	Alternating groups of four rows of AL-HEU TRIGA-FSV	1.00287
5-alg1fsv.o:	Alternating groups of five rows of AL-HEU TRIGA-FSV	1.01517

These cases show a hierarchy in the preferred arrangement of fuels to guide the potential rearrangement of fuels with a goal to give the lowest possible k_{eff}. The worst arrangement is to group the most reactive fuels, generally high fissile mass and high moderation, in a single collection with more than two rows adjacent. Collections of three or more canisters wide should be avoided. An arrangement with a lower k_{eff} would be to uniformly arrange the fuels. Even more preferable is to arrange the fuels in alternating rows. Either of these two arrangements increases the potential for neutron leakage and reduce the degree of effective neutron moderation over a larger volume. A more ideal arrangement is with the fuels in a configuration where the well moderated, more reactive fuels can be isolated near the edge of the array, especially if the resultant number of rows is two deep or less. This maximizes the neutron leakage for the most reactive canisters, and decreases interaction with the other fuels. A sufficient number of low moderation canisters can also serve to isolate separate regions of high moderation fuels. Likewise, a large number of truly low fissile mass fuels that have high moderation would also be able to serve as a lower reactivity isolation zone between more reactive fuels.

A final set of calculations is performed that are a variation of the concentric case with AL-plate fuel at the center and HEU TRIGA at the perimeter. These cases introduce sixteen canisters of Fermi fuel to the low moderation region of the array. Recall that Fermi is an especially high fissile mass fuel with over twice the fissile mass per canister as AL-plate. This fuel type is also very reactive when present in a large grouping based strictly on the quantity of fissile mass present. It has also been shown previously that this fuel results in a large reactivity increase when present in a region with significant moderation. In these cases the number of AL-plate canisters is reduced as some are replaced by Fermi. Therefore the total fissile mass in the array is significantly increased and the number of high reactivity canisters (single canister array fill k_{eff} >1.0) is increased. The cases in Table 19 however show that this very high fissile mass fuel (in these quantities) can essentially be “hidden”

if placed in the low moderation region of the array. The increase in the array k_{eff} is very minimal, and the difference between the two vertical row cases is statistically insignificant (less than a two-sigma change for the calculation statistical uncertainty). The fuel is placed with a sufficient number of rows intervening between the Fermi fuel and the well moderated fuels such that there is minimal interaction of thermal neutrons from the moderated fuels with the very high fissile mass fuel. Also, arranging the Fermi canisters in groups one row wide ensures that a fissile density sufficient for a high k_{eff} in a fast neutron spectra is not obtained. Demonstration of this ability to minimize the potential impact to increase k_{eff} by these very high fissile mass fuels is an important result for the goal of minimizing the overall array k_{eff}. Case conc1a-frm-midv2 is shown in Figure 16. This case was the arrangement that had the lowest k_{eff} with the 16 Fermi canisters added.

Table 19 – Concentric arrangement case 1 with Fermi fuel added to AL-plate region.

Case Name	Description	k_{eff} (without bias)
conc1a.o:	Baseline case with no Fermi in the center	0.95615
conc1a-frm-mid.o:	Place 16 canisters of Fermi fuel in a long singe horizontal row at the center of the AL-plate region between rows 10 and 26.	0.95900
conc1a-frm-midv1.o:	Place 16 canisters of Fermi fuel in the center of the AL-plate region in groups four tall in rows 10, 15, 20, and 25.	0.95759
conc1a-frm-midv2.o:	Place 16 canisters of Fermi fuel in the AL-plate region in groups eight tall in rows 14 and 23.	0.95702

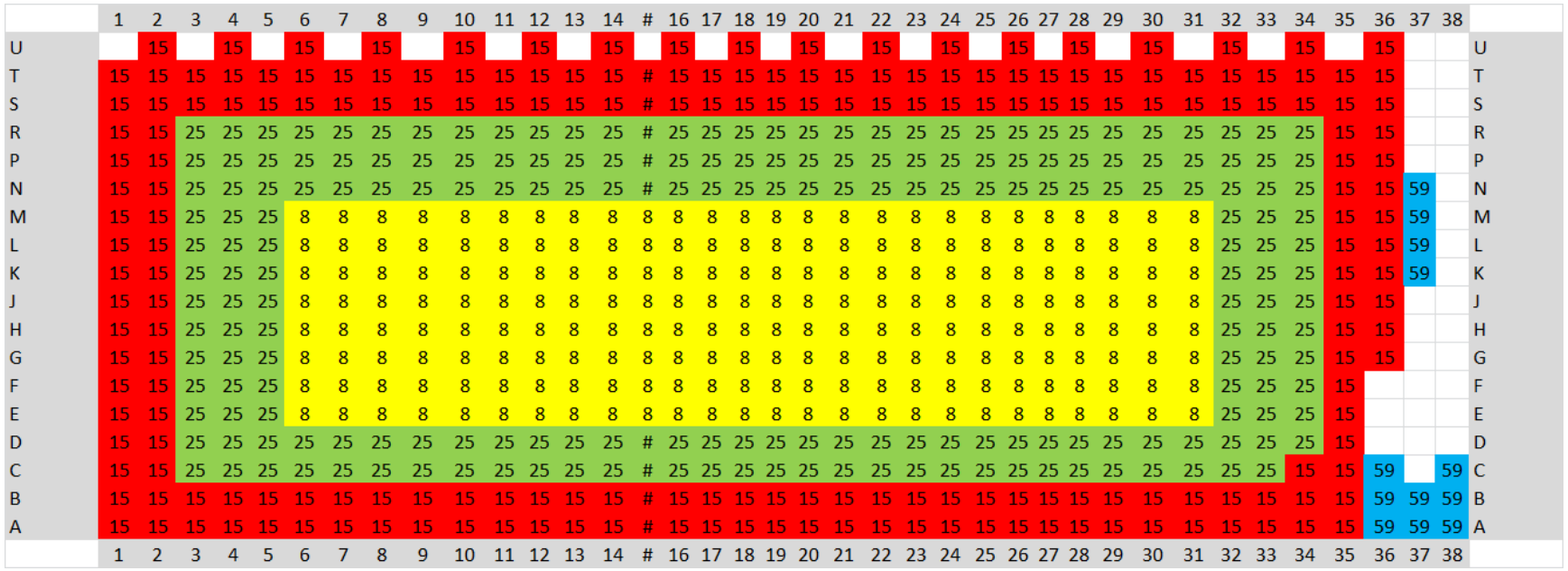

Figure 14 – Arrangement for case “conc2.o”

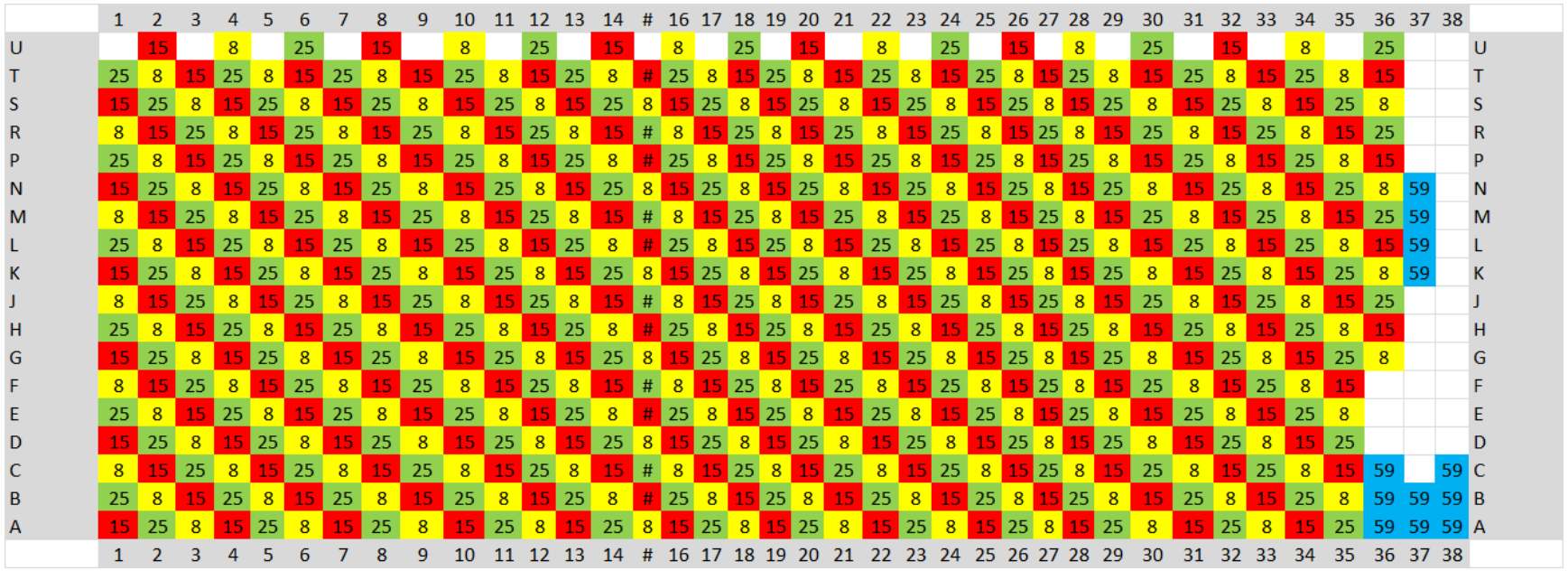

Figure 15 – Arrangement for case “uniform”

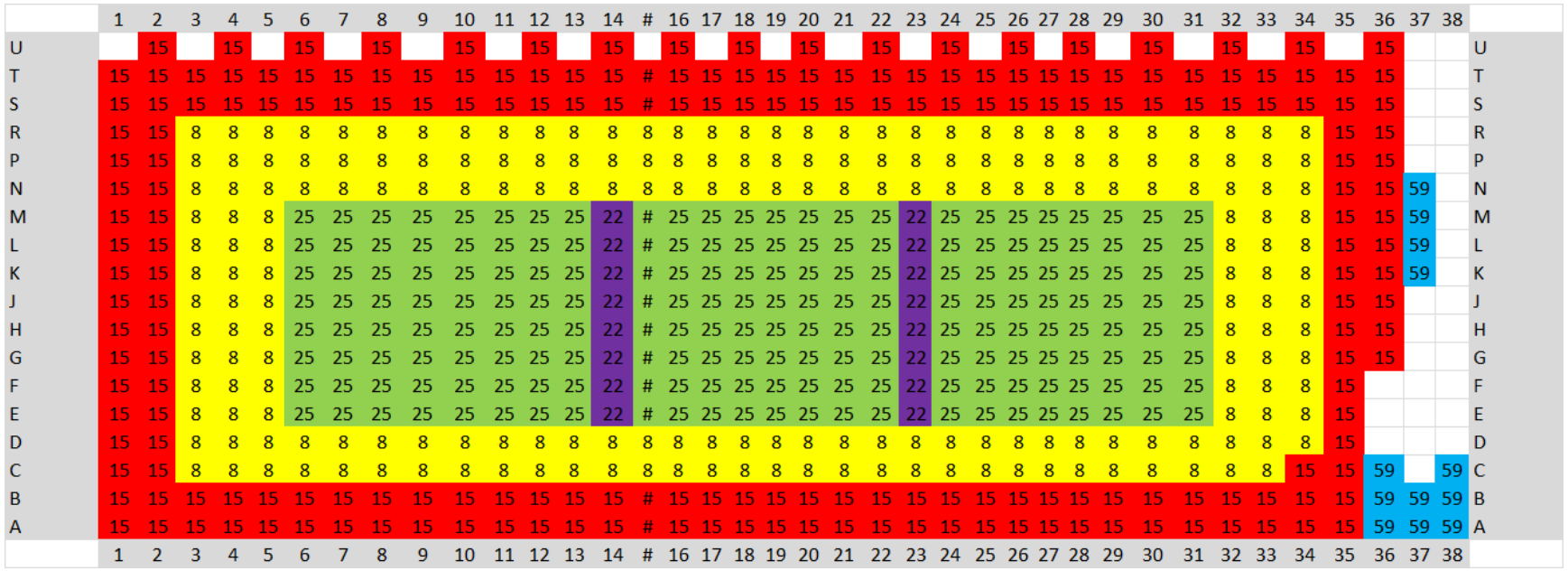

Figure 16 – Arrangement for case “conc1a-frm-midv2.o”

6.2 Empirical Model

The empirical model takes a weighted average from a given canister and the 60 canisters that form four concentric rings around that canister based on the single-canister k_{eff} value for each of the fuel canister positions. The weighted averages were based on data fits of the MCNP calculations that considered well moderated fuels. The single canister k_{eff} values are then modified to include additional multiplying factors for unmoderated fuels when they are present in regions of the array with a threshold degree of moderation. These factors were determined from the two and three fuel mixing cases, as well as from the array fill cases and some of the concentric cases. The moderation multiplying factors range from 1.02 to 1.61 depending on the subject unmoderated fuel type and the degree of moderation of the array region. The k_{eff} value of the central canister in a group of 60 is divided by 10.24, the sum of the immediately adjacent six canister's k_{eff} surrounding the canister of concern is divided by 4.63, the sum of the twelve canister's k_{eff} values in the second ring around the canister of concern is divided by 3.38, the sum of the eighteen canister's k_{eff} values in the third ring around the canister of concern is divided by 5.53, and the sum of the twenty-four canister's k_{eff} values in the fourth ring of the canister of concern is divided by 6.3. In all cases the k_{eff} value is the single canister array fill value as modified for the degree of array region moderation. These resultant values are summed to produce the ultimate k_{eff} value produced by the subject group of sixty canisters, and this value is applied to the center canister position in the final matrix result view of the array. The highest resultant value for any of the array positions is the ultimate k_{eff} value of the empirical model that simulates the overall array k_{eff} value that would be returned by MCNP. In this way the empirical model is returning a greater amount of information than an MCNP calculation, since the MCNP calculation result does not state what region of the array is producing the overall result, since a more reactive fraction of the array can produce the same k_{eff} value as the entire array. The empirical model however shows a distribution of k_{eff} values by position that shows an effective fission distribution present in the array. In this way the empirical model is more useful for optimization purposes than MCNP results since the empirical model shows the regions of the array with greater neutron multiplication and the regions with less neutron multiplication.

A fit was performed after applying the basic empirical model developed from the all-moderated fuel arrangements to the arrangements that involved mixing of the unmoderated fuels with the moderated fuels. The empirical model at this point was applied to the arrangements that considered concrete walls around smaller sections of the array. The concrete walls are treated by considering them as canisters, but with lower k_{eff} values assigned, which accounts for the proportion of neutrons returned by the reflector. The applicable wall k_{eff} assigned are 0.5 for two equivalent rows of wall

depth, 0.4 for the third equivalent row of depth, and 0.3 for a forth equivalent row of depth. These values were determined from fitting the data to the partial array cases with concrete walls. This aspect of the model is the least well developed, as the impact of the reflector does vary to some degree depending on the moderation state of the adjacent fuel. This is not a large concern for the fundamental problem to be addressed because the reactivity of the current storage arrangement is dominated by the neutron multiplication from fuels in the center of the east side of the array. If complete rearrangements of the IFSF were the goal of the analysis then the importance of a more precise treatment of the wall reflection would be greater.

Table 20 presents a view of the empirical model calculation for a given point of the array and the values of the weighting factors for neighboring canisters, the moderation correction factors, and the wall reflection. Figure 17 shows a depiction of the final empirical model spreadsheet view that shows the array k_{eff} value as determined by canister contribution. The ultimate array k_{eff} value returned by the array empirical model is the maximum k_{eff} value of the various array positions. In this way the array empirical model determines the array peak reactivity contribution location, as well as the location(s) of minimum neutron multiplication.

Table 20 – View of a representative section of the empirical model spreadsheet calculation.

Highlight of moderation-adjusted single canister fill k_{eff} values used to calculate positional k_{eff} for position J-29.

24	25	26	27	28	29	30	31	32	33	34	35
0.3	0.3	0.3	0.3	0.3	0.3	0.3	0.3	0.3	0.3	0.3	0.3
0.4	0.4	0.4	0.4	0.4	0.4	0.4	0.4	0.4	0.4	0.4	0.4
0.5	0.5	0.5	0.5	0.5	0.5	0.5	0.5	0.5	0.5	0.5	0.5
0.5	0.5	0.5	0.5	0.5	0.5	0.5	0.5	0.5	0.5	0.5	0.5
0.813	0.5	0.194	0.5	0.951	0.5	0.951	0.5	0.194	0.5	0.010	0.5
0.813	0.860	0.194	0.951	0.951	0.951	0.951	1.050	1.002	1.267	0.844	0.010
0.813	0.860	0.860	0.951	0.951	0.951	0.951	1.208	1.002	0.680	0.844	1.267
0.813	0.860	0.860	0.951	0.951	0.951	0.951	1.050	1.002	0.680	0.844	0.844
0.813	0.860	0.860	0.951	1.028	1.028	1.028	1.050	0.844	0.680	0.844	0.844
0.813	0.860	0.951	0.951	1.028	1.028	0.951	1.050	0.844	0.680	0.844	0.844
0.813	0.860	0.951	0.951	0.951	0.951	0.951	1.050	0.844	0.680	0.844	1.100
0.813	0.860	0.951	0.951	0.951	0.951	0.951	1.050	0.844	0.680	0.844	1.100
0.810	0.951	0.951	0.951	1.267	1.100	0.844	1.050	0.844	0.680	1.100	0.922
0.810	0.951	0.951	0.951	0.844	1.100	0.844	1.050	0.844	0.790	0.844	0.844
0.951	0.951	0.951	0.951	0.844	1.100	0.844	1.050	0.844	0.790	0.844	0.844
0.951	0.951	0.951	0.951	0.844	1.100	0.844	1.050	0.844	0.790	0.844	0.844
0.951	0.951	0.951	0.951	0.844	1.100	0.844	1.050	0.844	0.398	0.844	0.844
1.028	0.951	0.951	0.951	0.844	1.100	0.844	1.050	0.844	0.398	0.844	0.844
1.028	1.028	0.951	0.951	0.844	1.100	0.844	1.050	0.844	0.680	0.844	0.844
0.951	0.951	0.951	0.951	0.844	1.100	0.997	1.050	0.844	0.844	0.844	1.100
0.951	0.951	0.951	0.951	0.844	1.100	0.537	1.050	0.844	0.844	0.844	1.100
0.951	0.951	0.951	0.951	1.267	1.100	0.537	1.050	1.267	0.844	0.194	1.100
0.5	0.5	0.5	0.5	0.5	0.5	0.5	0.5	0.5	0.5	0.5	0.5
0.5	0.5	0.5	0.5	0.5	0.5	0.5	0.5	0.5	0.5	0.5	0.5
0.4	0.4	0.4	0.4	0.4	0.4	0.4	0.4	0.4	0.4	0.4	0.4
0.3	0.3	0.3	0.3	0.3	0.3	0.3	0.3	0.3	0.3	0.3	0.3

	1	2	3	4	5	6	7	8	9	10	11	12	13	14	15	16	17	18	19	20	21	22	23	24	25	26	27	28	29	30	31	32	33	34	35	36	37	
U		0.619		0.575		0.523		0.512		0.561		0.596		0.602		0.602		0.602		0.602		0.599		0.587		0.544		0.633		0.648		0.564		0.471		0.396		U
T	0.621	0.679	0.662	0.630	0.587	0.560	0.541	0.542	0.547	0.605	0.640	0.659	0.667	0.672	0.670	0.672	0.670	0.672	0.670	0.672	0.670	0.665	0.661	0.652	0.650	0.628	0.689	0.718	0.746	0.742	0.739	0.698	0.648	0.575	0.468	0.420		T
S	0.658	0.721	0.708	0.665	0.617	0.584	0.558	0.557	0.570	0.633	0.680	0.704	0.718	0.722	0.724	0.722	0.724	0.722	0.724	0.722	0.724	0.716	0.720	0.717	0.720	0.741	0.772	0.802	0.832	0.828	0.835	0.777	0.697	0.652	0.609	0.478		S
R	0.677	0.744	0.729	0.687	0.632	0.594	0.568	0.560	0.578	0.648	0.700	0.731	0.744	0.751	0.752	0.751	0.752	0.751	0.752	0.751	0.753	0.750	0.753	0.760	0.774	0.797	0.831	0.862	0.876	0.880	0.865	0.816	0.757	0.699	0.643	0.547		R
P	0.686	0.756	0.741	0.698	0.638	0.598	0.568	0.551	0.582	0.655	0.709	0.743	0.758	0.768	0.763	0.765	0.763	0.767	0.765	0.767	0.766	0.770	0.771	0.782	0.805	0.836	0.868	0.897	0.909	0.912	0.891	0.826	0.770	0.745	0.704	0.670		P
N	0.689	0.763	0.748	0.704	0.642	0.599	0.569	0.553	0.581	0.653	0.712	0.746	0.764	0.770	0.766	0.764	0.762	0.764	0.766	0.766	0.767	0.770	0.780	0.795	0.823	0.861	0.889	0.913	0.924	0.914	0.893	0.848	0.800	0.784	0.760	0.726	0.643	N
M	0.688	0.761	0.748	0.707	0.652	0.608	0.577	0.571	0.586	0.656	0.712	0.746	0.761	0.766	0.755	0.750	0.745	0.750	0.751	0.754	0.755	0.762	0.776	0.801	0.834	0.870	0.899	0.917	0.921	0.911	0.887	0.845	0.811	0.802	0.809	0.753	0.684	M
L	0.688	0.767	0.754	0.721	0.663	0.630	0.595	0.587	0.594	0.661	0.713	0.747	0.759	0.761	0.746	0.733	0.726	0.727	0.728	0.732	0.736	0.749	0.768	0.799	0.837	0.873	0.897	0.918	0.914	0.904	0.883	0.845	0.818	0.814	0.813	0.773	0.694	L
K	0.678	0.762	0.758	0.730	0.679	0.647	0.617	0.600	0.603	0.663	0.714	0.746	0.755	0.754	0.734	0.693	0.698	0.696	0.695	0.700	0.709	0.728	0.758	0.797	0.847	0.880	0.902	0.935	0.924	0.902	0.884	0.851	0.824	0.837	0.806	0.756	0.698	K
J	0.683	0.761	0.793	0.748	0.719	0.679	0.664	0.620	0.618	0.671	0.718	0.744	0.754	0.747	0.727	0.678	0.668	0.653	0.652	0.654	0.670	0.695	0.746	0.796	0.848	0.880	0.902	0.907	0.921	0.900	0.885	0.856	0.831	0.812	0.786	0.732		J
H	0.676	0.744	0.769	0.766	0.740	0.725	0.682	0.644	0.634	0.681	0.722	0.741	0.754	0.746	0.725	0.676	0.652	0.628	0.623	0.622	0.644	0.679	0.738	0.807	0.853	0.878	0.897	0.902	0.915	0.897	0.886	0.859	0.833	0.804	0.759	0.698		H
G	0.664	0.741	0.773	0.776	0.751	0.748	0.715	0.669	0.653	0.697	0.728	0.748	0.756	0.755	0.738	0.721	0.657	0.622	0.609	0.609	0.629	0.671	0.738	0.808	0.858	0.883	0.894	0.897	0.910	0.900	0.888	0.864	0.833	0.802	0.746	0.678		G
F	0.666	0.745	0.797	0.786	0.771	0.763	0.720	0.689	0.678	0.712	0.734	0.755	0.762	0.766	0.754	0.735	0.669	0.626	0.604	0.604	0.622	0.666	0.740	0.813	0.861	0.884	0.895	0.898	0.909	0.898	0.890	0.866	0.862	0.796	0.741			F
E	0.671	0.754	0.814	0.796	0.777	0.767	0.733	0.711	0.721	0.727	0.745	0.763	0.769	0.771	0.769	0.749	0.686	0.636	0.616	0.612	0.628	0.671	0.745	0.820	0.865	0.884	0.898	0.897	0.911	0.896	0.900	0.872	0.863	0.801	0.746			E
D	0.668	0.752	0.820	0.797	0.777	0.768	0.745	0.745	0.735	0.742	0.750	0.763	0.769	0.773	0.768	0.753	0.694	0.650	0.625	0.623	0.636	0.677	0.745	0.819	0.863	0.881	0.891	0.887	0.899	0.886	0.880	0.853	0.819	0.795	0.744			D
C	0.663	0.741	0.797	0.780	0.761	0.743	0.734	0.728	0.732	0.740	0.741	0.753	0.760	0.762	0.765	0.755	0.708	0.669	0.654	0.642	0.655	0.683	0.746	0.800	0.846	0.864	0.875	0.875	0.883	0.870	0.859	0.837	0.801	0.780	0.746	0.710		C
B	0.637	0.703	0.749	0.737	0.721	0.703	0.712	0.695	0.704	0.707	0.711	0.721	0.723	0.726	0.727	0.725	0.680	0.656	0.645	0.634	0.637	0.666	0.711	0.757	0.798	0.811	0.824	0.824	0.827	0.785	0.812	0.792	0.765	0.742	0.739	0.696	0.648	B
A	0.604	0.653	0.694	0.680	0.672	0.648	0.653	0.644	0.661	0.665	0.671	0.677	0.679	0.689	0.691	0.712	0.668	0.697	0.681	0.681	0.640	0.694	0.685	0.722	0.744	0.759	0.769	0.786	0.769	0.730	0.752	0.747	0.714	0.651	0.691	0.610	0.625	A

Figure 17 – View of array empirical model spreadsheet result.

This view corresponds to the optimization starting point of the current array configuration with the empty interior canisters filled with LEU TRIGA fuel. The overall array k_{eff} is the highest value of any of the positions (in this case 0.935 without 0.05 bias). In the array empirical model spreadsheet the color red represents positions with k_{eff} greater than 0.90, orange represents k_{eff} between 0.85 and less than 0.899, yellow represents k_{eff} between 0.80 and less than 0.849, light green represents k_{eff} between 0.75 and less than 0.799, medium green represents k_{eff} between 0.70 and less than 0.749, dark green represents k_{eff} between 0.60 and less than 0.699, and blue represents k_{eff} less than 0.60.

6.3 Application of the empirical model to determine optimized fuel storage arrangements.

6.3.1 Initial Optimization Results

The empirical model was used to perform interrogations of the array arrangement by iterating different canister arrangements and searching for the resultant lowest maximum k_{eff}. The process focused on performing relocations of the fuel canisters from positions that produced the highest k_{eff} result in the empirical model. The k_{eff} change primarily resulted from decreasing the density of the more reactive canisters and the specific fuel that the canister was swapped for, or in later cases when more canisters are moved, from the resulting location that the higher reactivity canister is moved to. The movements are primarily guided by the inherent understanding of the system gained from chapter 6.1. The basic focus includes movement of the higher reactivity fuels away from other higher reactivity fuels, towards the perimeter or to borders with lower moderation or low fissile mass fuel groupings and where the replacement canister is a lower fissile mass and lower moderation canister. The next priority is to decrease the presence of very high fissile mass fuels in the high moderation regions. The emphasis remained on the highest reactivity region of the array until the highest reactivity production moved to a different location of the array. The taboo constraints were imposed on the interrogation of the empirical model through prohibitions on possible movements. The preferred movements were applied by initial targeted swap movements and also by a fitness function. Random movements were applied through a random number generated movement applied to the grid coordinate system.

The heuristic rules applied to perform the optimization search are as follows:

- “taboo” events
  - No swapping with the same canister fuel type
  - No swapping with a more reactive fuel
  - No swapping with a higher moderation fuel to a moderated location
  - No swapping with nearby locations
- Prefer to swap high moderation with lower moderation or lower fissile
- Prefer to move reactive fuels (high moderation/high fissile mass) to the perimeter or bordering low moderation

- Focus swaps on general region of canister returning the max. k_{eff} in the array empirical model
- Impose random swaps that break the preference rules

The optimization searches focused on a range of two, six, twelve, 16, 20, 24, 27, 29 and 30 canister swaps. For the initial, smaller number of swaps the optimal canister movements are essentially a sequential process. The best candidate solutions returned by the empirical model iterations were verified by performing an MCNP calculation with the arrangement of interest. The results of the MCNP calculations that returned the lowest results for the respective number of canister swaps are presented in Table 21. Full results of arrangements confirmed with MCNP calculations are presented in Appendix A. The results show that the moderated Pulstar and the central row 28 Rover and central row 29 HEU TRIGA are the initial fuels that provide the most benefit from relocation. The initial best fuel for the swap is PBF, because this is a fuel canister with a particularly low fissile mass and moderation that comes from a region that can tolerate the insertion of a number of high moderation/high fissile mass reactive fuel canisters in a row. This is because PBF fuel is in a single row between two wide collections of AL-plate and FSV fuels, which is an ideal border location for placement of well moderated fuels. This arrangement is favorable until it becomes necessary to move Fermi fuel into the western AL-plate region, since Fermi is the next priority fuel to be moved after a significant number of row 29 HEU TRIGA have been relocated (those that are not against the wall). Fermi should be placed in a low moderation region of the array with at least three rows of low moderation canisters providing spacing to moderated canisters. Once Fermi is moved into the west AL-plate region, there is not a sufficient buffer of three rows of AL-plate fuel between the HEU TRIGA in the former PBF location and other reactive fuels. HEU TRIGA cannot remain in the PBF row, and therefore the HEU TRIGA should be moved to the walls in a single row bordering the wall. The optimal re-arrangement for 29 canister swaps is shown in Figure 18 with the resulting empirical model output as well.

Table 21 – Optimal canister relocation results for 4 to 60 canister relocation movements.

Case	Canister Swaps	Canister Movements	Description	MCNP k_{eff} w/ 0.05 bias All sigma <0.0005
Fbc-g2	0	0	Initial current arrangement with empty interior positions filled with LEU TRIGA (6x5 bucket). Results in 31 newly filled canisters.	0.9815
m2-plstr-PBF	2	4	Swap two row 33 Pulstar with north row 9 PBF.	0.9723
bf-g2-6m-a2a	6	12	Swap two row 33 Pulstar, row 28 central Rover, and three center row 29 HEU TRIGA with north row 9 PBF.	0.9534
bf-g2-12m-a2	12	24	Like above case, except two Pulstar to south row 11 and 13 FSV. Swap three more centermost row 29 HEU TRIGA with row 9 PBF, and row 30 PB-mod and south row 29 PB-mod with FSV from north wall of rows 18 and 20.	0.9366
bf-g2-16m-a2	16	32	Like above but swap remaining row 29 PB-mod and south row 28 PB-mod with N wall FSV of rows 14 and 16, swap south row 32 TRIGA-IN(MPR) with north wall row 19 FSV, and swap one more HEU TRIGA from row 29 with row 9 PBF.	0.9338
bf-g2-20m-b	20	40	Change from above. Swap center eight HEU TRIGA from row 29 to north wall FSV, row 29 center rover to north wall FSV also. Two row 33 Pulstar to south rows 11 and 13 FSV. South row 32 TRIGA–IN to north FSV wall. Center row 28 PB-mod, and rows 29 and 30 PB-mod to north wall FSV, and row 33 Fermi adjacent to PB fuel swapped with AL-plate of north row 6.	0.9300
bf-g2-24m-b4	24	48	Like above, but move PB-mod from row 25 and adjacent PB from row 26 to south wall FSV rows 12 and 14. Swap HTGR to south row 10 FSV. Swap row 31 Fermi-mod and one more Fermi to AL-plate in row 6, with the Fermi-mod placed next to the wall.	0.9252
bf-g2-27m-b4	27	54	Like above, but swap three more Fermi from row 31 with AL-plate fuel in center of AL-plate region in row 20.	0.9235
bf-g2-29m-c	29	58	Like above but swap two more row 31 Fermi to row 20 AL-plate, centered. Maintain spacing of two AL-plate canister spacing between wall Rover canister and FSV region. See Figure 18.	0.9233
m6-2b-5pbm	30	60	Different than above. Same movement of Pulstar, HEU TRIGA and center Rover, but all row 31 Fermi except three to row 6 and row 20 AL-plate regions. HTGR and TRIGA-IN is not swapped. All four north PB-mod are swapped with south wall FSV, no south region PB-mod is moved.	0.9243

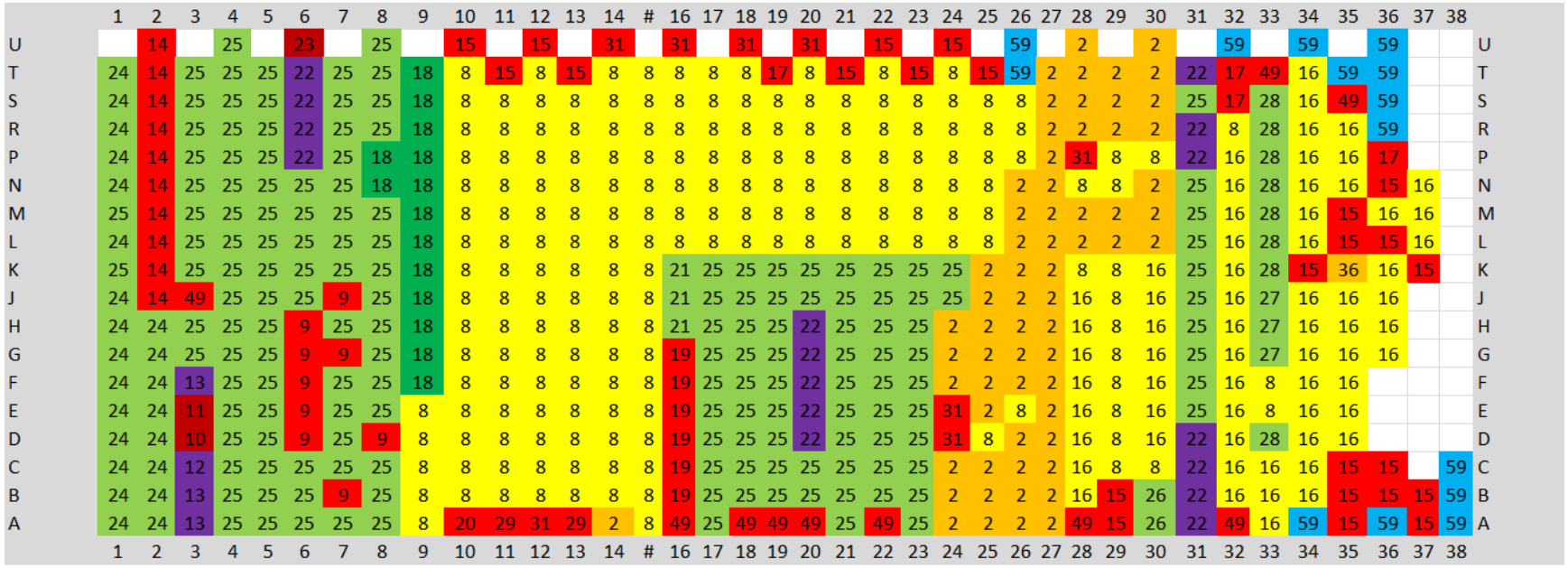

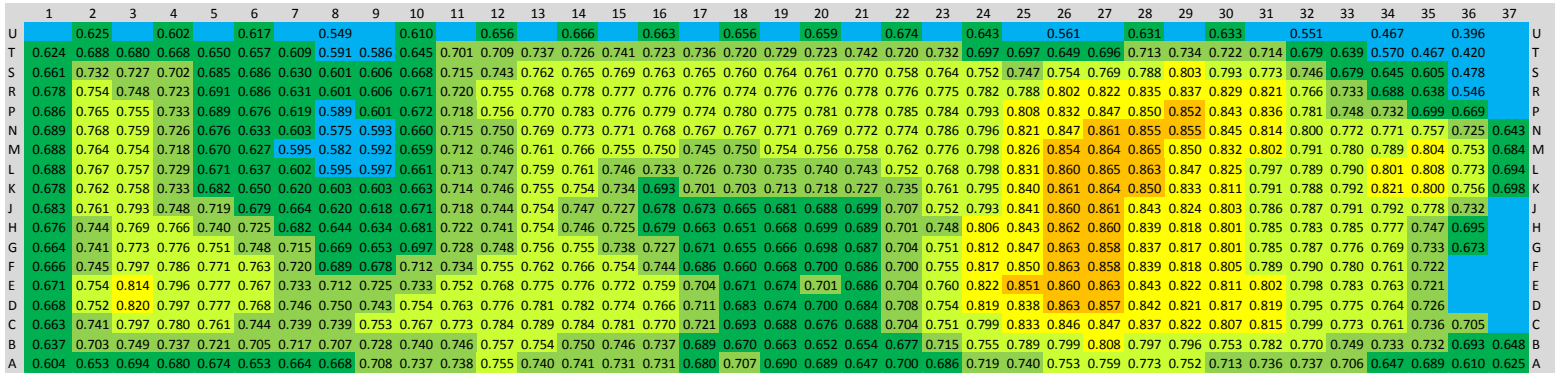

Figure 18 – Plot of optimal arrangement for 29 canister swap movements and empirical model result. This figure corresponds to case “bf-g2-29m-c”.

Note that it is important in the decision on which canisters to move to consider the end-state desired result in k_{eff} reduction, since the optimal movements with an increasing number of movements is not always a progressive process. For example, initial need may mean that the required arrangement and k_{eff} reduction for 16 canister swaps is initially desired, and accomplished. If at a later date the arrangement for 27 canister swaps is desired, then ultimately a greater number of canister movements will be required than if the movements were originally performed for the 27 swap configuration. Many of the optimal 16 swap movements are not optimal for the 27 swap configuration.

6.3.2 Full array optimization scoping attempts

An attempt is made to determine the potential reduction in k_{eff} if the entire array were re-arranged. Various configurations were iterated in the empirical model guided by the behavior learned from the analysis of chapter 6.1.7 with concentric arrangements. Various candidate arrangements were also confirmed with MCNP as documented in Appendix A. The MCNP result for the best arrangement determined from this initial scoping is presented in Table 22.

Table 22 – Potential near-optimal arrangement for entire array.

Case	Canister Swaps	Canister Movements	Description	k_{eff} w/ 0.05 bias sigma <0.0005
Fbc-g2	0	0	Initial current arrangement with empty positions filled with LEU TRIGA (6x5 bucket)	0.9815
bf-g2-m-all-a5-g9b	203	406	See Figure 19	0.9131

Note that various purely concentric based arrangements similar to those determined in chapter 6.1.7 did not yield a better k_{eff} than the arrangement depicted in Figure 19. This may be due to the fact that a greater proportion of middle reactivity (k_{eff} between 0.8 and 0.9) low mass/high moderation fuels (251 total) are present in the actual storage arrangement for optimization compared to the chapter 6.1.7 hypothetical mix of equal thirds of HEU TRIGA, FSV, and AL-plate considered in the initial scoping of concentric arrangements. This increased number of middle reactivity fuels results in a thicker layer of the ring from the standpoint of the number of rows of this type. Also, the chapter 6.1.7 concentric ring calculations considered the middle reactivity fuel all to the FSV fuel. FSV has a single canister type array fill value of ~0.81, Compared to the LEU TRIGA single canister array fill

value of ~0.84. The actual array has a significant quantity (64 canisters) of LEU TRIGA present in the array to be optimized. LEU TRIGA also introduces more moderation than FSV which can have a large influence on neighboring fuels compared to FSV. The optimal arrangement that was determined again shows the importance of edges or borders of lower moderation regions or regions of lower reactivity fuels as ideal places to locate linear rows of high moderation/high reactivity fuels. Placement at these borders optimizes the balance of minimum interaction of these more reactive fuels with themselves while also placing them with the best possible neighboring fuels to maximize axial leakage and reduce overall moderation over a local region of the array. The optimal arrangement found also makes use of the ability to "hide" a row of the very high mass fuels such as Fermi in a low moderation region of sufficient size, such as in an AL-plate region. Fortunately, the current IFSF arrangement has similar regional fuel arrangements, where low moderation and low fissile mass fuels are present in "block" arrangements, in which to place the fuels of concern. Ultimately, this work demonstrates the sensitivity of the full array to positioning of some fuels, and the fact that ever increasing effort must be employed to achieve progressively smaller gains in the attempt to find the optimal state for the entire array.

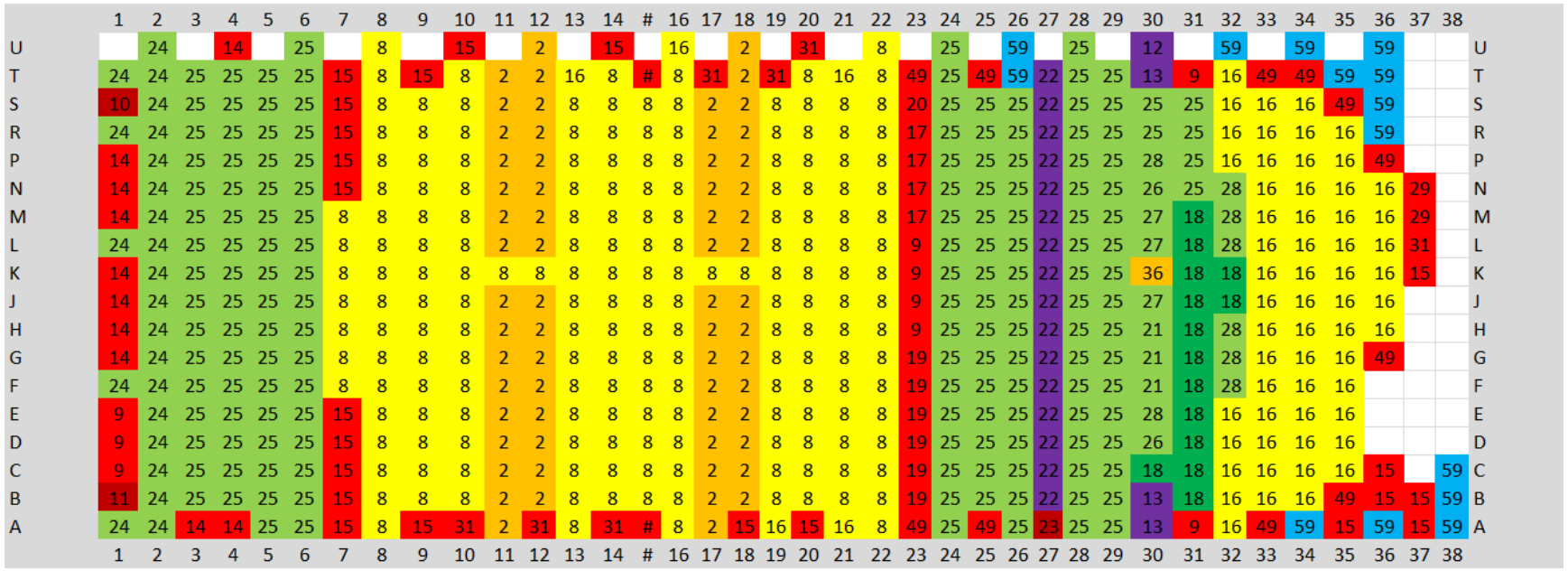

	1	2	3	4	5	6	7	8	9	10	11	12	13	14	#	16	17	18	19	20	21	22	23	24	25	26	27	28	29	30	31	32	33	34	35	36	37	38	
U		24		14		25		8		15		2		15		16		2		31		8		25		59		25		12		59		59		59			U
T	24	24	25	25	25	25	15	8	15	8	2	2	16	8	#	8	31	2	31	8	16	8	49	25	49	59	22	25	25	13	9	16	49	49	59	59			T
S	10	24	25	25	25	25	15	8	8	8	2	2	8	8	8	8	2	2	8	8	8	8	20	25	25	25	22	25	25	25	25	16	16	16	49	59			S
R	24	24	25	25	25	25	15	8	8	8	2	2	8	8	8	8	2	2	8	8	8	8	17	25	25	25	22	25	25	25	25	16	16	16	16	59			R
P	14	24	25	25	25	25	15	8	8	8	2	2	8	8	8	8	2	2	8	8	8	8	17	25	25	25	22	25	25	28	25	16	16	16	16	49			P
N	14	24	25	25	25	25	15	8	8	8	2	2	8	8	8	8	2	2	8	8	8	8	17	25	25	25	22	25	25	26	25	28	16	16	16	16	29		N
M	14	24	25	25	25	25	8	8	8	8	2	2	8	8	8	8	2	2	8	8	8	8	17	25	25	25	22	25	25	27	18	28	16	16	16	16	29		M
L	24	24	25	25	25	25	8	8	8	8	2	2	8	8	8	8	2	2	8	8	8	8	9	25	25	25	22	25	25	27	18	28	16	16	16	16	31		L
K	14	24	25	25	25	25	8	8	8	8	8	8	8	8	8	8	8	8	8	8	8	8	9	25	25	25	22	25	25	36	18	18	16	16	16	16	15		K
J	14	24	25	25	25	25	8	8	8	8	2	2	8	8	8	8	2	2	8	8	8	8	9	25	25	25	22	25	25	27	18	18	16	16	16	16			J
H	14	24	25	25	25	25	8	8	8	8	2	2	8	8	8	8	2	2	8	8	8	8	9	25	25	25	22	25	25	21	18	28	16	16	16	16			H
G	14	24	25	25	25	25	8	8	8	8	2	2	8	8	8	8	2	2	8	8	8	8	19	25	25	25	22	25	25	21	18	28	16	16	16	49			G
F	24	24	25	25	25	25	8	8	8	8	2	2	8	8	8	8	2	2	8	8	8	8	19	25	25	25	22	25	25	21	18	28	16	16	16				F
E	9	24	25	25	25	25	15	8	8	8	2	2	8	8	8	8	2	2	8	8	8	8	19	25	25	25	22	25	25	28	18	16	16	16	16				E
D	9	24	25	25	25	25	15	8	8	8	2	2	8	8	8	8	2	2	8	8	8	8	19	25	25	25	22	25	25	26	18	16	16	16	16				D
C	9	24	25	25	25	25	15	8	8	8	2	2	8	8	8	8	2	2	8	8	8	8	19	25	25	25	22	25	25	18	18	16	16	16	16	15		59	C
B	11	24	25	25	25	25	15	8	8	8	2	2	8	8	8	8	2	2	8	8	8	8	19	25	25	25	22	25	25	13	18	16	16	16	49	15	15	59	B
A	24	24	14	14	25	25	15	8	15	31	2	31	8	31	#	8	2	15	16	15	16	8	49	25	49	25	23	25	25	13	9	16	49	59	15	59	15	59	A
	1	2	3	4	5	6	7	8	9	10	11	12	13	14	#	16	17	18	19	20	21	22	23	24	25	26	27	28	29	30	31	32	33	34	35	36	37	38	

Figure 19 – Potential near-optimal complete rearrangement of the IFSF storage array. This arrangement corresponds to case “bf-g2-m-all-a5-g9b”.

6.3.3 Final Results

Figure 20 presents a plot of the Pareto Front for four to 60 canister movements, with error bars at the data points that determine the curve. The figure plots the results for the optimal movements as confirmed by MCNP calculations for swaps of 2 to 30 canisters as present in Table 21. Uncertainty on the Pareto Front for a lower k_{eff} for a given number of movements is determined from the square root of the sum of the squares of the two sigma calculation statistical uncertainty of 0.001 and an estimate of the optimal arrangement uncertainly for that number of movements. As the difficulty in determining the optimal arrangement increases as the number of movements increases, this estimate of uncertainty increases with the number of movements as well. However, as more iterations are performed with the empirical model, the potential gains become smaller and smaller. Ultimately, the estimated uncertainty for the 24 through 30 swap cases is 0.003, resulting in a collective uncertainty of 0.0032 when combined with the MCNP calculation uncertainty for these Pareto Front data points. This uncertainty estimate is determined from the maximum degree of change that has been found between the candidate solutions that resulted from the empirical model for proposed relocation arrangements for a given number of relocation movements. That is, from the arrangements that were verified by MCNP and the best possible result that was determined by MCNP for the candidate new arrangements.

Figure 21 repeats the plot of the Pareto Front but at a reduced scale and with inclusion of the proposed optimal complete array rearrangement of Figure 19 and calculated by case "bf-g2-m-all-a5-g9b". The final results in Figure 21 demonstrate that the overall current array arrangement is not far from an approximately optimal arrangement, with the key exception of a few rows and fuels types that are stored in the east end of the array. A reasonable number of canister relocation movements can result in an appreciable reduction in the overall array k_{eff}. This is due to the fact that for the remainder of the array, the more reactive and better moderated fuels are placed in rows among groupings of low moderation fuel canisters or groupings of fuel canisters such as FSV that are higher moderation but lower fissile mass. The analysis of this document has shown that placing more reactive fuel canisters at the edges of these regions can result in the best configuration for reducing reactivity and finding the optimal balance between decreasing interaction of more reactive fuels, while maximizing leakage of neutrons from moderated fuels and minimizing significant mixing of moderated fuels with high fissile mass undermoderated canisters. Specifically, the current rows of MTR, Rover UBM, and ORSNF are well placed near Tory and AL-plate fuels. The SB-TRIGA fuel, while not strictly optimally arranged, is well placed in the AL-plate region, since SB-TRIGA is the preferred fuel of the higher reactivity fuels to be in such a region because it is on the lower end of reactivity and fissile mass for the higher reactivity group.

In Figure 20 the decrease in the slope between 24 and 32 canister relocation movements corresponds to the shift in the optimal relocation sequence when it is no longer optimal to swap the HEU TRIGA with PBF fuel. The initial optimal movements prevent the west AL-plate region from being a sufficiently-sized low-moderation zone to adequately isolate the Fermi fuel. Fermi fuel is the next priority fuel that requires movement from the high moderation east end of the array. This shows that while a continuous incremental improvement in k_{eff} reduction is possible with an increasing number of canister movements, it is not a cleanly sequential process, even for a relatively small number of overall canister movements. The small upturn in the curve from the 58 canister movement point to the 60 canister movement point results from the presence of a degree of statistical uncertainty in the confirmatory calculations that is significant relative to the rather flat slope for this region of the optimization front. A significant effort was invested to attempt to determine a preferable arrangement for this number of canister movements, but no statistically significant improvement was found, which supports the determination of the uncertainty present for the data points.

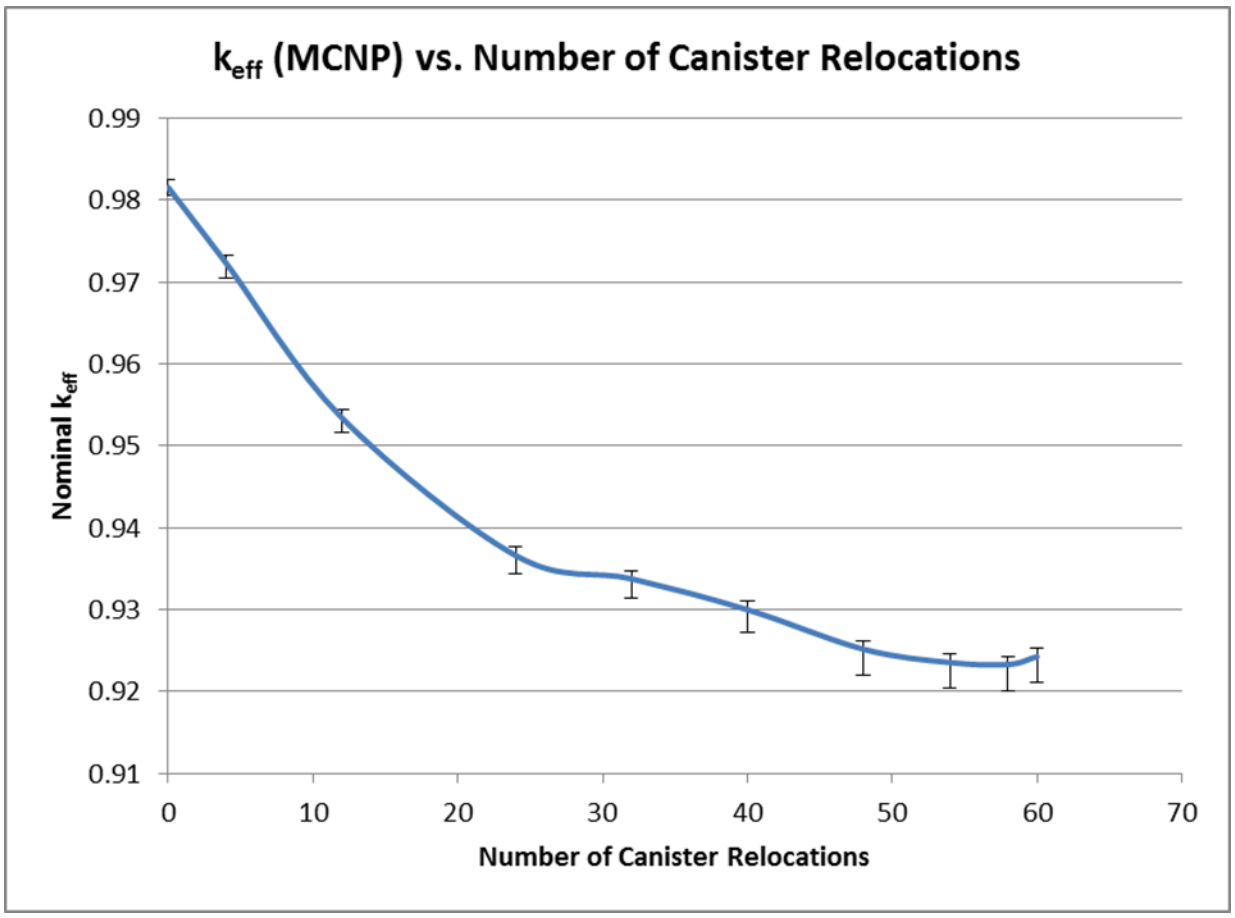

Figure 20 – Pareto Front plot – MCNP calculated minimum possible k_{eff} for canister relocation movements between four and sixty.

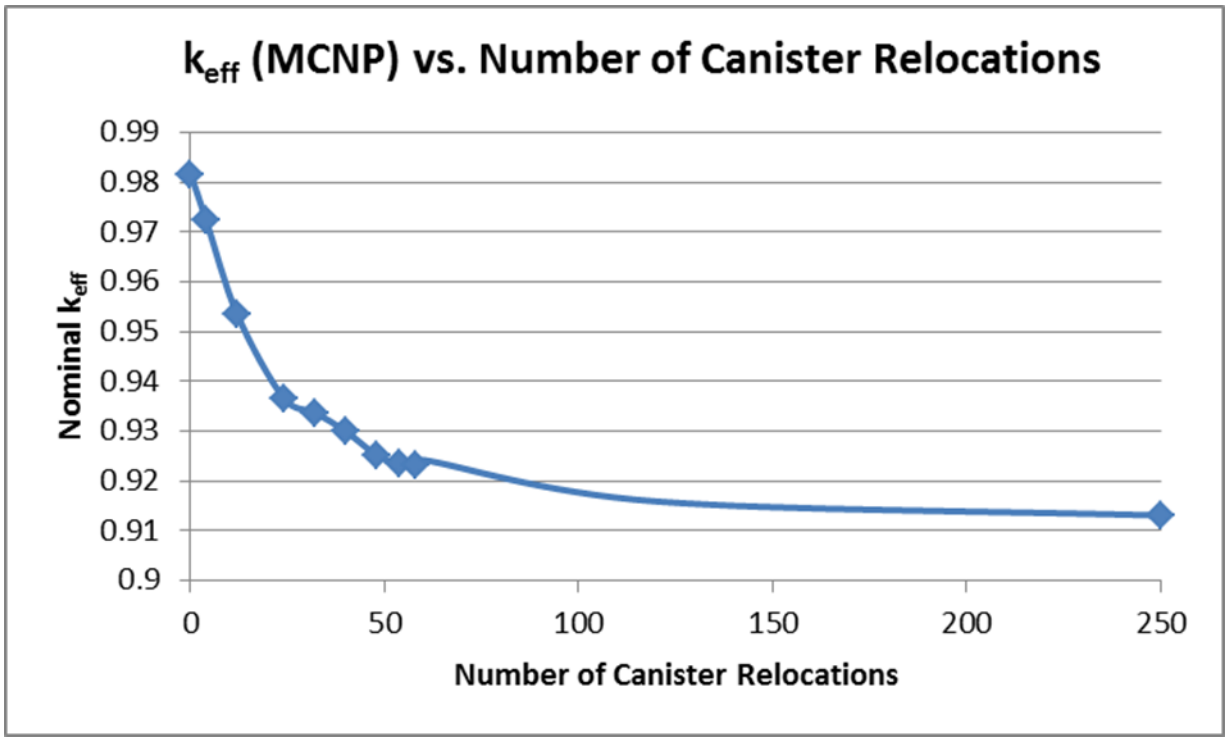

Figure 21 – Pareto Front plot with comparison to potential complete re-arrangement.

A key detail to be noted from the plot of the Pareto Front in Figure 20 is the presence of a region of the curve that shows a marked change in the slope. The transition region indicates that a point is reached where diminishing returns become more pronounced regarding the further relocation of additional canisters. This point occurs after a significant portion of the potential k_{eff} reduction has been achieved. Therefore a reasonable expenditure of operational effort can achieve a considerable gain in the potential reduction in array k_{eff}, and the resulting commensurate increase in capacity utilization from this k_{eff} reduction. Essentially, the steep slope that precedes the 24 canister movement data point shows that there are 12 canisters that are particularly not optimally placed in the current arrangement, and that relocating these canisters can provide a substantial benefit to array k_{eff} reduction.

It is noted that the result for 30 canister swaps is not as low as for 27 or 29 canister swaps. This raises a question over whether there is a true disconnect where consistent, progressive (monotonic) improvement is not necessarily possible, or perhaps the course of optimization is that has been followed by this sequence is a dead-end and that no meaningful further improvement can be made. Specifically, that there is a need to back up and pursue a different course or sequence of

movements. By definition this later case would mean that the 30 swap data point is not Pareto optimal. So the question remains whether the Pareto Front is truly smooth or if disconnects or dislocations are possible. A further degree of randomness in the optimization algorithm could perhaps provide more insight on this question.

Ultimately the results show that a limited number of relocation movements can obtain the majority of the k_{eff} reduction benefit that could be achieved from a much larger scale relocation of the majority of the canisters in the array. This allows for the realization of a practical solution to the multiple-objective optimization problem where by nature there is not one single answer. From a cost-benefit standpoint an important answer to the problem can result from the demonstration of the point of diminishing returns and that this point occurs after sufficient performance improvement has been attained to meet the need at hand.

Chapter 7.0 - Conclusions

The IFSF is an important resource to the DOE for the storage of UNF. The storage array of the IFSF is unique among centralized facilities for dry UNF storage from an NCS standpoint due to the large variety of different fuels currently stored and the fact that there is significant neutronic interaction between the stored fuels. These conditions present a challenge regarding nuclear criticality safety, particularly since the facility has nearly reached the safety limit for the allowable neutron multiplication factor with the current analyzed arrangement that does not consider the facility loaded to capacity. The determination of a new arrangement for the IFSF fuel storage array that would allow the remaining operationally in-service positions to be filled while remaining acceptably subcritical is the fundamental problem to be solved.

The primary objectives established in the effort to address this problem included: 1) improving the knowledge of the interaction effects between the different fuel types stored, particularly regarding the controlled NCS parameters of fissile mass and moderation, which are the crucial variables regarding the stored fuels; 2) development of an empirical model of the IFSF storage array that determines the system neutron multiplication factor for different arrangements of fuels; and 3) establishment of an optimization method that can be applied to the empirical model and which will allow a determination of a fuel storage arrangement that reduces reactivity of the array sufficiently for the remaining empty positions to be filled, and preferably with a minimal number of fuel canister relocation movements.

The first objective was accomplished through new MCNP analysis of the IFSF array with controlled arrangements of fuels to gain a more fundamental knowledge of the interplay of the canister fissile mass and moderation states regarding the effectiveness of neutronic interaction within and neutron leakage from the storage array. These relationships were then applied in the determination of an empirical model that could compute the array k_{eff} for different arrangements of the stored fuel canisters. This model is possible because of the number of other NCS parameters that remain constant within the array, particularly geometry and spacing. This array empirical model produces a fast result, allowing the application of the optimization search algorithm.

The work then accomplished the third objective by developing a search algorithm for the optimal arrangement to produce a minimal k_{eff} through a combination of metaheuristic search methods (specifically a Tabu search) and stochastic methods applied to the empirical model. The empirical model provided an ideal starting point due to the ability to locate the minimal and maximal neutron multiplication produced by the localized regions of the array. Also, the information obtained from the

analysis performed for the first objective was applied in the determination of the rules or exclusions followed by the Tabu search.

The resultant application of the optimization method to the array empirical model was able to determine a solution to the multiple objective optimization problem to minimize the IFSF array k_{eff} with a minimum number of canister relocation movements. This was possible by determining the different array arrangements that resulted in the minimum k_{eff} for various respective numbers of total canister movements. The final results show that the currently empty positions in the IFSF array that are in-service can be filled while remaining below the NCS acceptance criterion for subcriticality if some rearrangement is performed. This condition can be realized with a limited number of canister relocation movements that would be operationally practical to perform. An increase in overall safety margin can also be attained, in that the k_{eff} of the filled array can be reduced below the current array k_{eff} value by up to 0.018 Δk_{eff}. This will allow the utilization of 31 positions that are modelled as empty in the current array arrangement that is approaching the acceptance criterion for subcriticality. The results of this work demonstrate that between 30 to 60 canister movements will achieve the majority of the possible reduction of the k_{eff} of the array that could occur from a major canister relocation effort. Such a major relocation effort would require rearrangement of the majority of the canisters present in the current array, with minimal further benefit.

The empirical models that have been developed provide a beneficial tool for evaluating the addition of new fuel types to the storage array, or to consider changes to the quantities or arrangements of the fuels stored. The overall optimization method and array empirical model that has been developed can be applied to determine new array arrangements that may be needed in order to fill the array with a different fuel type other than the one considered in this analysis. If the future operational need is to fill the array with an AL-plate type fuel, as would be the case with additional ATR fuel that will need dry storage, this is a less difficult condition than the one solved in this analysis. AL-plate fuels produce a smaller increase in the array k_{eff} compared to the LEU TRIGA fuel that was considered, since LEU TRIGA fuel introduces more moderation to the array system. The undermoderated state of the array is a primary factor allowing storage of this significant quantity of fissile material while remaining subcritical.

Additional value of the work includes:

1. An overall advancement of the knowledge of the array interaction behavior, from both a fundamental level, and regarding the range of fuels that are currently stored in the array. Aspects include demonstration of the importance of axial leakage in limiting the array k_{eff}.

2. The determination of the range of significant effect of the presence of moderated canisters relative to unmoderated canisters (particularly with high fissile mass). The analysis has also determined the degree of allowable grouping of the high mass-high moderation (most reactive) canisters.
3. Demonstration of the impact of moving higher reactivity fuels to the perimeter of the array, and the limitations of such movements depending on the proportion of fuel types present. The analysis has improved the knowledge of which fuels are the primary cause for the east side of the array resulting in a much higher k_{eff} than other regions of the array, to the degree that the empty positions in the east side cannot be filled. Further, an understanding has been obtained regarding which areas of the array are in fact well-arranged for the collection of fuels that are currently stored, such as the placement of MTR fuel and Rover UBM fuel adjacent to Tory IIC and AL-plate fuels. Similarly, ORSNF is well-placed between regions of FSV and AL-plate fuels.
4. Demonstration of the capability to "hide" very high fissile mass canisters in low moderation regions of the array, which is essential to the ability to place these canisters in locations that have a minimal impact on overall array reactivity.

References

i "Methods to Improve Efficiency of Fissile Material Storage," T. H. Brown, Los Alamos National Laboratory, *Criticality Safety in the Storage of Fissile Material*, Proceedings of a Topical Meeting, Jackson, Wyoming, Nuclear Criticality Safety Division, American Nuclear Society, September, 1985.

ii LA-14244-M, "Hand Calculation Methods for Criticality Safety – A Primer," D. G. Bowen and R. D. Busch, Los Alamos National Laboratory, November 2006.

iii "A simple, Practical Method for Calculating Interaction," H. K. Clark, Savannah River Laboratory, *Criticality Control of Fissile Materials,* Proceedings of the Symposium on Criticality Control of Fissile Materials, Stockholm, Sweden, International Atomic Energy Agency, November 1965.

iv F. Glover, "Tabu Search – Part I," ORSA Journal of Computing, Vol. 1 Issue 3, August 1989.

v Marler and Arora, "Multi-Objective Optimization - Concepts and Methods for Engineering," VDM Verlag Dr. Muller, Saarbrucken, Germany, 2009.

vi John R. Lamarsh, "Introduction to Nuclear Engineering," Addison-Wesley Publishing Co., Reading, MA, 1983.

vii LA-88-20, "The Hansen-Roach Cross Sections," N. L. Pruvost and M. L. Prueitt, Los Alamos National Laboratory, October 1988.

viii DOE-HDBK-1019/1-93, "DOE Fundamentals Handbook, Nuclear Physics and Reactor Theory, Volume 1 of 2," U. S. Department of Energy, January 1993.

Appendix A – MCNP calculations not reported in Chapter 6

Additional 50/50 proportion, two-fuel grouping calculations

Case Name	Arrangement	K_{eff}
FSV fuel and HEU TRIGA		
	Alternating rows	
fsv2dg1-2.o:	Alternating 2 rows of each type grouped – FSV-FSV-HEU T-HEUT-FSV-FSV-HEUT-HEUT-etc.	1.01715
fsv2dg1-3.o:	Alternating 3 rows grouped – FSV-FSV-FSV-HEU T-HEU T-HEU T, etc.	1.01947
fsv2dg1-4.o:	Alternating 4 rows grouped	1.02739
fsv2dg1-5.o:	Alternating 5 rows grouped	1.03297
fsv2dg1-6.o:	Alternating 6 rows grouped	1.04248
fsv2dg1-7.o:	Alternating 7 rows grouped	1.04441
fsv2dg1-8.o:	Alternating 8 rows grouped	1.04943
fsv2dg1-9.o:	Alternating 9 rows grouped	1.05984
fsv2dg1-10.o:	Alternating 10 rows grouped	1.06537
fsv2dg1-11.o:	Alternating 11 rows grouped	1.07154
fsv2dg1-12.o:	Alternating 12 rows grouped	1.07514
fsv2dg1-13.o:	Alternating 13 rows grouped	1.07953
fsv2dg1-14.o:	Alternating 14 rows grouped	1.08354
fsv2dg1-15.o:	Alternating 15 rows grouped	1.08114
fsv2dg1-16.o:	Alternating 16 rows grouped	1.07742
fsv2dg1-17.o:	Alternating 17 rows grouped	1.07527
fsv2dg1-18.o:	Alternating 18 rows grouped	1.06986

Case Name	Arrangement	K_{eff}
Peach Bottom fuel and HEU TRIGA		
	Alternating rows	
pb2dg1-2.o:	Alternating 2 rows grouped	1.0313
pb2dg1-3.o:	Alternating 3 rows grouped	1.04017
pb2dg1-4.o:	Alternating 4 rows grouped	1.04307
pb2dg1-5.o:	Alternating 5 rows grouped	1.04716
pb2dg1-6.o:	Alternating 6 rows grouped	1.04948
pb2dg1-7.o:	Alternating 7 rows grouped	1.05186
pb2dg1-8.o:	Alternating 8 rows grouped	1.05584
pb2dg1-9.o:	Alternating 9 rows grouped	1.06285
pb2dg1-10.o:	Alternating 10 rows grouped	1.06681
pb2dg1-11.o:	Alternating 11 rows grouped	1.07458
pb2dg1-12.o:	Alternating 12 rows grouped	1.07943
pb2dg1-13.o:	Alternating 13 rows grouped	1.08232
pb2dg1-14.o:	Alternating 14 rows grouped	1.08063

pb2dg1-15.o:	Alternating 15 rows grouped	1.08266
pb2dg1-16.o:	Alternating 16 rows grouped	1.07993
pb2dg1-17.o:	Alternating 17 rows grouped	1.07512
pb2dg1-18.o:	Alternating 18 rows grouped	1.07522

Case Name	Arrangement	K_{eff}
Fermi fuel and HEU TRIGA		
	Alternating rows	
frm2dg1-2.o:	Alternating 2 rows grouped	1.08767
frm2dg1-3.o:	Alternating 3 rows grouped	1.08257
frm2dg1-4.o:	Alternating 4 rows grouped	1.08376
frm2dg1-5.o:	Alternating 5 rows grouped	1.08174
frm2dg1-6.o:	Alternating 6 rows grouped	1.07812
frm2dg1-7.o:	Alternating 7 rows grouped	1.0793
frm2dg1-8.o:	Alternating 8 rows grouped	1.07757
frm2dg1-9.o:	Alternating 9 rows grouped	1.08002
frm2dg1-10.o:	Alternating 10 rows grouped	1.07744
frm2dg1-11.o:	Alternating 11 rows grouped	1.08521
frm2dg1-12.o:	Alternating 12 rows grouped	1.08721
frm2dg1-13.o:	Alternating 13 rows grouped	1.08591
frm2dg1-14.o:	Alternating 14 rows grouped	1.08867
frm2dg1-15.o:	Alternating 15 rows grouped	1.09004
frm2dg1-16.o:	Alternating 16 rows grouped	1.08364
frm2dg1-17.o:	Alternating 17 rows grouped	1.08437
frm2dg1-18.o:	Alternating 18 rows grouped	1.0798

MCNP verification calculations for empirical model optimization results. The best configuration for a given number of swaps is highlighted in bold.

Case Name	Number of swaps	Description	k_{eff} w/ bias
fbc-g2.o:	0	Comparison case for below	0.98153
m2-frm	2	replace 2 fermi (near ctr Pb) w/ FSV	0.98032
m2-g1	2	replace 2 G1 at ctr w/ FSV	0.97487
m2-pbm-a	2	replace two pb-m (ctr near g1 and rover) w/ FSV	0.97879
m2-pbm-b	2	replace two pb-m (near fermi) w/ FSV	0.9786
m2-plstr	2	replace two pulstar w/ FSV	0.97295
m2-plstr-PBF	**2**	**Pulstar swapped with PBF**	**0.97228**
m2-rg1	2	replace rover and centermost G1 w/ FSv	0.97366
mr-rg1-PBF	2	swap center Rover and G1 w/ PBF	0.97326

bf-g2-6m-a	6	2 pulstar, 2 RovG1, 2 more G1	0.95824
bf-g2-6m-a2	6	Like above but swap the Rover and G1 for PBF	0.95348
bf-g2-6m-a2a	**6**	**Like above but with Pulstar also swapped for PBF**	**0.95339**
bf-g2-6m-b	6	2 pulstar, 2 RovG1, 2 PBm	0.96121
bf-g2-12m-a	12	2 pulstar, 8 RovG1, 2 PBm	0.94182
bf-g2-12m-a2	**12**	**like above, but swap the 7 G1 to/with PBF instead of N-FSV**	**0.9366**
bf-g2-12m-b	12	2 pulstar, 6 RovG1, 4 PBm	0.94444
bf-g2-16m-a	16	from 12m-a is two more PBm, one G1, and 1 G3, from 12m-b is 3 more G1 and one G3	0.93675
bf-g2-16m-a2	**16**	**Like above, but swap G1 with PBF instead of FSV**	**0.93376**
bf-g2-16m-b	16	from 12m-b, is 4 new Fermi, 3 more G1 and the G3 relative to 16m-a	0.94234
bf-g2-20m-a	20	Like-16m-a but move HTGR, F-23, two F22	0.93152
bf-g2-20m-b	**20**	**like -16m-a but move four F22**	**0.92999**
bf-g2-20b-b2	20	Like above, but swap G1 w/ PBF instead of FSV	0.93443
bf-g2-20b-b2a	20	Like above, but Fermi is in center instead of west AL	0.93333
bf-g2-20b-b2b	20	Like above, but put one Fermi back and remove one S-PBm	0.93187
bf-g2-20b-b3	20	Like "b", but move F23 to west and only 3 F22 instead of 4	0.93054
bf-g2-20b-b4	20	Like "b', but put one Fermi back and take out one S-PBm, shift location of one previously moved G1 away from PB	0.93103
bf-g2-20m-c	20	Like -16m-a but move four PB south	0.9334
bf-g2-20m-d	20	Like -16m-a but move two PB south, HTGR, F23	0.93213
bf-g2-24m-a	24	Like 20-a, but move four F22, (20a and 20b) (6 total)	0.92783
bf-g2-24m-b	24	Like m20a, but move 4 PB south (20a and 20c)	0.92662
bf-g2-24m-b2	24	Like above, but swap G1 w/ PBF instead of FSV	0.93281
bf-g2-24m-b3	24	like "b", but move Fermi 23 to west instead of south	0.92753
bf-g2-24m-b4	**24**	**Like above, but move two more F22 instead of south PB,PBm (now 2 there instead of 4)**	**0.92517**
bf-g2-24m-c	24	Like m20a, but move 1 PBm south, 1 PBm north, two more F22, (similar to 20 a, 20b and 20 D)	0.92783

bf-g2-m6-7.o:	13	move 8-frm and 4-G1 in groups of 2, and one Rover	0.95685
bf-g2-m4-23.o:	23	Like below, also move the one F-23	0.93451
bf-g2-m4.o:	22	Move 8-G1 to FSV-north, 13-Frm to AL, 1-Rov to FSV-N	0.93766
bf-g2-m5.o:	22	Like -m4 but swap G1 w/ PBF	0.93789
bf-g2-m6-2a.o:	25	Like -m4-23 but also 2-G3 to FSV-N	0.93563
bf-g2-m6-2b.o:	25	Like -m4-23 but also 2-pulstar to FSV-S	0.92774
bf-g2-m6-4.o:	27	comb. -m6-2a and -2b (2-G3 and 2-pulstar)	0.92748
bf-g2-m6-6.o:	29	Like above but move2-G1 east to FSV-N	0.92935
m4-23-2pbm-fsv	25	Like bf-g2-m4-23 but also move 2 moderated pb with FSV south	0.93128
m4-23-2pbm-g2	25	Like bf-g2-m4-23 but also move 2 moderated pb with east g2	0.93369
m4-23-2pbm-al	25	Like bf-g2-m4-23 but also move 2 moderated pb with pbf	0.93212
m4-23-2pbm-pbf	25	Like bf-g2-m4-23 but replace two mod pb with AL	0.93131
bf-g2-27m-b	27	Like 24m-b, but move three more Fermi	0.92543
bf-g2-27m-b4	**27**	**Like 24m-b4, but move three more Fermi**	**0.92353**
m6-2b-2pbm	27	move two in N pbm	0.92588
m6-2b-2pbm-b	27	Like above, but move 2 more Npbm, one Spbm, move 3 Frm back	0.92696
m6-2b-2pbm-2a	27	move two in S pbm	0.92833
m6-2b-4pbm	29	Move two in each (N and S) (4 total)	0.92519
bf-g2-29m-a	29	Like m27-b4 but more two F22 from north to west	0.92688
bf-g2-29m-b	29	Like m27-b4, but from two F22 from SE to west	0.92545
bf-g2-29m-c	**29**	**Like m29-b, but move the two F22 from SE to center**	**0.9233**
bf-g2-30m-b4-c	30	Like m29-b4-c, but one SBT	0.92504
bf-g2-30m-b4-c1	30	Like m29-b-c, but move one east G1	0.9266
m6-2b-5pbm	**30**	**move 5 in N pbm**	**0.92426**
m6-2b-5pbm-b	30	move 4 in N pbm, one in S pbm	0.92649
m6-2b-5pbm-c	30	move 3 in N pbm, 1 in S pbm, one G3	0.9264
m6-2b-5pbm-d	**30**	**move 4 in N pbm, one G3**	**0.92441**
m6-2b-5pbm-d2	30	Like above but swap G1 with PBF, not FSV.	0.93546

m6-2b-5pbm-d3	30	Like above, but put two Frm back, move last PBmn and HTGR to FSVn	0.93569
m6-2b-5pbm-d4	30	Like above but move one more Frm back for one PBm-s	0.93325
m6-2b-5pbm-e	30	Like 5pbm but move three Fermi back, move one G3, HTGR, and one PBm-s instead	0.9276
bf-g2-30m-b4	30	Like 27m-b4 but move four F22, put G3 back to east	0.92747
bf-g2-30m-b5	30	Like 27m-b4, but move three F22, all in Row 6	0.92638
bf-g2-30m-b5a	30	Like above with one F22 in r7 instead of r6	0.92979
bf-g2-30m-b5b	30	Like m30-b5, but rearrange red walls to be closer to 5pbm	0.92592
bf-g2-30m-b5c	30	Like m30-b5b, but Move two F22 to center	0.92446
bf-g2-30m-b5d	30	Like m30-b5c, but Move two more F22 from east, put a Pbm and HTGR back	0.92568
bf-g2-30m-b6	30	Like 27m-b4, but move one F22 to r6, two F22 to r20	0.92722
bf-g2-30m-b7	30	Like 27m-b4, but move two F22 to r6, move final N-PBm	0.92723

Entire array optimization cases

Case Name	Swaps	Description	K_{eff} w/ bias
bf-g2-m-all-a		Initial move all case - best est. concentric	0.94108
bf-g2-m-all-b		Move more FSV to south, more AL to east	0.94324
bf-g2-m-all-c		Like above and group Fermi in fours	0.94115
bf-g2-m-all-d		Like above, but move pulstar out of corner	0.94323
bf-g2-m-all-e		Like "c", but move Rover-UBM out of corner	0.94123
bf-g2-m-all-f		Like "c", but more ROV-UBM 12/13 out of center	0.94106
bf-g2-m-all-a2		Re-arrange of "a", 2 groups of fermi, UBM to east, all BER, tory, PBF to perimeter, G2 outside of FSV	0.94278
		Below all like bf-g2-m-all-a2 except:	
bf-g2-m-all-a2-a		replace all Fermi w/ AL	0.94309
bf-g2-m-all-a2-b		replace all Tory w/ AL	0.94413
bf-g2-m-all-a2-c		rows 36,37 empty	0.94442
bf-g2-m-all-a2-d		rows 34 thru 37 empty	0.94252
bf-g2-m-all-a2-e		empty row 1	0.94071
bf-g2-m-all-a2-f		replace all G2 with FSV	0.94401
bf-g2-m-all-a3-a		Like -a2 but swap yellow for green	0.94135
bf-g2-m-all-a3-b		Like above but remove west Fermi	0.93904
bf-g2-m-all-a3-c		Like above but move W PB over 2 rows	0.93197

bf-g2-m-all-a3-d		Like above but Move W MTR over 2 rows, PB over to FSV border	0.94525
bf-g2-m-all-a4-a		Re-arrange w/ red on three side, yellow on one, green between	0.93197
bf-g2-m-all-a5-a		Re-arrange with blocks and rows	0.94099
bf-g2-m-all-a5-b		Like above, break up G1 row	0.93098
bf-g2-m-all-a5-c		Break up Fermi row	0.94341
bf-g2-m-all-a5-d		Break up PB	0.93716
bf-g2-m-all-a5-e		Combine all three above	0.93194
bf-g2-m-all-a5-f		Like above, but swap West wall rover w/ AL	0.9279
bf-g2-m-all-a5-g		Like above, but break up PB more	0.92671
bf-g2-m-all-a5-h		Like above, but split row 23, and spread row 30 more	0.92717
bf-g2-m-all-a5-g1	207	Like -a5-g but move Fermi back to one row	0.92314
bf-g2-m-all-a5-g2	200	Like above, but move row 1 east one row, Tory against wall	0.92815
bf-g2-m-all-a5-g3	201	Like above, but add more space and move UBM away from wall	0.92191
bf-g2-m-all-a5-g4	206	Like above, but move row back to wall (like "g1"	0.91744
bf-g2-m-all-a5-g5	204	Like above but move UBM 12/13 to wall (move two wall Rovers over)	0.91594
bf-g2-m-all-a5-g6	204	Like above, but move east end Rover from corners to walls	0.91606
bf-g2-m-all-a5-g7		Like g5 but mess with Row 1 more	0.91844
bf-g2-m-all-a5-g8		Like above but also mess with east Rover and G2	0.92079
bf-g2-m-all-a5-g9		Like a5-g5 but move PB to two groups of two rows full width	0.91432
bf-g2-m-all-a5-g9a		Like a5-g9 but move red fuels at the edges and add break to PB rows	0.91352
bf-g2-m-all-a5-g9b	**203**	**Like a5-9a, but move SBT away from UBM, move one rover to NE corner, center T66 and BER more**	**0.91311**
bf-g2-m-all-a5-g9c		Move east SBT over one more row, put displaced row 32 TG2 inward, move path to where SBT was	0.91805